NEESR Summary Report
Earthquake Response and Rehabilitation of Critical Lifelines

Award No. CMMI-1041498

Prepared by
Cornell University,
University at Buffalo, and
California State University at Los Angeles

August 27, 2014

TABLE OF CONTENTS

TABLE OF CONTENTS (completed)

LIST OF TABLES

LIST OF FIGURES

LIST OF FIGURES (continued)

LIST OF FIGURES (continued)

LIST OF FIGURES (continued)

LIST OF FIGURES (completed)

NEESR Summary Report
Earthquake Response and Rehabilitation of Critical Lifelines
Prepared by Cornell University, University at Buffalo, and California State University at Los Angeles
August 27, 2014

1. 0 ACTIVITIES AND FINDINGS

This report summarizes the activities and findings from the NEESR project "Earthquake Response and Rehabilitation of Critical Lifelines" (Award No. CMMI-1041498) The report is organized into sections that include activities of each of the partners in the project. Separate sections cover the Project Summary, and then activities at Cornell University, University at Buffalo, and Education, Outreach and Training (EOT) at California State University at Los Angeles.

Project Summary

This research will transform the seismic mitigation of lifelines by 1) qualifying in situ lining technology to retrofit existing underground infrastructure, 2) developing fundamental understanding and analytical capabilities for the in-situ reinforcement of lifelines, 3) combining full-scale experimental validation and computational simulation in design and construction guidelines, 4) developing undergraduate classroom projects related to seismic vulnerability and design of lifelines, and 5) delivering short courses for industry and students, with web-based lectures, seminars, and notes. The research will correct a critical deficiency in current practice, namely the lack of verification of in situ pipe lining technologies for seismic retrofitting. It will use flexible electronics for combining micro sensor systems with in situ linings. This fusion of flexible electronics and pipe lining technology has the potential to transform underground utilities into real-time condition monitoring and data collection networks.

The research is performed through physical modeling at the Cornell Large-Scale Lifelines Testing Facility, University at Buffalo (UB) Dual Shake Table Facility, and California State University at Los Angeles (CSULA) Strength of Materials instructional laboratory, all of which will be used in combination with advanced computational simulation to characterize the behavior of underground lined piping systems. The research involves a university-industry partnership with support from Insituform Technologies, Inc., the largest company worldwide for in situ lining installation, Los Angeles Department of Water and Power (LADWP), and the Center for Advanced Microelectronics Manufacturing (CAMM).

Intellectual Merit: The research will substantially reduce the seismic vulnerability of US pipeline networks through the systematic investigation and validation of pipelines with polymeric linings for seismic retrofit by full-scale testing and numerical modeling of lined pipe under permanent and transient ground deformation. The split-box testing capabilities at Cornell are ideally suited for simulating ground rupture effects on pipelines to reproduce upper bound conditions of permanent ground deformation in the field. The dual shake table capabilities at UB are uniquely qualified for simulating seismic wave interaction with pipelines, especially for replicating the critical condition of closely spaced weak joints and defects, where axial movements and rotations will be driven by simultaneous shake table operation. Guided by full-scale simulations, which are essential to discover and refine 3-D soil-lifeline interaction, numerical models will be developed, including 3-D models of the composite pipeline, liner, and soil system. The research will combine state-of-the-art, full-scale experiments with advanced computational procedures to develop and validate the next generation analytical models. These models will support design and construction to apply in situ lining technologies broadly for seismic risk reduction as well as improve the general practice associated with liner rehabilitation of critical underground infrastructure. The research also has begun to explore the use of flexible electronics to embed micro-sensors, and thus create "intelligence", in lining systems.

Broader Impacts: There are more than 2.1 million km of pipelines in water and wastewater systems throughout the US, with nearly half consisting of cast iron pipelines that are at least 50-100 years old. There is a strong need to rehabilitate aging, underground lifelines throughout the country, especially those located in areas with seismic risk and constructed of brittle materials such as cast iron. The proposed research has the capacity to reduce utility system costs through the extension of pipeline service life with intelligent liners.

2.0 CORNELL UNIVERSITY

Large-scale testing at Cornell is performed with an integrated system of large-stroke hydraulic actuators that are mounted on a reaction wall with their movable pistons connected to a split test basin. The basin can contain up to 90 metric tons of soil. The system can be configured to test multiple full-scale pipes simultaneously, in either tension or compression, and the fault modified for a range of crossing angles. Figure 2.0.1 shows a layout of the facility with the split test basin. The test basin at Cornell consists of a fixed and movable section displaced by four hydraulic actuators. The basin is 3.2 m wide and 13 m long, with a maximum 2.1 m depth. It is split in the center along a 50-degree sliding plane, which can be seen in Figure 2.0.1. Four actuators, mounted parallel to the direction of fault displacement, will be electronically grouped and operated under displacement control, thus assuring identical actuator commands and uniform test basin movement.

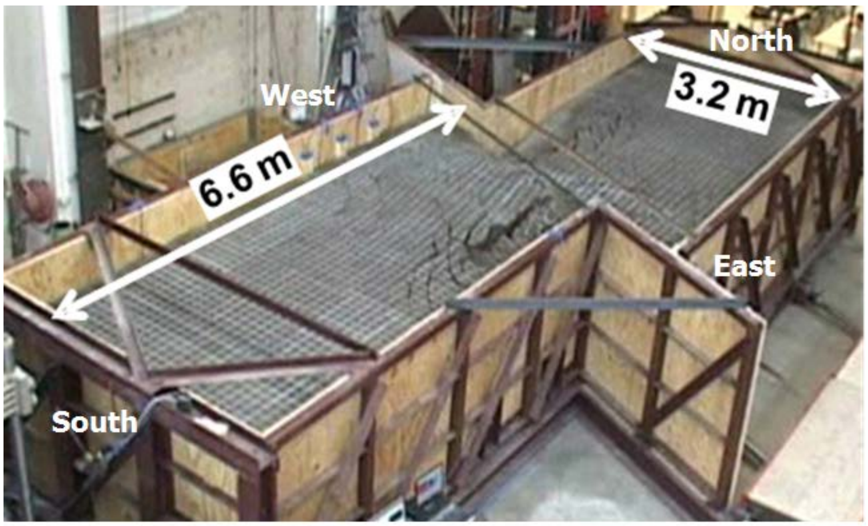

Figure 2.0.1. Cornell Large Scale Test Basin

Experimental Study

This report describes several sets of full-scale experiments conducted at Cornell.

The tests consist of:

1) Axial push tests on unlined ductile iron pipes connected with bell-spigot joints performed at the Cornell large scale test basin in May 2012,

2) Large-scale tension test on lined ductile iron (DI) pipe connected with bell-spigot joints performed at the Cornell large-scale test basin in June 2012. The liner material was InsituformMain® System, referred to as IMain in this report. In this test, the central portion of the experimental pipe was centered on the fault. This is referred to as a pipe centered (PC) experiment.

3) This report presents the results of a large-scale tension test on lined DI pipe connected with bell-spigot joints performed at the Cornell large-scale test basin in June 2012. The liner material was InsituformMain® System. In this test, a joint of the experimental pipe was centered on the fault. This is referred to as a joint centered (JC) experiment.

4) Axial pull tests on IMain lined DI pipe connected with bell-spigot joints performed at Cornell in September through November, 2012, and

5) Axial pull tests on Starline 2000® lined DI pipe connected with bell-spigot joints performed at Cornell in December, 2012 through May, 2013.

2.1 Axial Push Tests

2.1.1 Test Purpose and Descriptions

The primary purpose of these tests was to study the axial frictional resistance of the pipes, through an experimental process which involves progressive axial "push-through" of a ductile iron pipe through the soil. The frictional resistance between the pipe and the soil depends on the properties of the pipe and the surrounding soil, and the geometry of the joint connection. Six different tests were performed using different joint configurations and joint restraints to quantify the resulting frictional resistance developed along the pipe. The first test (PT1) involved a straight ductile iron pipe without joints, and the second test (PT2) was a push-through test of a single-joint pipe specimen, with the bell "tail" being progressed through the soil. During the third test (PT3) a single-joint pipe specimen with the joint being restrained by a special restraint (Cornell Joint Restraint) was pushed through the soil. The fourth test (PT2a) was a repeat of PT2 to substantiate repeatability and correct for a slip at the jack/pipe connection. The fifth push-through tests (PT4) was a single-joint pipe specimen axial push, with the bell "face" being progressed through the soil. The sixth test (PT5) was a push-through of a single-joint pipe specimen that was restrained by a specially designed clamp (UB clamp). A separate report describes the UB clamps and their testing capacity. ("Capacity Testing of UB Clamps," Cornell University NEESR Group, Dec., 2012.) Table 2.1.1 briefly describes the six tests. A more complete description of the test procedures and experimental results is given in "Axial Push Tests on Ductile Iron Pipes, "Cornell University NEESR Group, January 23, 2013.

Figures 2.1.1 and 2.1.2 show plan and profile views of Push Test 1 (PT1). Figures 2.1.3, 2.1.4, 2.1.5, and 2.1.6show the plan views of PT2, PT2a, PT3, PT4, and PT5, respectively. The profile views of the tests are similar to that of PT1, with the exception of the bell, restraint, or clamp position (see Table 2.1.1)

Table 2.1.1. Descriptions of Axial Push Tests

Test	Date	Description	Push Direction	Instrumentation
1	5/16/2012	Straight DI Pipe followed by bell.	South to north. Bell faces direction south.	Pressure Transducer, String Pot, Two DCDTs
2	5/17/2012	Bell 33.5 in. into test basin.	South to north. Bell faces direction south.	Pressure Transducer, String Pot, Two DCDTs
2a	5/21/2012	Bell 33 in. into test basin.	South to north. Bell faces direction south.	Pressure Transducer, String Pot, Two DCDTs
3	5/18/2012	Bell with a restraint center 33.5 in. into test basin.	South to north. Bell faces direction south.	Pressure Transducer, String Pot, Two DCDTs
4	5/23/2012	Bell 33 in. into test basin in soil.	South to north. Bell faces direction north.	Pressure Transducer, String Pot, Two DCDTs
5	5/24/2012	Straight pipe with clamp 7 in. north of the southern bulkhead.	South to north.	Pressure Transducer, String Pot, Two DCDTs

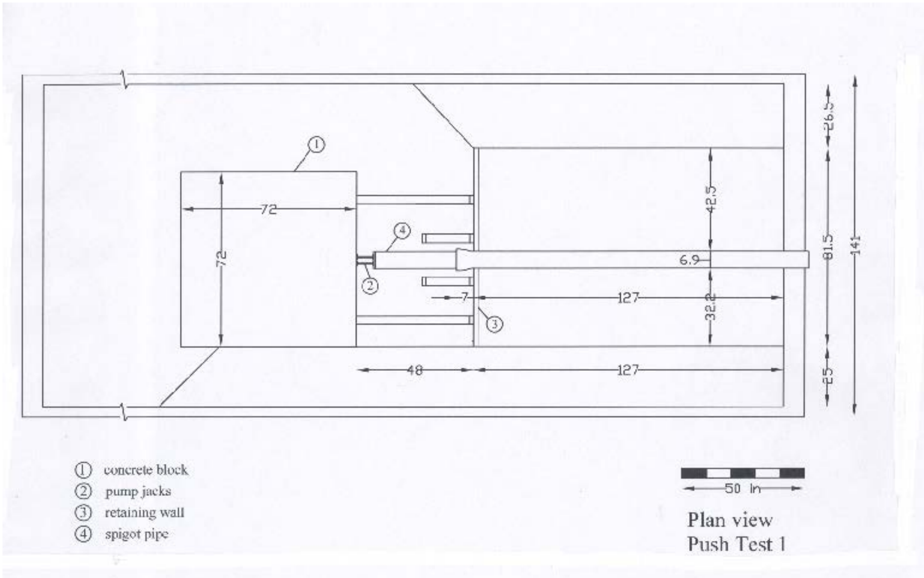

Figure 2.1.1. Plan View of Push Test 1

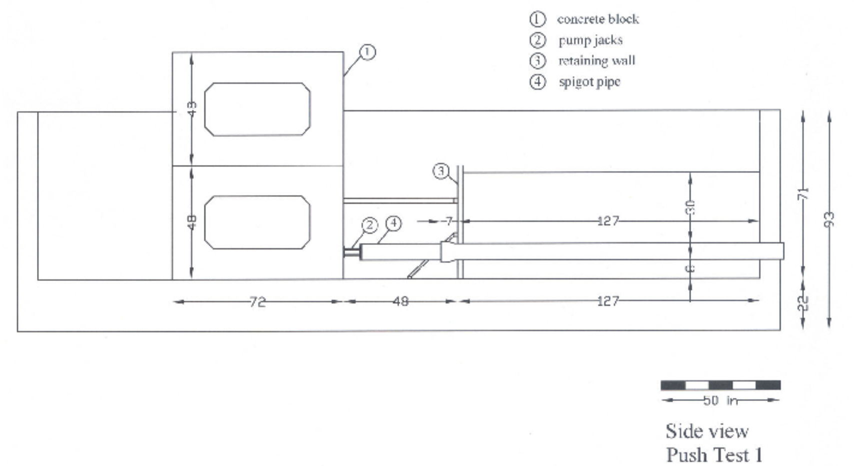

Figure 2.1.2. Profile View of Push Test 1

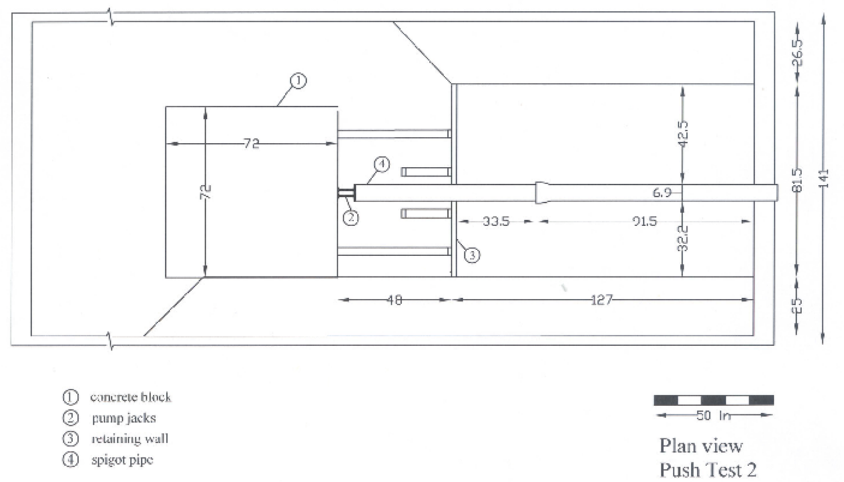

Figure 2.1.3. Plan View of Push Test 2 and Push Test 2a

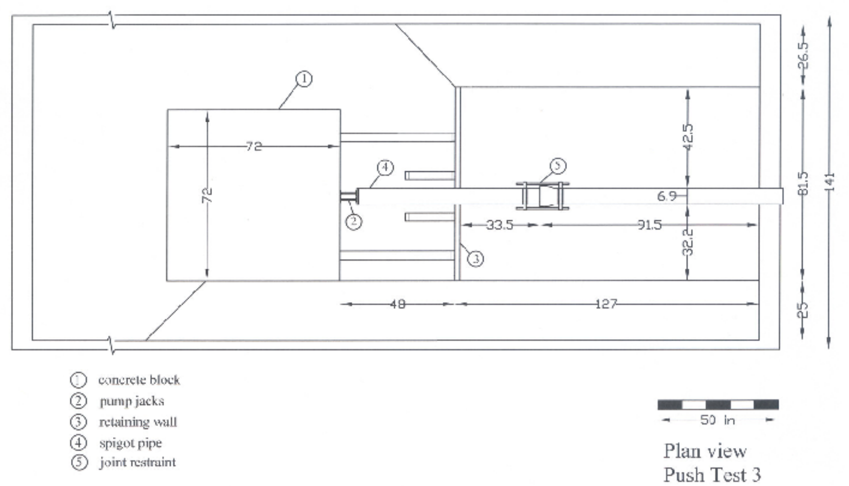

Figure 2.1.4. Plan View of Push Test 3

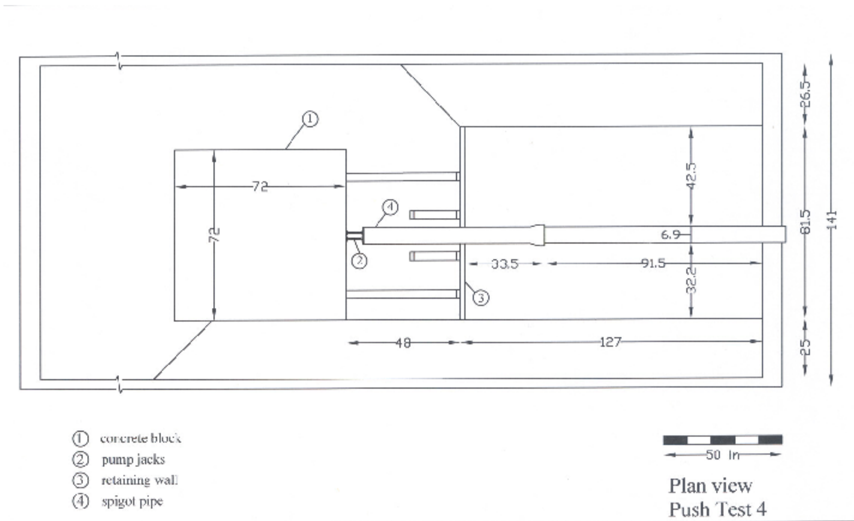

Figure 2.1.5. Plan View of Push Test 4

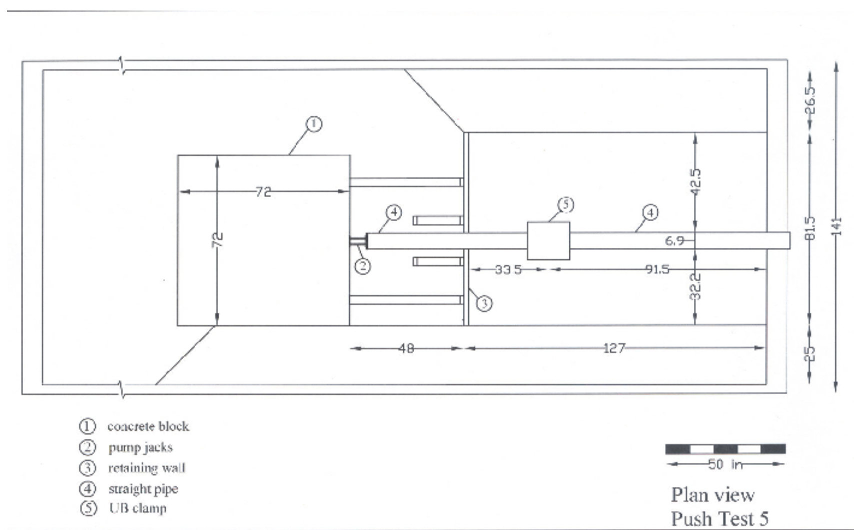

Figure 2.1.6. Plan View of Push Test 5

The pipe specimen that was used during the axial push-through tests was a 13-ft-long (4-m-long) ductile iron (DI) pipe specimen with 6 in. (150 mm) nominal diameter. The standard DI pipes used in the tests were provided by the Los Angeles Department of Water & Power (LADWP) and have bell-and-spigot joint connections. Figure 2.1.7 shows a cross-section of the bell-spigot connection. The pipe specimen wall thickness was approximately 0.30 in. (7.6 mm). The outer and inner diameter of the DI pipe was respectively 6.87 in. (175 mm) and 6.01 in. (153 mm). The DI pipe joint consists of a standard bell and spigot connection sealed with a greased rubber gasket, as shown in Figure 2.1.7. The connection is prepared by inserting the spigot into the bell until metal contact between the spigot and toe of the bell is achieved.

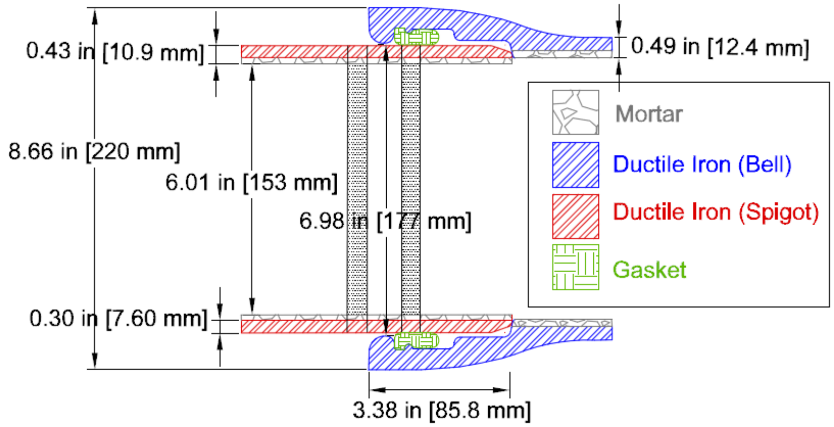

Figure 2.1.7. Ductile Iron Joint Cross Section.

2.1.2 Soil Preparation and Compaction Data

The soil that was used during the push-through tests was crushed, washed, glacio-fluvial sand produced by RMS Gravel consisting of particles mostly passing the ¼ in. (6.25 mm) sieve. Eight in. (203.2 mm) of compacted sand was placed in the test basin, followed by the pipe section, followed by roughly 8-in.thick (203-mm) lifts until there was 30 in. (762 mm) cover of compacted sand above the pipe crown. Every layer was compacted to the same extent and moistened with water in a similar way to achieve uniformity. Dry density measurements for each layer at four representative spots (NW, NE, SE, SW) were obtained using a Troxler Model 3440 densitometer. Moisture content measurements were obtained using both soil samples and the densitometer at the same locations. The target value of dry density was γ_{dry} = 106 pcf (17 kN/m3) and of moisture content w = 4.0 %.

2.1.3 Test Basin and Equipment

The push-through tests on DI pipes were performed at the Cornell NEES testing facility, in the 10.5-ft-wide (3.2-m) and 43-m-long (13-m) test basin. Only one third of the length of the basin was necessary for these tests. A 48-in.-high (1.2-m) wooden retaining wall was constructed for the restraint of the soil layer. The wooden retaining wall constructed roughly 10 ft from the north end of the test basin. The bulkhead had an opening cut into it so that the pipe would protrude through the bulkhead. The other end of the pipe exited the test basin on the north end. Figure 2.1.8 shows the general set-up of the tests. The pipe specimens were pushed with the aid of a manual pump, placed at the south end of the DI pipe section, which are shown in Figure 2.1.9. Two 6 ft by 6 ft by 4 ft high (1.83 m by 1.83 m by 1.22 m high) reaction wall blocks, each weighing 13.5 kips (60.1 kN) were placed in the open area of the test basin to provide a resistance to the pushing force that was applied by two hand-operated hydraulic jacks. The capacity of the blocks against sliding was in excess of approximately 12.5 kips (55.6 kN). The hydraulics for the jacking system were connected to a calibrated pressure transducer so the push forces could be measured.

Figure 2.1.8. Overview of Test Basin for Axial Push Tests

Figure 2.1.9. Overview of Hydraulic Pumps and for Axial Push Tests

2.1.4 Instrumentation

The force imposed at the south end of the pipe from the hydraulic pumps was monitored during the push-through tests based on the pressure of the pump, which was calibrated accordingly with an electronic pressure transducer and connected to the data acquisition system. The displacement imposed on the DI pipe was measured by a string potentiometer (pot) and two DCDTs placed at the north end of the pipe. The string pot was expected to provide measurements at large pipe displacements up to roughly 40 in. (1016 mm) and the DCDTs at very small displacements up to 1.5 in. (3.8cm). Figure 2.1.10 shows the setup of the string pot and the DCDTs on the north side of the test basin.

2.1.5 Testing Protocol

The general testing protocol consisted of:

a. Place the first soil layer with measurements of density (unit weight) and water content,
b. Place the pipe in the test basin,
c. Place the remaining soil in lifts with measurements of density (unit weight) and water content,
d. Add a pipe section to the “pushed” end so the jacks could be positioned against the reaction blocks,
e. Connect all instrumentation to the data acquisition system,
f. Operate the hand-pumped jacks. Note that the maximum stroke of the jacks was approximately 5 in. (127 mm),
g. When the jacks reached their limiting stroke, release the jack pressure, retract the jacks and install additional blocking to continue pushing the pipe section.

a) Small Displacement

b) Large Displacement

Figure 2.1.10. Instrumentation for Displacement Measurements for Axial Push Tests

2.1.6 Test Comparisons

Selected results of the axial push test are presented. The full test results are given in a separate report, as referenced previously.

<u>Push Tests 2 and 2a</u>

Push Test 2 (PT2) was a section of the DI pipe with the bell face roughly 33 in. (838 mm) inside the soil, with the bell face in the south direction. Push Test 2a (PT2a) was a repeat of PT2, with the bell face in the south direction 33 in. (838 mm) inside the soil. Figure 2.1.11 compares the two tests to a 0.2 in (5.14 mm) displacement. There is practically no difference in the test results. Figure 2.1.12 shows the test results to a displacement of 1 in. (25.4 mm). At a bit larger displacement in PT2 there was a possible misalignment of the jack and additional movements within the loading system, leading to an increase in the resistance. This increase in resistance is clearly shown in Figure 2.1.13. At a displacement of about 3.2 in. (81.3 mm) the push force in Test 2 was 6.8 kips (30.2 kN) as compared to 4.7 kips (20.9 kN) in Test 2a. At a displacement of 3.2 in. (81.3 mm) the jacking system in Test 2 was realigned. Figure 2.1.14 shows that following the realignment the push forces at large displacements in Tests 2 and 2a were nearly the same.

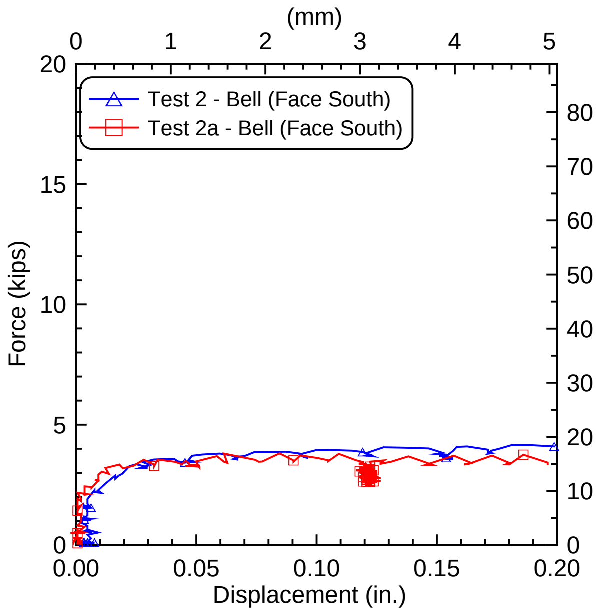

Figure 2.1.11. Force-Displacement for Axial Push Tests 2 and 2a to 0.2 in. (5.1 mm) Displacement

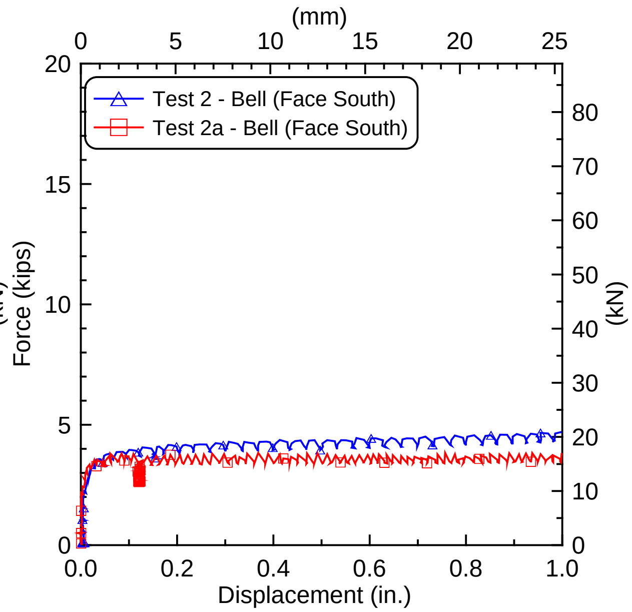

Figure 2.1.12. Force-Displacement for Axial Push Tests 2 and 2a to 1 in. (25.4 mm) Displacement

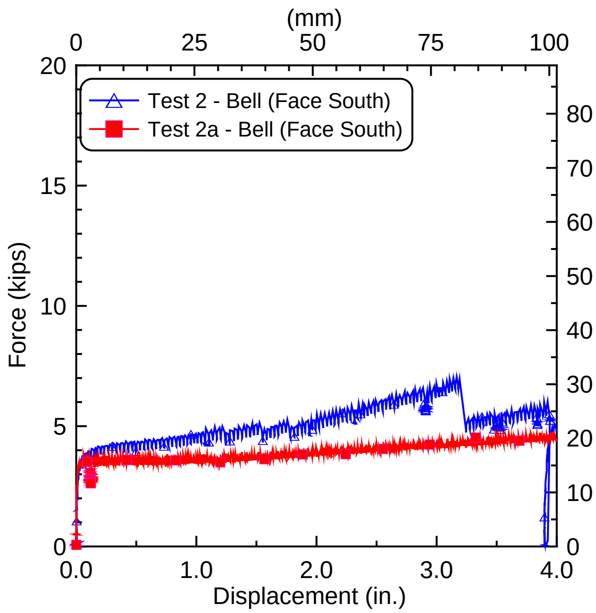

Figure 2.1.13. Force-Displacement for Axial Push Tests 2 and 2a 1 to 4 in. (101.6 mm) Displacement

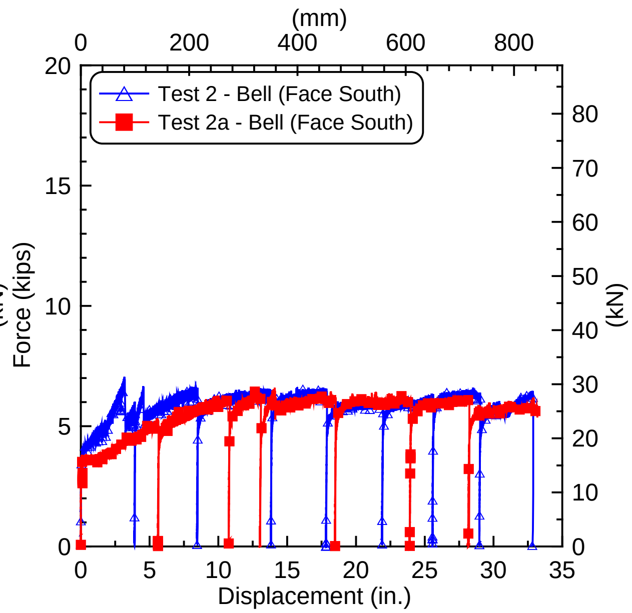

Figure 2.1.14. Force-Displacement for Axial Push Tests 2 and 2a Maximum Displacement

Push Tests 2a and 4 – Bell South and Bell North

Push Test 2a and Push Test 4 both had the bell 33 in. (838 mm) but with the face of the bell in the south and north directions, respectively. Thus, they are a direct comparison of the effects of the direction of the bell. Figure 2.1.15 compares the two tests to 0.2 in. (5.1 mm) displacement. The test results are virtually the same, indicating at the small displacements necessary to mobilize the soil resistance there is no difference in the axial force-displacement relationship when the bell faces either direction. Figures 2.1.16, 2.1.17, and 2.1.18 show comparisons of PT2a and PT4 at 1 in. (24.4 mm), 4 in. (101.6 mm), and maximum test displacements, respectively. At a displacement of about 1 in. (25.4 mm) the bell north (PT4) began to pick up more force than the bell south test, as seen in Figure 2.1.17. Figure 2.1.18 shows that after a displacement of 3 in (76.2 mm) the force-displacement results are the once again the same.

Push Tests 1, 2a and 4 – Straight Pipe and Joint

Tests PT1 (straight pipe) and PT2a and PT4 (joints) were typical of jointed pipes without any external clamping of joining features. Up to displacements of about 1 in. (76.2 mm) the behavior of all of these combinations were similar, but some differences did exist. This is seen in Figures 2.1.19 and 2.1.20. After that displacement there were substantial variations in the force-displacement relationships. This is shown in Figures 2.1.21 and 2.1.22.

Push Tests 3 and 5 – Restraint and Clamp

Figure 2.1.23 shows the results from PT3 that had the restraint and PT5 that had the UB clamp. up to a displacement of 0.2 in. At small displacements the two joining systems showed similar results, with the clamp showing slightly greater resistance. Figures 2.1.24, 2.1.25, and 2.1.26 show that the UB clamped pipe develops substantially greater resistance at larger displacements.

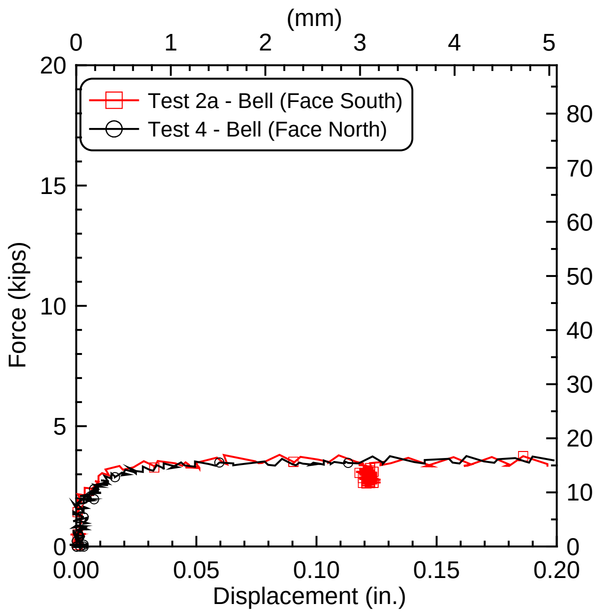

Figure 2.1.15. Force-Displacement for Axial Push Tests 2a and 4 to 0.2 in. (5.1 mm) Displacement

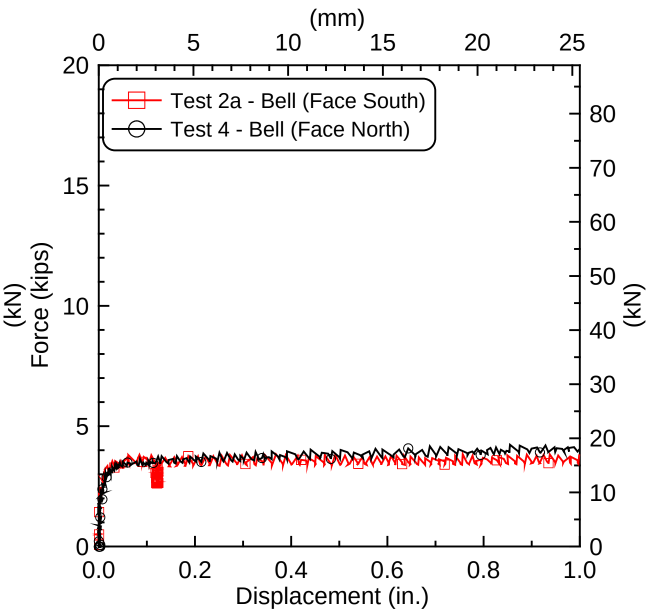

Figure 2.1.16. Force-Displacement for Axial Push Tests 2a and 4 to 1 in. (25.4 mm) Displacement

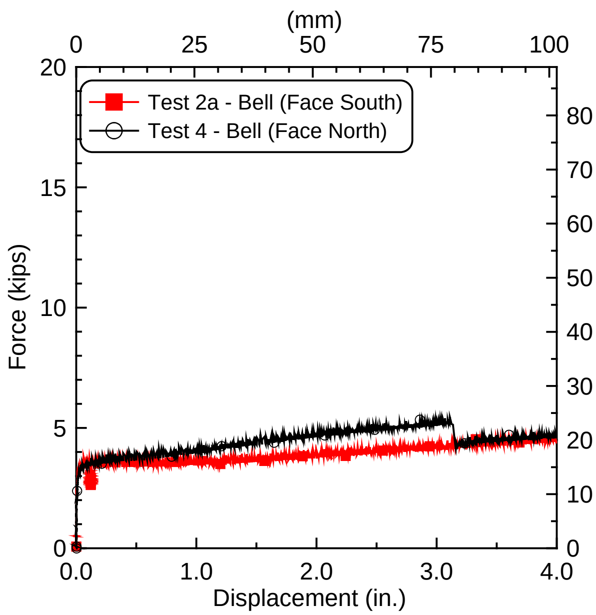

Figure 2.1.17. Force-Displacement for Axial Push Tests 2a and 4 to 4 in. (101.6 mm) Displacement

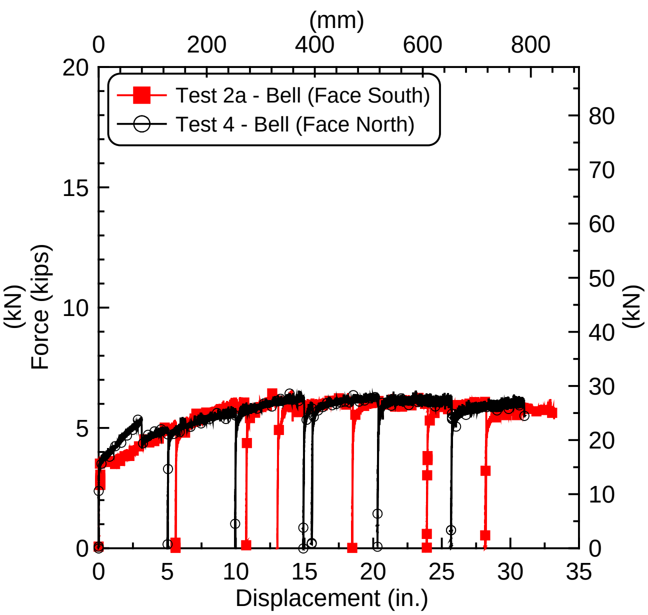

Figure 2.1.18. Force-Displacement for Axial Push Tests 2a and 4 to Maximum Displacement

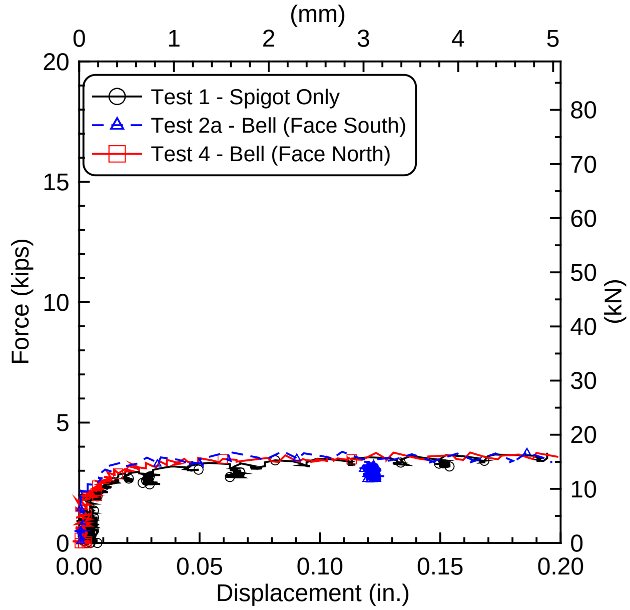

Figure 2.1.19. Force-Displacement for Axial Push Tests with and without a Joint to 0.2 in. (5.1 mm) Displacement

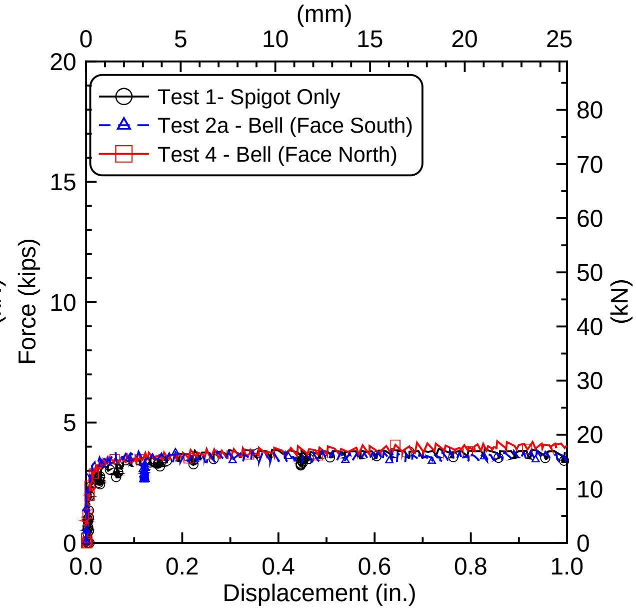

Figure 2.1.20. Force-Displacement for Axial Push Tests with and without a Joint to 1 in. (25.4 mm) Displacement

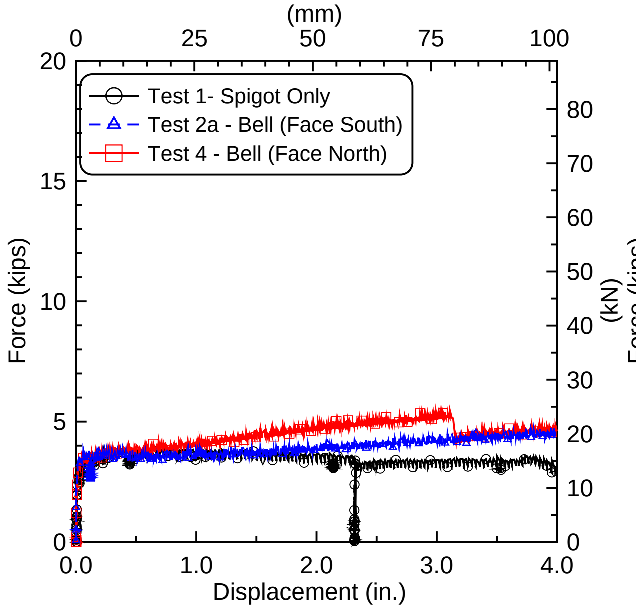

Figure 2.1.21. Force-Displacement for Axial Push Tests with and without a Joint to 4 in. (101.6 mm) Displacement

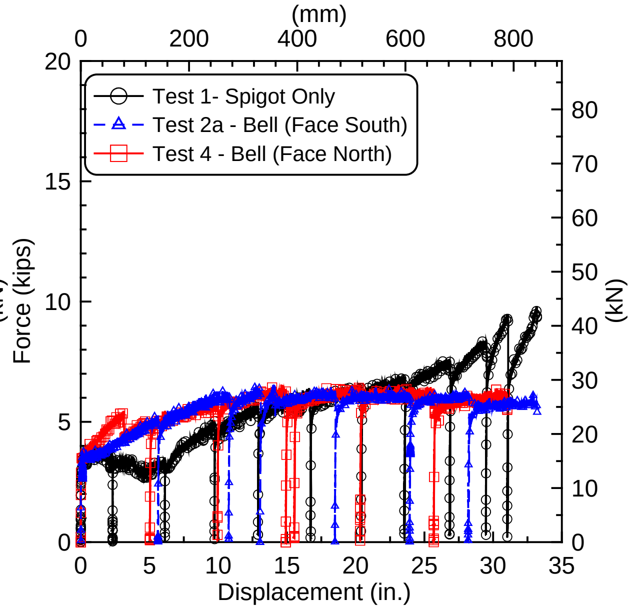

Figure 2.1.22. Force-Displacement for Axial Push Tests with and without a Joint to Maximum Displacement

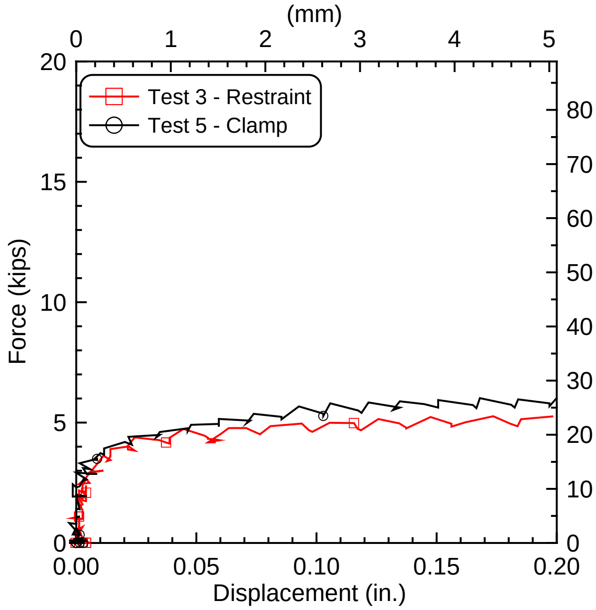

Figure 2.1.23. Force-Displacement for Axial Push Tests with Restraint and Clamp to 0.2 in. (5.1 mm) Displacement

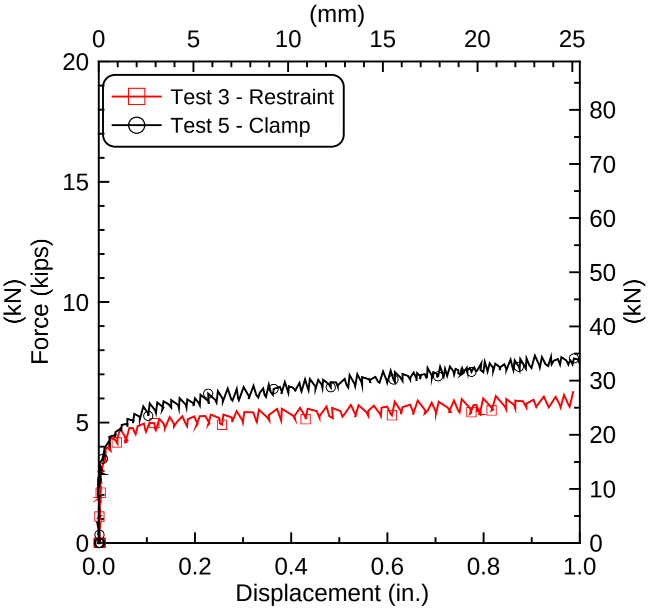

Figure 2.1.24. Force-Displacement for Axial Push Test with Restraint and Clamp to 1 in. (25.4 mm) Displacement

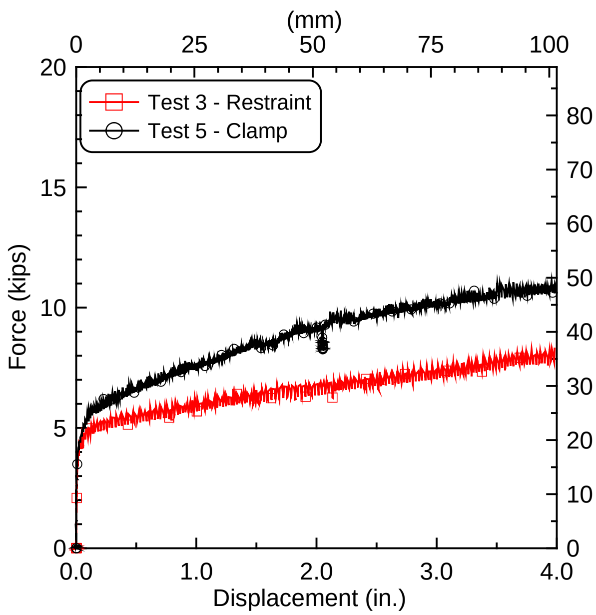

Figure 2.1.25 Force-Displacement for Axial Push Tests with Restraint and Clamp to 04 in. (101.6 mm) Displacement

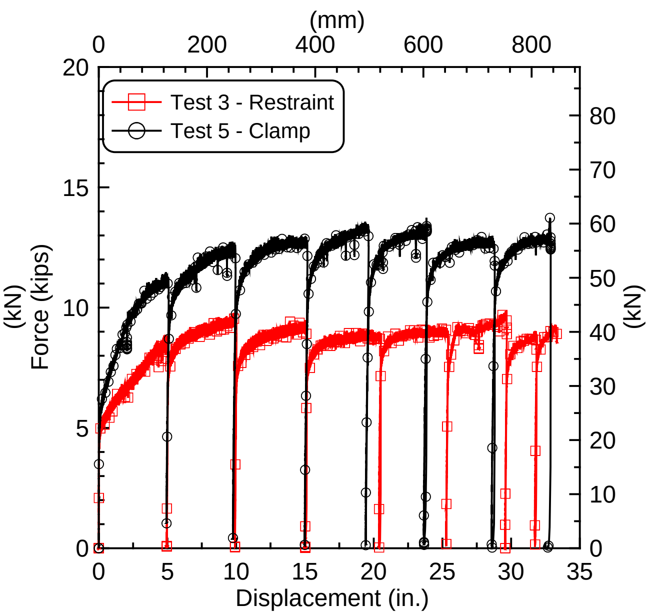

Figure 2.1.26. Force-Displacement for Axial Push Tests with Restraint and Clamp to Maximum Displacement

2.1.7. Summary of Axial Push Tests

Six large-scale push tests were performed on nominal 6-in (152-mm)-diameter ductile iron pipe. The arrangements included straight pipe, pipe with bells facing both possible directions, and pipes jointed with two types of special clamping arrangements. All pipe section had 30 in. (762 mm) of compacted soil cover above the pipe crown. Displacements were measured at the pipe end extending through the test basin, using one string potentiometers and two DCDTs. Previous sections of this report provide all of the force-displacement measurements and also present comparisons between tests having generally similar characteristics. Table 2.1.2 gives brief summary descriptions of the push tests. Table 2.1.3 presents a summary table of push force at selected displacements from the six tests.

Table 2.1.2. Brief Descriptions of Axial Push Tests

Test	Description	Push Direction
1	Straight DI Pipe followed by bell.	South to north. Bell faces direction south.
2	Bell 33.5 in. into test basin.	South to north. Bell faces direction south.
2a	Bell 33 in. into test basin.	South to north. Bell faces direction south.
3	Bell with a restraint center 33.5 in. into test basin.	South to north. Bell faces direction south.
4	Bell 33 in. into test basin in soil.	South to north. Bell faces direction north.
5	Straight pipe with clamp 7 in. north of the southern bulkhead.	South to north.

Table 2.1.3. Forces at Selected Displacements for Axial Push Tests

Displacement (in.)	Force (kips)					
	PT1	PT2	PT2a	PT3	PT4	PT5
0.000	0	0	0	0	0	0
0.025	3.0	3.4	3.3	3.8	3.4	4.5
0.050	3.0	3.5	3.3	4.7	3.5	4.9
0.100	3.5	4.0	3.6	5.0	3.5	5.7
0.25	3.8	4.2	3.4	5.2	3.9	6.3
0.50	3.8	4.0	3.4	5.5	4.0	6.8
1.00	3.7	4.7	3.8	6.3	4.2	7.4
2.50	3.1	6.1	4.3	7.2	5.1	9.6
5.00	3.1	5.4	5.1	8.8	4.9	11.3

1 in. = 25.4 mm 1 kip = 4.448 kN

2.2 Pipe Centered Test with InsituformMain® System Liner

This section presents the results of a large-scale tension test on lined ductile iron (DI) pipe connected with bell-spigot joints performed at the Cornell large-scale test basin in June 2012. The pipe material was ductile iron (DI) pipe specimen with 6 in. (150 mm) nominal diameter, as described previously. The liner material was InsituformMain® System, referred to as IMain in this report. The InsituMain® System is an internal, cured-in-place pipe (CIPP) composite material made up of polyester fiber, fiberglass and a specially formulated epoxy resin system. A thin polyethylene layer also is adhered to the on the inside surface increases the liner to reduces friction and provide an additional corrosion barrier. More information about the IMain liner can be found at http://www.insituform.com/CompanyInformation/~/~/media/Corporate/Files/Insituform/InsituMain%20Brochure.ashx. Figure 2.2.1 is a schematic of the lining system. Three sections of DI pipe were lined at the Insituform factory in Missouri, using their standard liner installation procedure. The total pipe specimen was 30 ft long, consisting of a 9 ft (2.74 m) pipe, a central 12 ft (3.66 m) section, and another 9 ft (2.74 m) section. The pipe was attached to a steel strongback and shipped to Cornell. The strongback was necessary so the pipe did not rotate and the joints were not disturbed during shipping.

2.2.1 Test Configuration and Procedure

Figure 2.2.2 is a plan view of the test layout. The length of the “test” portion of the pipe was 30 ft (9.15 m). The “test” section did not extend the full length of the split test basin. This 30 ft (9.15 m) length was necessary because of pipe handling considerations for the specially lined pipe. Figure 2.2.3 shows the test pipe being placed in the test basin. At this point the pipe is still secured to the strongback to avoid joint movements. The test section was joined to other pieces of DI pipe using special clamps (“Capacity Testing of UB Clamps,” Cornell University NEESR Research Group, Dec., 2012.). The overall test specimen then exited the test basin at the north and south ends. Additional clamps were installed so that tension could be imposed by moving the north, movable section of the test basin along the 50º fault in the test basin using four large-stroke hydraulic actuators. The central portion of the test basin was filled with compacted sand so that the pipe had 30 in. (0.76 m) of soil cover above the pipe crown.

The pipe was pressurized with water to approximately 75 psi (517 kPa). Figure 2.2.4 shows the end cap and pressurization system used. The north (movable) portion of the test basin is connected to four MTS hydraulic actuators with load cells controlled by a MTS Flextest GT controller. All of the actuators are operated in synchronized displacement control. The general test procedure, after all soil placement and instrumentation was installed was:

a) Synchronize the data acquisition systems,
b) Verify pipe internal pressure,
d) Move the test basin 0.1 in. (6.35 mm) at a rate of 12 in./minute (304.8 mm/minute),
e) Verify data collection,
f) Repressurize as necessary,
g) Repeat steps b – f until leakage occurred or the liner failed.

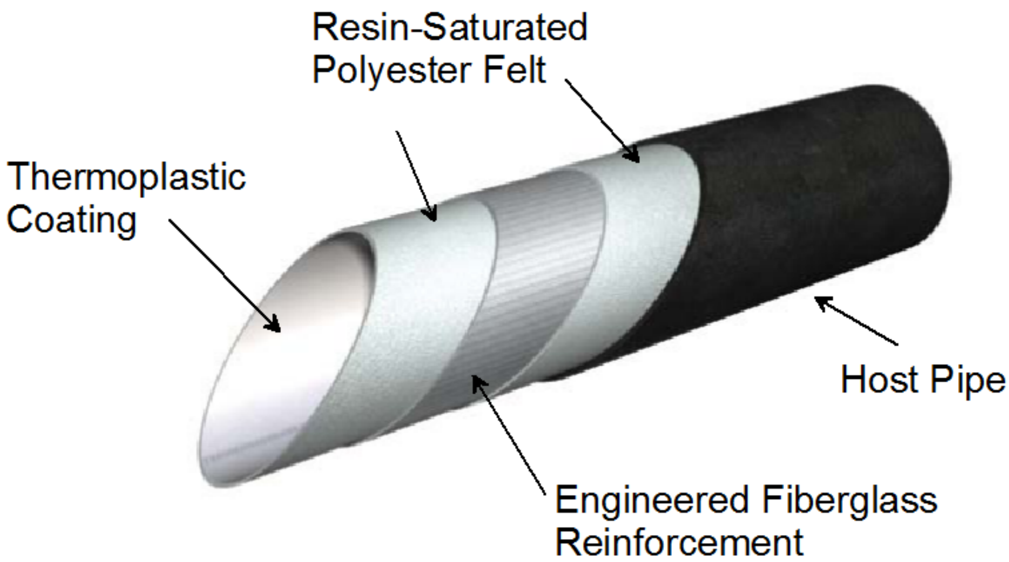

Figure 2.2.1. Schematic of InsituMain® System (courtesy of Insituform Technologies)

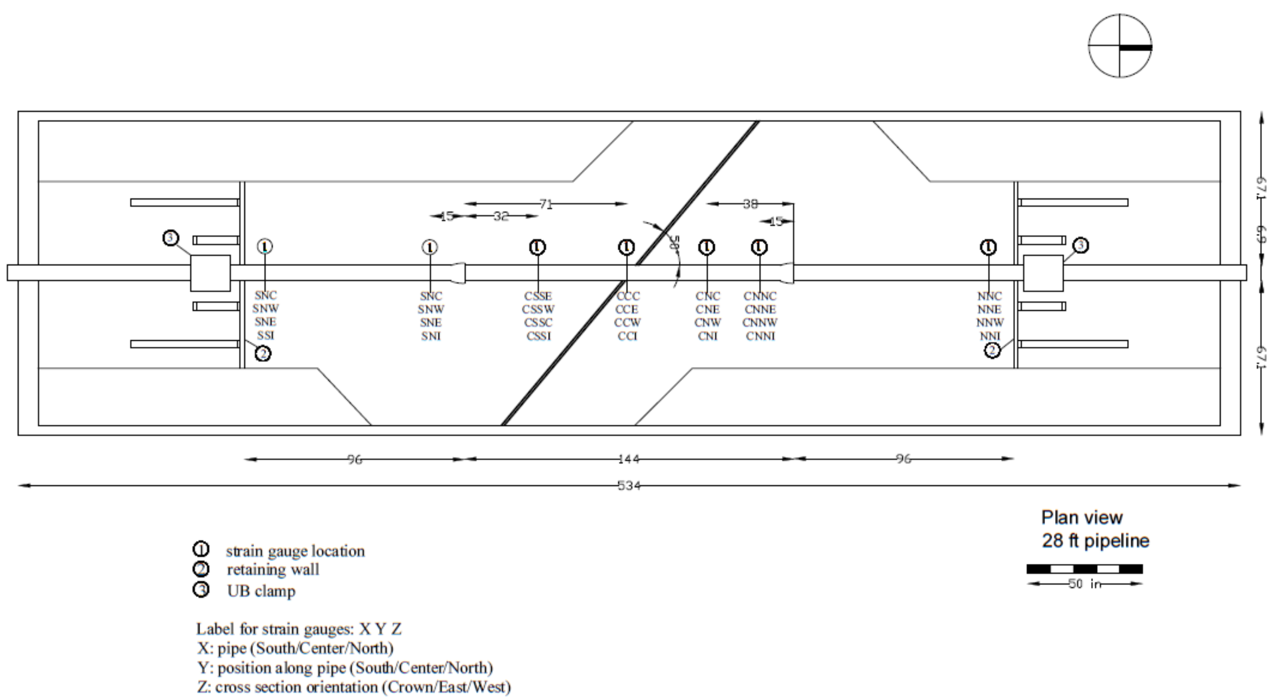

Figure 2.2.2. Plan View of IMain Lined Pipe Centered Ductile Iron Pipe in Test Basin

Figure 2.2.3. Positioning the Pipe Centered Specimen in the Test Basin

2.2.2. Soil Preparation and Compaction Data

The soil was prepared in the test basin using the same placement procedures described previously. Eight measurements of dry unit weight and moisture content were made for each soil lift. Four in the north portion of the test basin and four in the south portion. The average dry unit weight was γ_{dry} =105.9 lb/ft^3 (16.6 kN/m^3) with a standard deviation of 1.8 lb/ft^3 (0.28 kN/m^3). The average moisture content as w = 4.3% with a standard deviation of 1.3%.

2.2.3 Instrumentation

Twenty eight strain gages were installed at various locations along the pipe at the crown, invert, and springlines. Figure 2.22 also shows the strain gage locations and coding. Table 2.2.1 further provides locations and coding for the seven gage planes. DCDTs were positioned at the north and south joint at the crown and springlines. The purpose of the DCDTs was to measure both joint opening and joint rotation. Figure 2.2.5 shows the DCDTs positioned around the south joint. A similar configuration was used at the north joint. Protective covers of thin shim stock were placed around the DCDT system to protect them during the test. Four load cells were placed at each end of the test basin. These were mounted at the pipe springline elevations between the tension restraint on the pipe and the outside test basin structural steel frame and also in the inside of the test basin. These load cells were intended to measure the force in the pipe as the test basin was displaced along the 50º fault in the test basin. The inside load cells were intended to measure pipe load during pressurization. Table 2.2.2 lists the additional instrumentation used.

Table 2.2.1. Gage Locations and Coding System for IMain Pipe Centered Test

Gage Plane	Gages	Distance from Pipe Center
NN	NNE – East Springline NNC – Crown NNW – West Springline NNI – Invert	156 in. north of fault
CNN	CNNE – East Springline CNNC – Crown CNNW – West Springline CNNI – Invert	58 in. north of fault
CN	CNE – East Springline CNC – Crown CNW – West Springline CNI – Invert	35 in. north of fault
CC	CCE – East Springline CCC – Crown CCW – West Springline CCI – Invert	On fault (0 in.)
CSS	CSSE – East Springline CSSC – Crown CSSW – West Springline CSSI – Invert	36 in. south of fault
SN	SNE – East Springline SNC – Crown SNW – West Springline SNI – Invert	83 in. south of fault
SS	SSE – East Springline SSC – Crown SSW – West Springline SSI – Invert	204 in. south of fault

Table 2.2.2. Additional Instrumentation for IMain Lined, Pipe Centered Test

Instrument	Local Name	Location / Description
Load Cell	NW outside	North End Load, West, Outside Basin
Load Cell	NE outside	North End Load, East, Outside Basin
Load Cell	NW inside	North End Load, West, Inside Basin
Load Cell	NE inside	North End Load, East, Inside Basin
Load Cell	SW outside	South End Load, West,, Outside Basin
Load Cell	SE outside	South End Load, East, Outside Basin
Load Cell	SW inside	South End Load, East, Inside Basin
Load Cell	SE inside	South End, Inside Basin
Displacement	BNE	North Joint, East Springline
Displacement	BNC	North Joint, Crown
Displacement	BNW	North Joint, West Springline
Displacement	BSE	South Joint, East Springline
Displacement	BSC	South Joint, Crown
Displacement	BSW	South Joint, West Springline
Pressure Transducer	PX180B-100GV	North End, Internal Pressure

Figure 2.2.4. Photograph of UB Clamp and Pressurization System, North End

Figure 2.2.5. Photograph of DCDTs for Joint Displacements

2.2.4. Test Results

Test Basin Movements

Four actuators are connected between the movable portion of the test basin and the modular reaction wall in the laboratory. From south to north, the actuators are called short-stroke actuator 1 (SSA1), short-stroke actuator 2 (SSA2), long-stroke actuator 1 (LSA1), and long-stroke actuator 2. (LSA2). Each SSA actuator has a displacement range of ± 2 ft (0.61 m) [4 ft (1.22 m) total stroke] and load capacity of 100 kips (445 kN) tension and 145 kips (649 kN) compression. Each LSA actuator has a displacement range of ± 3 ft (0.91 m) [6 ft (1.83 m) total stroke] and load capacity of 63 kips (295 kN) tension and 110 kips (498 kN) compression.

Figure 2.2.6 shows the displacement of long-stroke actuator 2 (LSA2) versus time. All actuators are synchronized to move at exactly the same rate and displacement, so only LSA2 is shown. Since the actuators move the same, the forces in each actuator required to move the test basin at the 50º angle varied as the basin was displaced.

Figure 2.2.7 shows the forces in each actuator as the test basin was moved. SSA1 (closest to the fault) showed the maximum compression. The compressive forces to move the basin decreased with distance from the fault, and LSA2 (furthest from the fault) applied a tension (pull) force to maintain synchronous parallel movement.

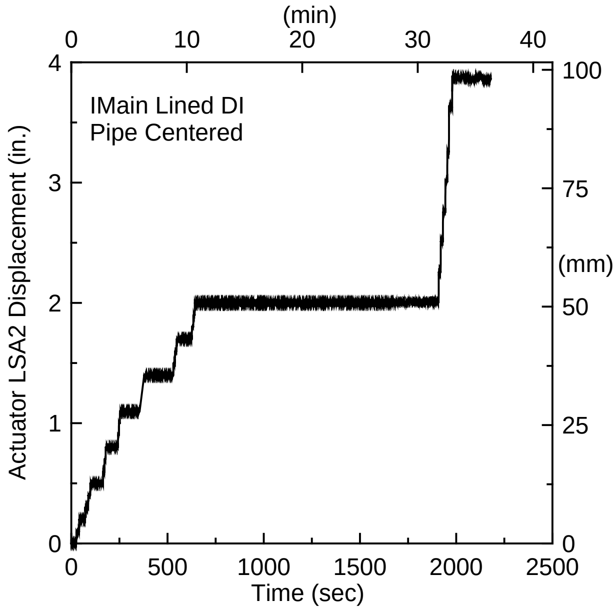

Figure 2.2.6 Actuator Displacements vs. Time

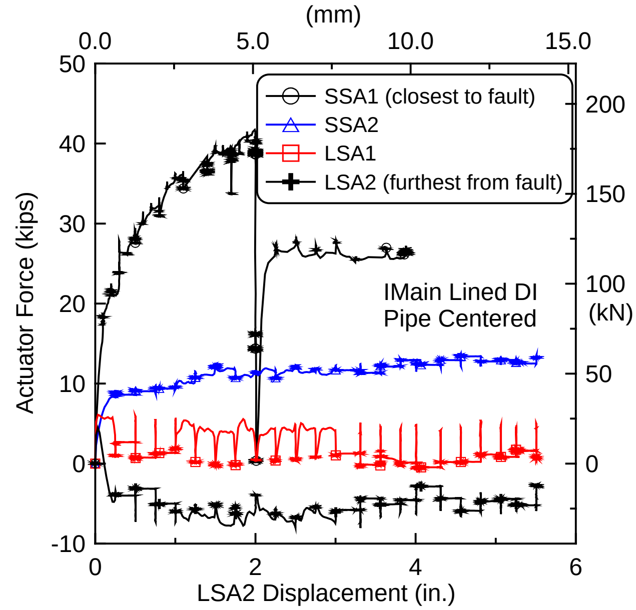

Figure 2.2.7. Actuator Forces vs. Displacement

Pipe Internal Pressure

The pipe was initially pressurized to 75 psi (517 kPa) prior to any basin movement. Each movement of the basin caused the pipe to increase slightly in overall length, causing the pressure to drop slightly (a few psi). Figure 2.2.8 shows the pipe internal pressure for each of the load steps. The pipe was repressurized to the target value and the next load step applied. In Figure 2.2.8 the upper axis is actuator movement times cosine 50º. This is the longitudinal movement of the north end of the test basin, since the actuators are parallel to the 50º fault. Figure 2.2.8 shows that at a total actuator displacement of roughly 2 in. (50 mm) there was a loss of pressure in the pipe, indicating a joint leak or liner breakage. The test was paused, the pipe repressurized and displacement continued until full pressure loss again at a displacement of roughly 4 in. (100 mm). At this point the test was stopped and the water drained from the pipe.

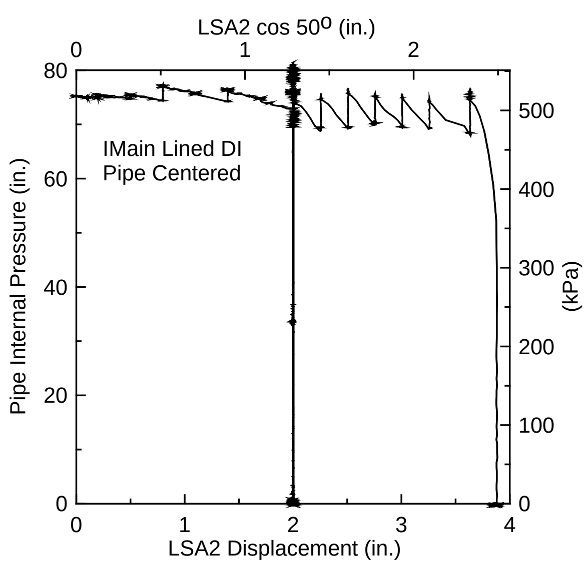

Figure 2.2.8. Pipe Internal Pressure vs. Test Basin Movement for IMain PC Test

Strain Gage Measurements

Figure 2.2.9 shows the pipe strains on the crown (NNC), east springline (NNE), and west springline (NNW), and invert (NNI) measured at the NN gage plane. This station was 24 in. (610 mm) from north the bell end of the northern most joint. Overall the NN gage plane was 156 in. (396 cm) north of the fault. The gages all showed similar strains until the liner ruptured at roughly 2 in. (50 mm) displacement. There was essentially no bending at this gage plane.

Figure 2.2.10 shows the pipe strains on the east springline (CNNE), crown (CNNC), west springline (CNNW), and invert (CNNI) measured at the CNN gage plane. This station was 15 in. (381 mm) from the south of the bell in the northern most joint. Overall the CNN gage plane was 58 in. (147.3 cm) north of the fault. These gages are on the central pipe section. Strains at the west and crown track each other, as do the strains at the east springline and invert. After the liner broke, the east and west springlines show about the same bending strain. Following liner breakage, the incremental strains at the crown and invert are near zero. This implies all of the strains are due to bending.

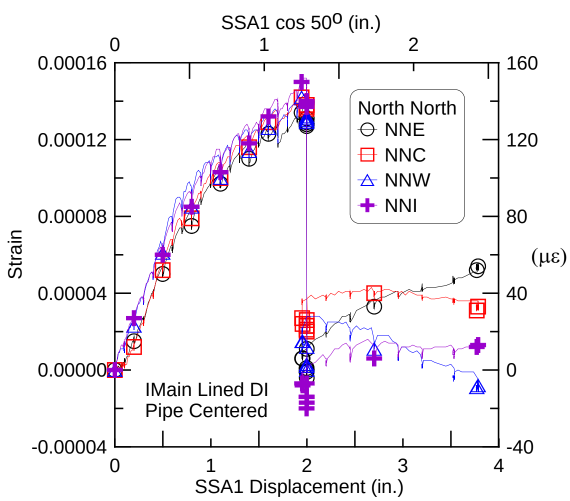

Figure 2.2.9. Strains at Gage Plane NN

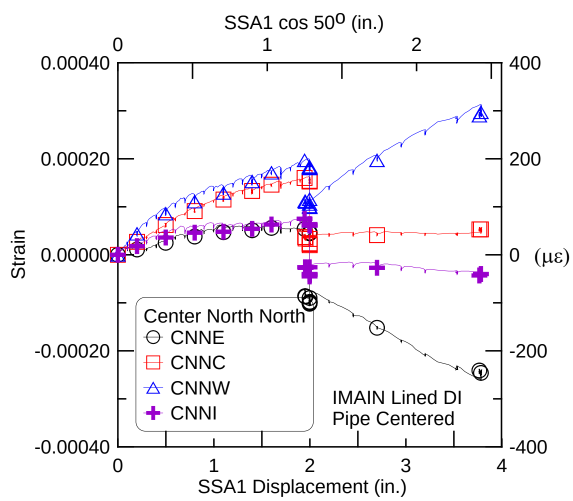

Figure 2.2.10. Strains at Gage Plane CNN

Figure 2.2.11 shows the pipe strains on the crown (CNC), invert (CNI), east springline (CNE), and west springline (CNW) measured at the CN gage plane. This station was 35 in. (88.9 cm) north of fault. These gages are on the central pipe section. Gages on the east springline showed very little strain until liner rupture. The gages indicate east-west bending following liner break.

Figure 2.2.12 shows the pipe strains on the crown (CCC), east springline (CCE), and west springline (CCW) measured at the CC gage plane. This station was on the fault at the center of the pipe segment. These gages are on the central pipe section. All the strains are similar until about 1 in. (25.4 mm) displacement. Following liner break, the gages again indicate east-west bending.

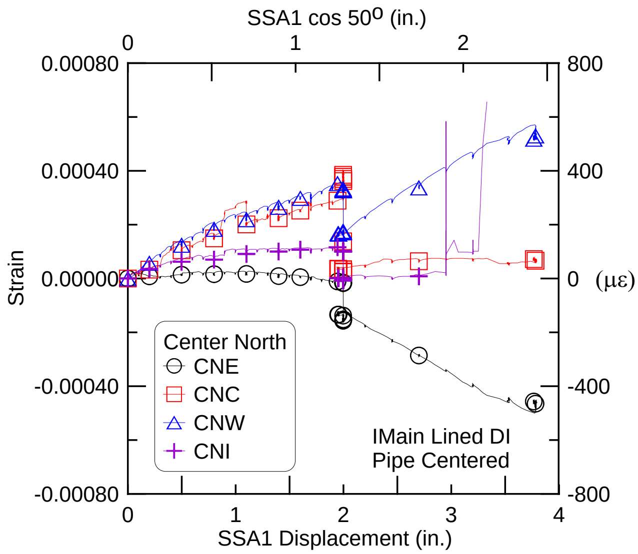

Figure 2.2.11. Strains at Gage Plane CN

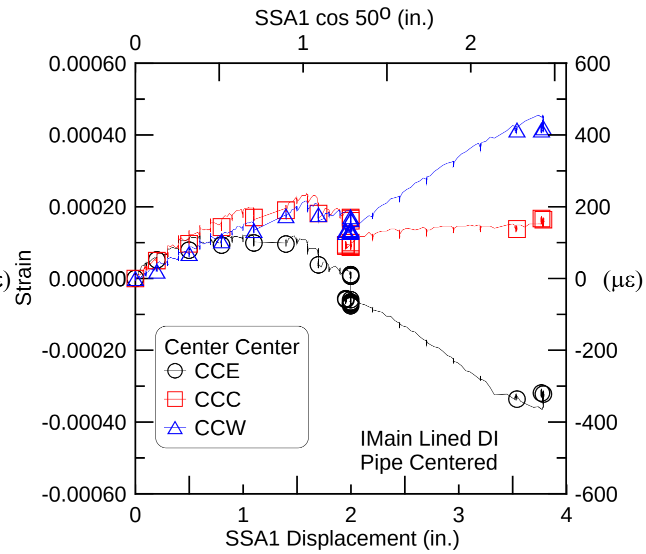

Figure 2.2.12. Strains at Gage Plane CC

Figure 2.2.13 shows the pipe strains on the crown (CSSC), east springline (CSSE), and west springline (CSSW), and invert measured at the CSS gage plane. This station was 36 in. (91.4 cm) south of the fault. These gages also are on the central pipe section. Axial strains at this gage plane were quite asymmetric.

Figure 2.2.14 shows the pipe strains on the crown (SNC), east springline (SNE), and west springline (SNW), and invert (SNI) measured at the SN gage plane. This gage plane was 15 in. (38.1 cm) south of the southern-most bell face and not on the central pipe section. Overall, this station was 83 in. (210.8 cm) south of fault. Strains at the all gage locations were similar until the liner broke. This indicates very little bending at this location.

Figure 2.2.15 shows the pipe strains on the crown (SSC), east springline (SSE), and west springline (SSW), and invert (SSI) measured at the SS gage plane. This gage plane was 204 in. (515.1 cm) south of fault. Strains at the crown, invert, and west springline gage locations were similar until the liner broke.

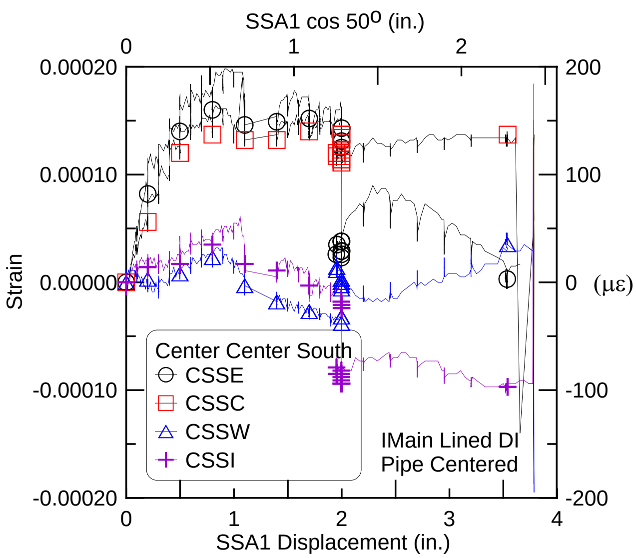

Figure 2.2.13. Strains at Gage Plane CSS

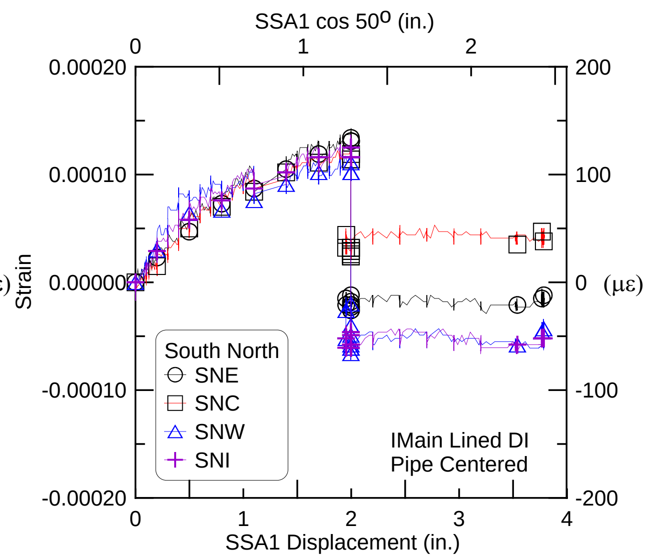

Figure 2.2.14. Strains at Gage Plane SN

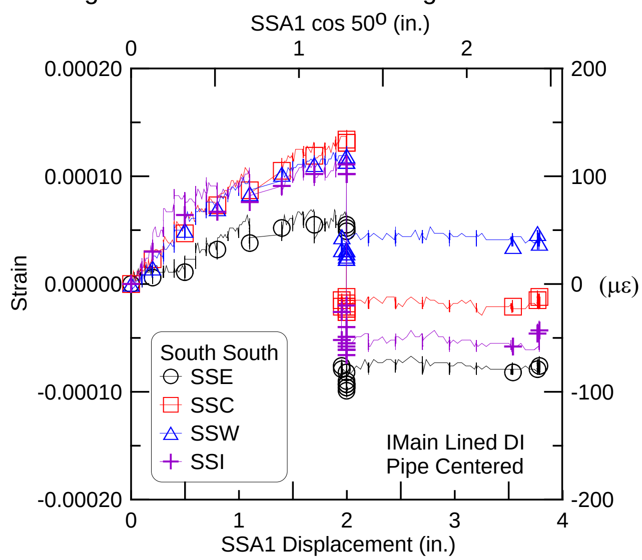

Figure 2.2.15. Strains at Gage Plane SS

Figures 2.2.16 and 2.2.17 show the strains at the east and west springline, respectively, versus distance for the center of the pipe, as actuator displacement increases. In this test the center of the pipe was at the fault. In the figures, the "crescent moon" symbol is at a joint location. The strains are not symmetric for east-west.

Figures 2.2.18 and 2.2.19 show the crown and invert strains along the pipeline for increasing actuator displacement. The east and west springline strains versus distance from the pipe center (fault). Here, the symmetry of the measured strains can be seen quite clearly.

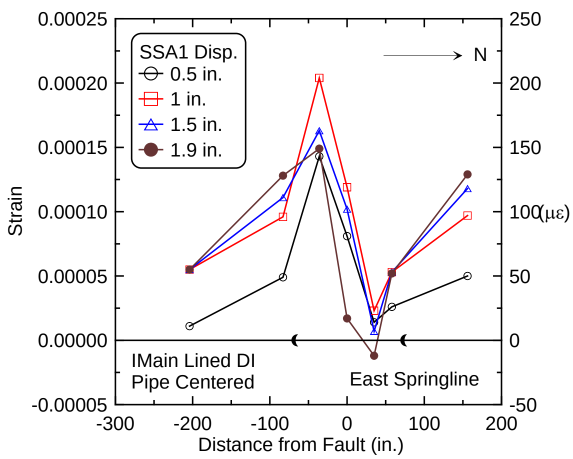

Figure 2.2.16. Strains at East Springline vs. Distance from Pipe Center

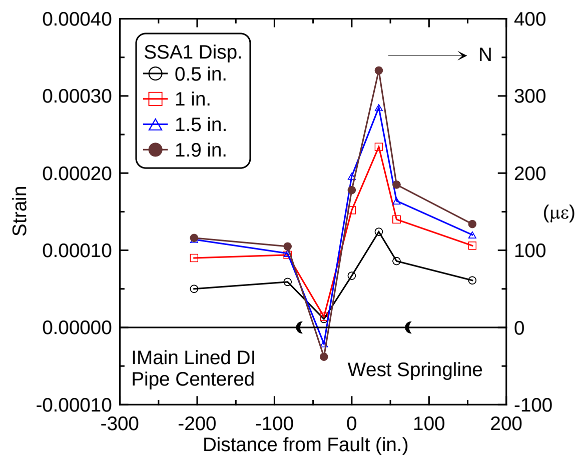

Figure 2.2.17 Strains at West Springline vs. Distance from Pipe Center

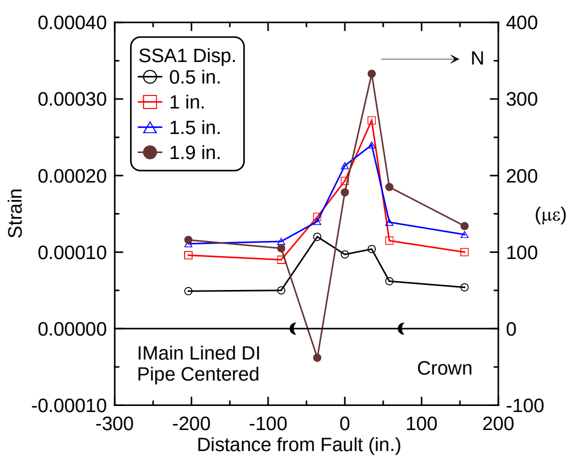

Figure 2.2.18. Strains at Crown vs. Distance from Pipe Center

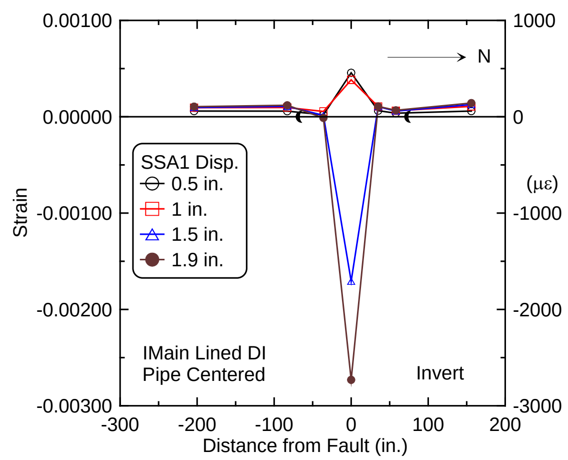

Figure 2.2.19. Strains at Invert vs. Distance from Pipe Center

<u>Joint Displacements</u>

Three DCDTs were placed at each of the two bell and spigot joints in the portion of the pipe that was buried in soil. Figures 2.2.20 and 2.2.21 show the displacements measured at the east and west springlines and crown of the pipe at the north and south joints, respectively. Displacements at the north joint are an order of magnitude smaller than those at the south joint. Prior to liner rupture the maximum joint opening of the north joint was roughly 0.1 in (2.5 mm) on the west springline. At the south joint, the displacements at the three locations were similar until the liner broke. At liner break the joint opening was just slightly less than 0.6 in. (15.2 mm) of actuator movement. This corresponds to an axial displacement of 0.39 in. (9.8 mm).

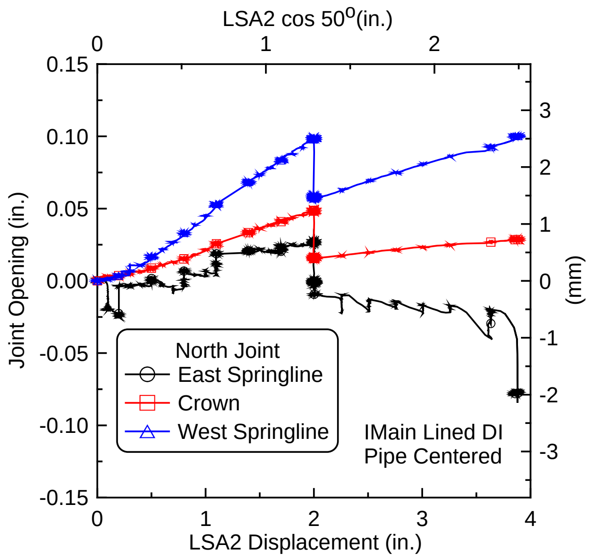

Figure 2.2.20. Displacements at North Joint

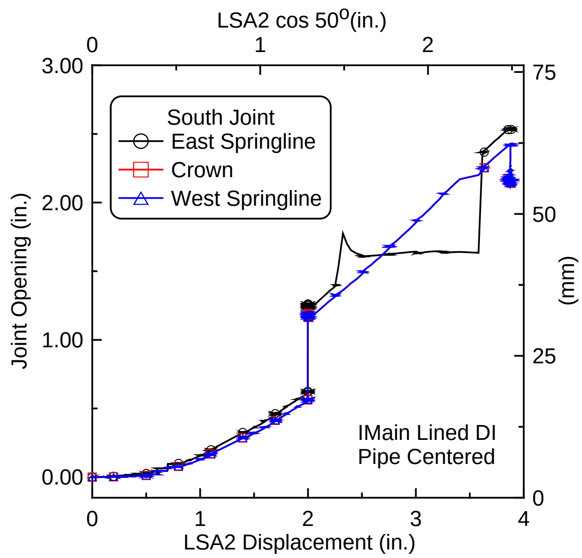

Figure 2.2.21. Displacements at South Joint

End Forces

Load cells were placed at the springline elevations of the test pipe, on the inside of the test basin and outside the test basin, to measure the end forces when the basin was displaced. Figures 2.2.22 through 2.2.23 show the end forces at the north end and south end of the test basin. Once the liner broke, the end forces reduced to zero.

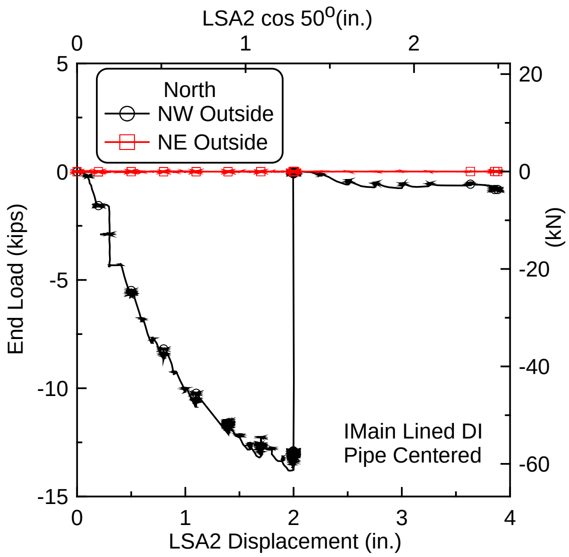

Figure 2.2.22. End Forces, North End, Outside Test Basin

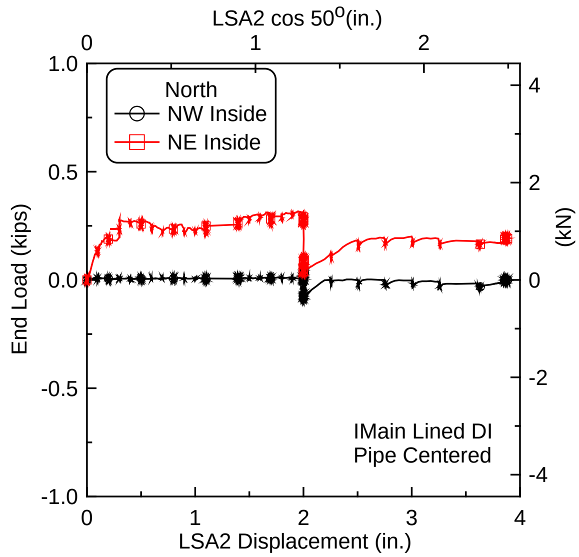

Figure 2.2.23. End Forces, North End, Inside Test Basin

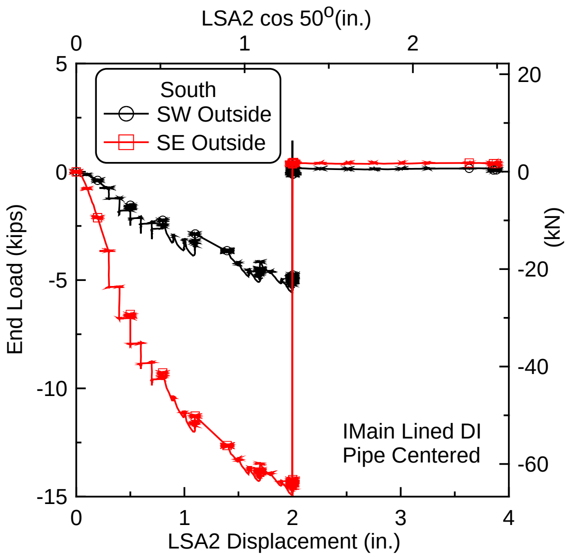

Figure 2.2.24. End Forces, South End, Outside Test Basin

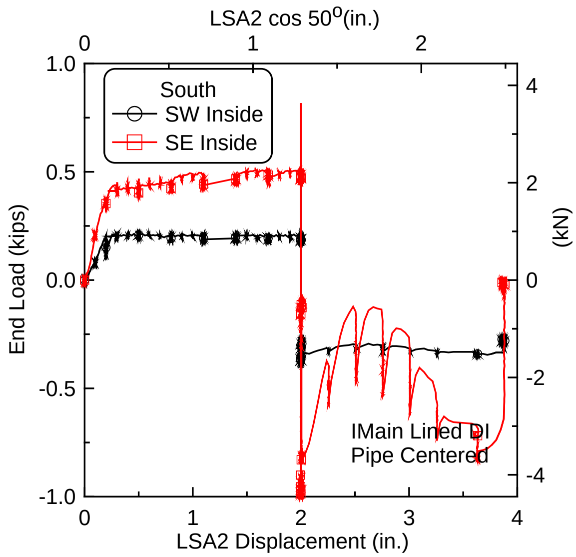

Figure 2.2.25. End Forces, South End, Inside Test Basin

2.2.5. Summary of IMain Pipe Centered Test

This section presents the measurements made during a large-scale “pipe centered” test of ductile iron pipe that was lined with the InsituformMain® System, referred to as IMain in this report. The test was performed in the large test basin in the Bovay Laboratory at Cornell University. The testing configuration and procedures are described. The central portion of the pipe was centered on the fault. The instrumentation is reported, along with the soil placement procedures. Data are given for the test basin movements, pipe internal pressures, strain gage measurement, joint displacements, and end forces. The liner failed at a axial joint opening of roughly 0.39 in. (9.8 mm). Figure 2.2.26 is a photograph of the ruptured joint taken after the pipe was excavated.

Figure 2.2.26. Photo of Separated Joint and Ruptured Liner at South Joint for Pipe Centered Test

2.3 Joint Centered Test with InsituformMain® System Liner

This section presents the results of a large-scale "joint centered" tension test on lined ductile iron (DI) pipe connected with bell-spigot joints performed at the Cornell large-scale test basin in June 2012. The liner material was InsituformMain® System. The pipe material was ductile iron (DI) pipe specimen with 6 in. (150 mm) nominal diameter. The liner and DI are the same as described previously

2.3.1 Test Configuration and Procedure

Figure 2.3.1 is a plan view of the test layout. The length of the "test" portion of the pipe was 30 ft (9.15 m). The "test" section did not extend the full length of the split test basin. This 30 ft (9.15 m) length was necessary because of pipe handling considerations for the specially lined pipe. Figure 2.3.2 shows the test pipe partially installed in the test basin. The test section was joined to other pieces of DI pipe using special clamps ("Capacity Testing of UB Clamps," Cornell University NEESR Group, Dec., 2012.). The overall test specimen then exited the test basin at the north and south ends. Additional clamps were installed so that tension could be imposed by moving the north, movable section of the test basin along the 50º fault in the test basin using four large-stroke hydraulic actuators. The central portion of the test basin was filled with compacted sand so that the pipe had 30 in. (0.76 m) of soil cover above the pipe crown.

The pipe was pressurized with water to approximately 75 psi (517 kPa). Figure 2.3.3 shows the end cap and pressurization system used. The north (movable) portion of the test basin is connected to four MTS hydraulic actuators with load cells controlled by a MTS Flextest GT controller. All of the actuators are operated in synchronized displacement control. The general test procedure, after all soil placement and instrumentation was installed was:

a) Synchronize the data acquisition systems,
b) Verify pipe internal pressure,
d) Move the test basin 0.1 in. (2.5 mm) at a rate of 12 in./minute (304.8 mm/minute),
e) Verify data collection,
f) Repressurize as necessary,
g) Repeat steps b – f until leakage occurred or the liner failed.

2.3.2. Soil Preparation

The soil was prepared in the test basin using the same placement procedures described previously. Eight measurements of dry unit weight and moisture content were made for each soil lift. Four in the north portion of the test basin and four in the south portion. The average dry unit weight was γ_{dry}= 106.7 lb/ft^3 (16.8 kN/m^3) with a standard deviation of 1.3 lb/ft^3 (0.20 kN/m^3). The average moisture content as w = 3.1% with a standard deviation of 0.5%.

2.3.3. Instrumentation

Thirty two strain gages were installed at various locations along the pipe at the crown, invert, and springlines. Figure 2.3.1 also shows the strain gage locations and coding. Table 2.3.2 further provides locations and coding for the eight gage planes. DCDTs were positioned at the north and south joint at the crown and springlines. The purpose of the DCDTs was to measure both joint opening and joint rotation. Figure 2.3.4 shows the DCDTs positioned around the north joint. A similar configuration was used at the south joint. Protective covers of thin shim stock were placed around the DCDT system to protect them during the test. Four load cells were placed at each end of the test basin. These were mounted at the outside the test basin just above and below the pipe springline elevations, on the east and west sides. These load cells were intended to measure the force in the pipe as the test basin was displaced along the 50º fault in the test basin. Table 2.3.3 lists the additional instrumentation used.

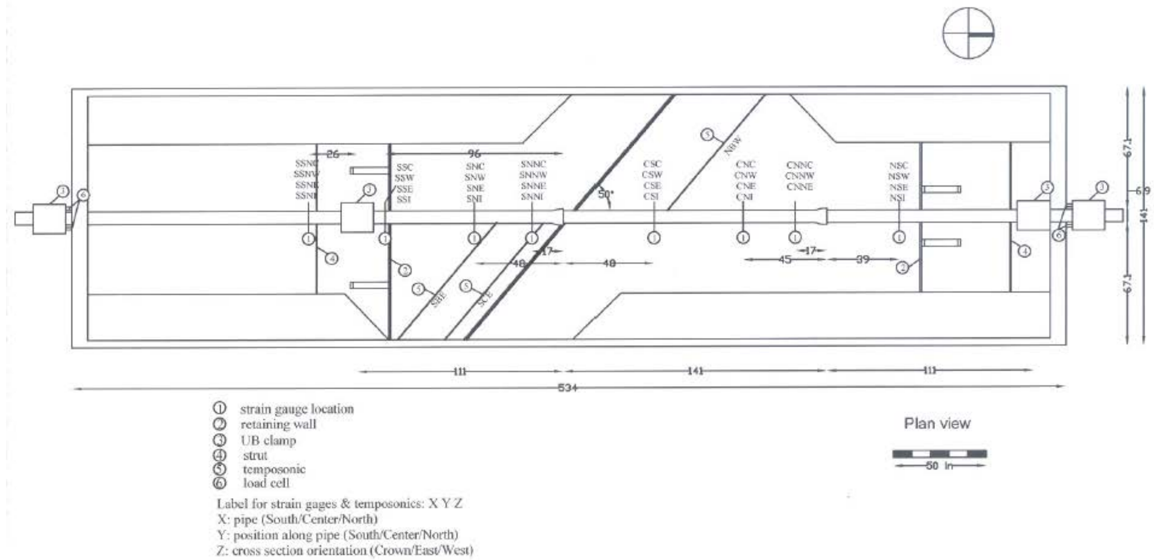

Figure 2.3.1. Plan View of IMain Lined Ductile Iron, Joint Centered Pipe in Test Basin

Figure 2.3.2. Positioning the Joint Centered Pipe in the Test Basin

Table 2.3.1 Gage Locations and Coding System for IMain Lined, Joint Centered Test

Gage Plane	Gages	Distance from Pipe Center
NS	NSE – East Springline NSC – Crown NSW – West Springline NSI – Invert	180 in. (457 cm) north of fault
CNN	CNNE – East Springline CNNC – Crown CNNW – West Springline	124 in. (315 cm) north of fault
CN	CNE – East Springline CNC – Crown CNW – West Springline CNI – Invert	96 in. (244 cm) north of fault
CS	CSE – East Springline CSC – Crown CSW – West Springline CSSI – Invert	48 in. (122 cm) north of fault
SNN	SNNE – East Springline SNNC – Crown SNNW – West Springline SNNI – Invert	17 in. (43 cm) south of fault
SN	SNE – East Springline SNC – Crown SNW – West Springline SNI – Invert	48 in. (122 cm) south of fault
SS	SSE – East Springline SSC – Crown SSW – West Springline SSI – Invert	96 in. (239 cm) south of fault
SSN	SSNE – East Springline SSNC – Crown SSNW – West Springline SSNI – Invert	140 in. (356 cm) south of fault

Table 2.3.2. Additional Instrumentation for IMain Lined, Joint Centered Test

Instrument	Local Name	Location / Description
Load Cell	NW outside top	North End Load, West, Outside Basin
Load Cell	NW outside bottom	North End Load, East, Outside Basin
Load Cell	NE outside top	North End Load, West, Inside Basin
Load Cell	NE outside bottom	North End Load, East, Inside Basin
Load Cell	SW outside top	South End Load, West,, Outside Basin
Load Cell	SW outside bottom	South End Load, East, Outside Basin
Load Cell	SE outside top	South End Load, East, Inside Basin
Load Cell	SE outside bottom	South End, Inside Basin
Displacement	BNE	North Joint, East Springline
Displacement	BNC	North Joint, Crown
Displacement	BNW	North Joint, West Springline
Displacement	BSE	South Joint, East Springline
Displacement	BSC	South Joint, Crown
Displacement	BSW	South Joint, West Springline
Pressure Transducer	PX180B-100GV	North End, Internal Pressure

Figure 2.3.3. Photograph of UB Clamp and Pressurization System, North End

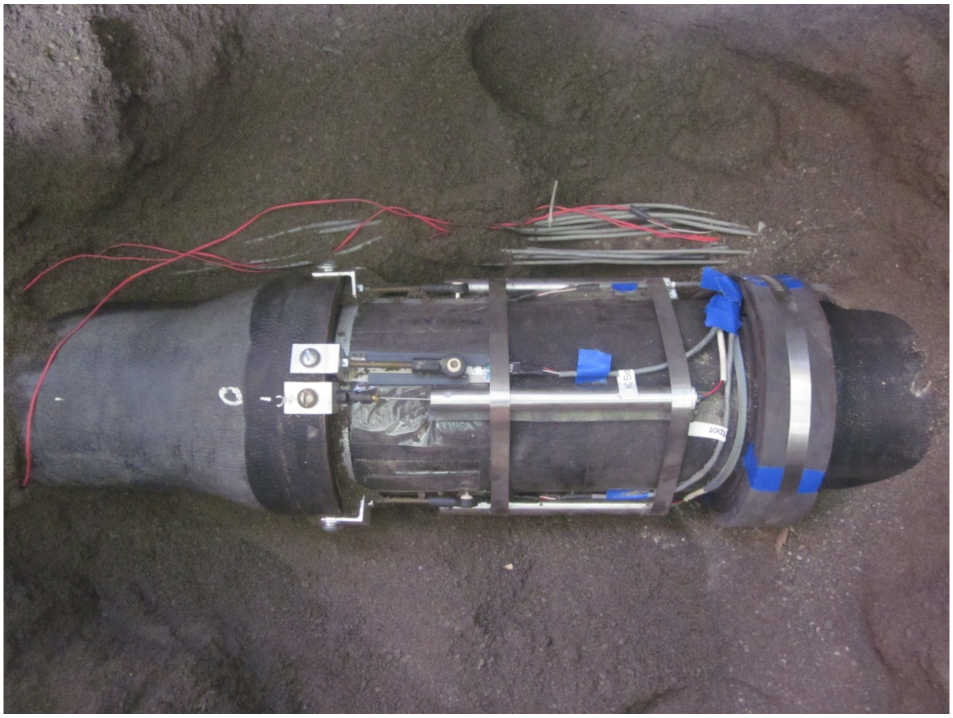

Figure 2.3.4. Photograph of DCDTs for Joint Displacements

2.3.4. Test Results

<u>Test Basin Movements</u>

Four actuators are connected between the movable portion of the test basin and the modular reaction wall in the laboratory. From south to north, the actuators are called short-stroke actuator 1 (SSA1), short-stroke actuator 2 (SSA2), long-stroke actuator 1 (LSA1), and long-stroke actuator 2. (LSA2). Each SSA actuator has a displacement range of ± 2 ft (0.61 m) [4 ft (1.22 m) total stroke] and load capacity of 100 kips (445 kN) tension and 145 kips (649 kN) compression. Each LSA actuator has a displacement range of ± 3 ft (0.91 m) [6 ft (1.83 m) total stroke] and load capacity of 63 kips (295 kN) tension and 110 kips (498 kN) compression. Figure 2.3.5 shows the displacement of long-stroke actuator 2 (LSA2) versus time. All actuators are synchronized to move at exactly the same rate and displacement, so only LSA2 is shown. Since the actuators move the same, the forces in each actuator required to move the test basin at the 50º angle varied as the basin was displaced.

Figure 2.3.6 shows the forces in each actuator as the test basin was moved. SSA1 (closest to the fault) showed the maximum compression. The compressive forces to move the basin decreased with distance from the fault, and LSA2 (furthest from the fault) applied a tension (pull) force to maintain synchronous parallel movement.

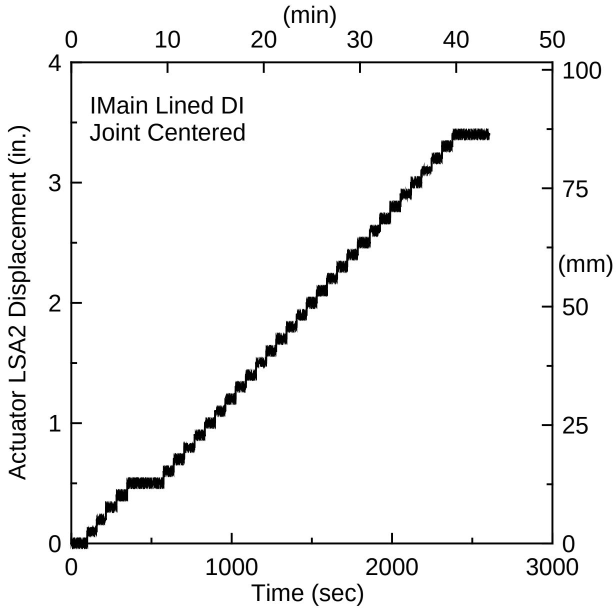

Figure 2.3.5 Actuator Displacements vs. Time

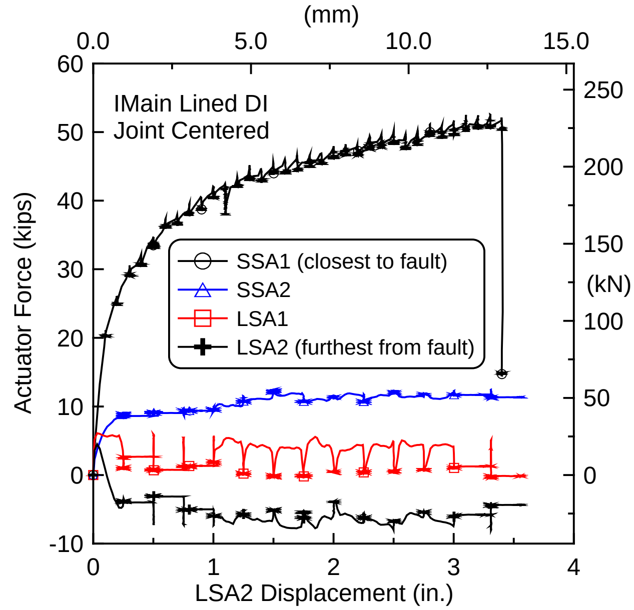

Figure 2.3.6. Actuator Forces vs. Displacement

Pipe Internal Pressure

The pipe was initially pressurized to 75 psi (517 kPa) prior to any basin movement. Each movement of the basin caused the pipe to increase slightly in overall length, causing the pressure to drop slightly (a few psi). Figure 2.3.7 shows the pipe internal pressure for each of the load steps. The pipe was repressurized to the target value and the next load step applied. In Figure 5.2 the upper axis is actuator movement times cosine 50º. This is the longitudinal movement of the north end of the test basin, since the actuators are parallel to the 50º fault. Figure 2.3.7 shows that at a total actuator displacement of roughly 3.4 in. (86.4 mm) of actuator displacement [2.2 in. (55.5 mm) of pipe axial movement] there was a loss of pressure in the pipe, indicating liner breakage. At this point the test was stopped and the water drained from the pipe.

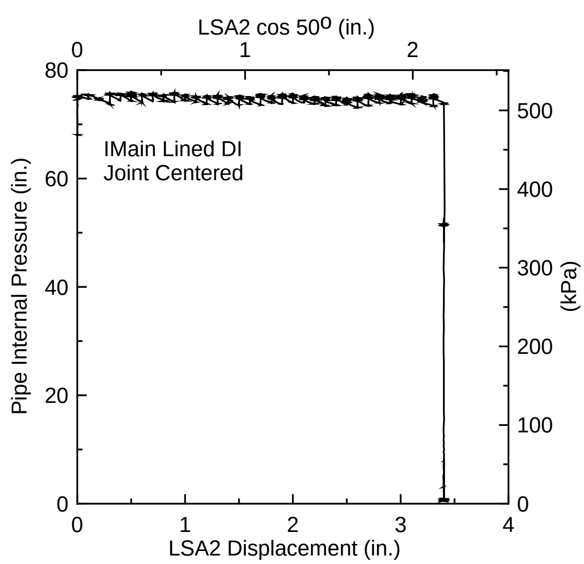

Figure 2.3.7. Pipe Internal Pressure vs. Test Basin Movement

Strain Gage Measurements

Figure 2.3.8 shows the pipe strains on the crown (NSC), east springline (NSE), and west springline (NSW), and invert (NSI) measured at the NS gage plane. This station was 39 in. (991 mm) from north the bell end of the northern most joint. Overall the NS gage plane was 180 in. (457 cm) north of the fault. The largest strains were on the east springline, followed by the crown and invert.

Figure 2.3.9 shows the pipe strains on the east springline (CNNE), crown (CNNC), west springline (CNNW) measured at the CNN gage plane. The invert gage (CNNI) did not function. This station was 17 in. (432 mm) from the south of the bell in the northern most joint. Overall the CNN gage plane was 124 in. (315 cm) north of the fault. Strains at the west and crown track each other reasonably closely up about 1 in. (25 mm) axial displacement. There was essentially east-west bending at this gage plane

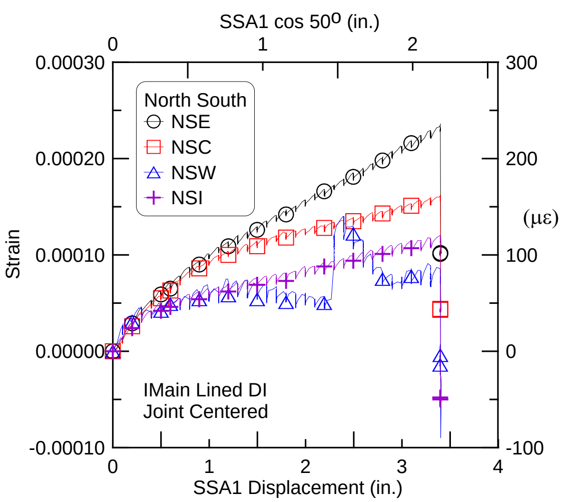

Figure 2.3.8. Strains at Gage Plane NS

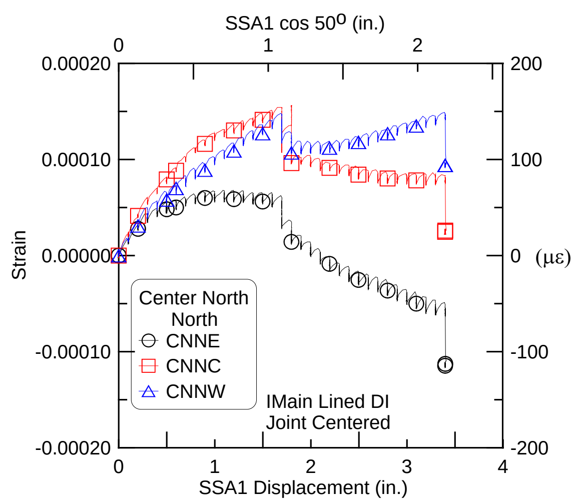

Figure 2.3.9. Strains at Gage Plane CNN

Figure 2.3.10 shows the pipe strains on the crown (CNC), invert (CNI), east springline (CNE), and west springline (CNW) measured at the CN gage plane. This station was 96 in. (244 cm) north of fault. The gages indicate east-west bending.

Figure 2.3.11 shows the pipe strains on the crown (CS), east springline (CSE), and west springline (CSW), and invert (CSI) measured at the CS gage plane. This station was 48 in. (122 cm) north of fault. The gages indicate east-west bending.

Figure 2.3.12 shows the pipe strains on the crown (SNNC), east springline (SNN), and west springline (SNNW), and invert (SNNI) measured at the SNN gage plane. This station was 17 in. (43 cm) south of the fault. The gages indicate substantial east-west bending. The crown and invert gages show similar amounts of axial strain.

Figure 2.3.13 shows the pipe strains on the crown (SNC), east springline (SNE), and west springline (SNW), and invert (SNI) measured at the SN gage plane. This gage plane was 48 in. (122 cm) south of fault. The gages indicate substantial east-west bending. The crown and invert gages show similar amounts of axial strain.

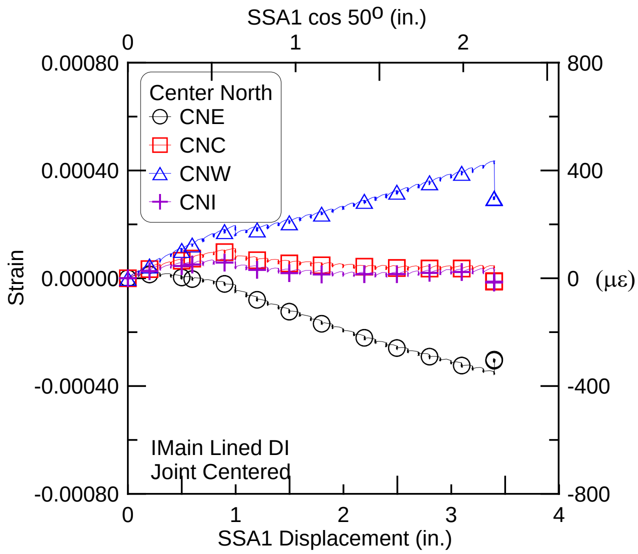

Figure 2.3.10. Strains at Gage Plane CN

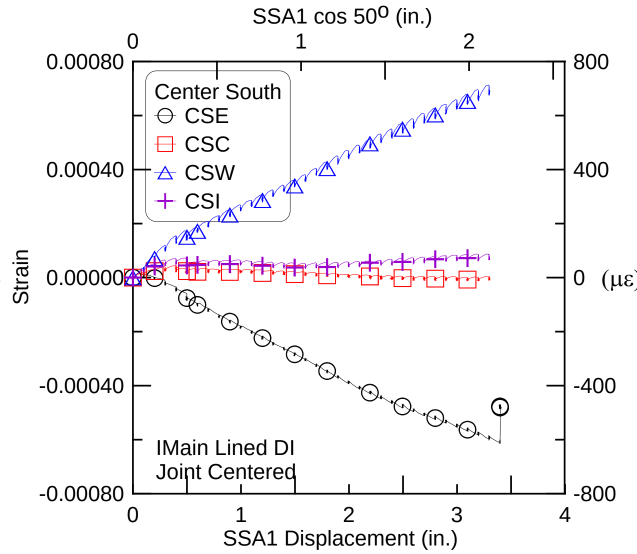

Figure 2.3.11. Strains at Gage Plane CS

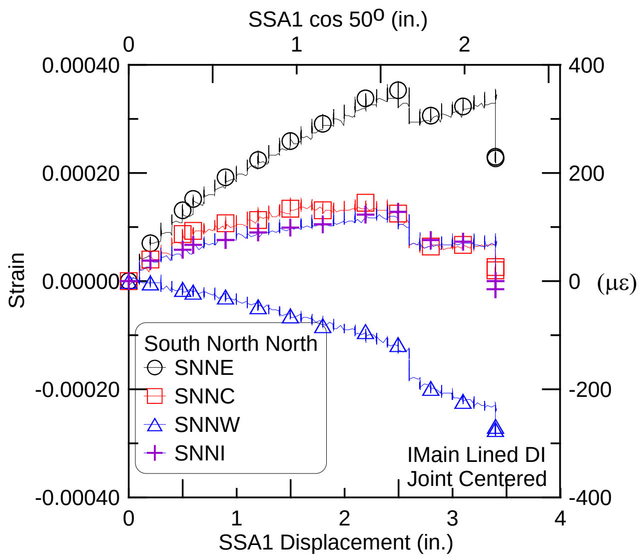

Figure 2.3.12. Strains at Gage Plane SNN

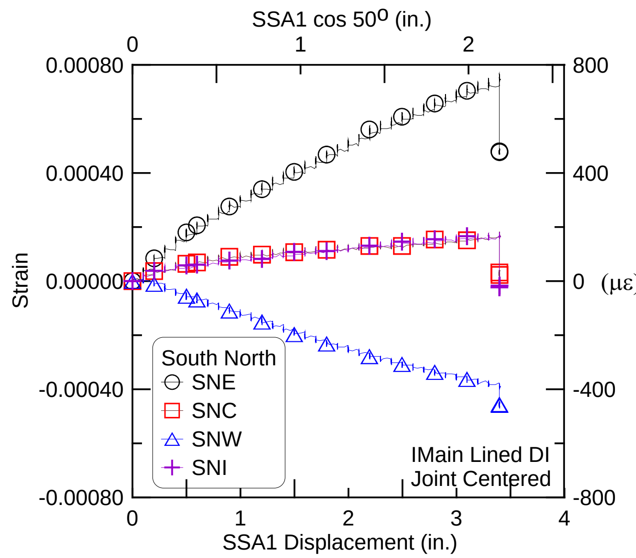

Figure 2.3.13 Strains at Gage Plane SN

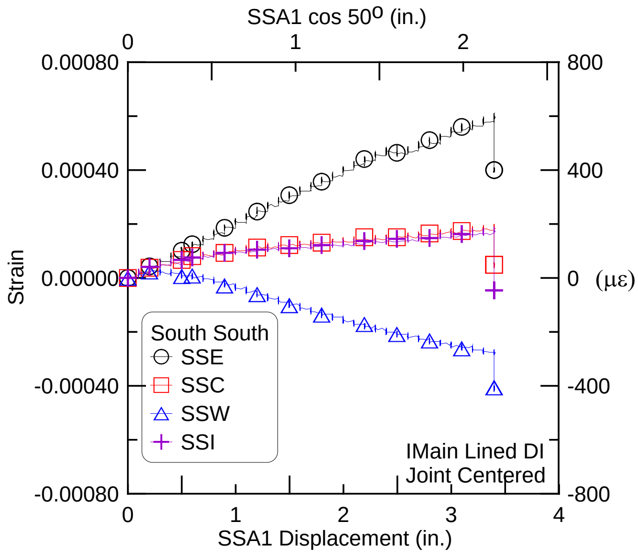

Figure 2.3.14. Strains at Gage Plane SS

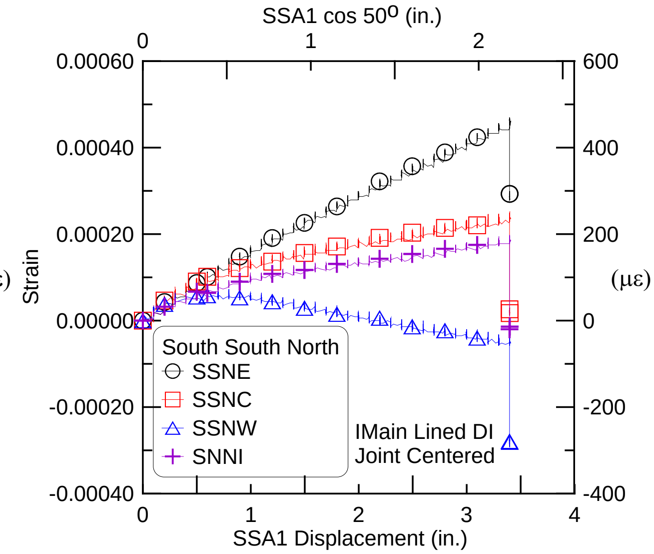

Figure 2.3.15. Strains at Gage Plane SSN

Figure 2.3.14 shows the pipe strains on the crown (SSC), east springline (SSE), west springline (SSW), and invert (SSI) measured at the SS gage plane. This gage plane was 96 in. (239 cm) south of fault and outside the soil backfill near the southern bulkhead. The gages indicate substantial east-west bending. The crown and invert gages show similar amounts of axial strain.

Figure 2.3.15 shows the pipe strains on the crown (SSNC), east springline (SSNE), west springline (SSNW), and invert (SSNI) measured at the SSN gage plane. This gage plane was 140 in. (356 cm) south of fault and outside the soil backfill. The gages indicate substantial east-west bending. The crown and invert gages show similar amounts of axial strain.

Figure 2.3.16 shows the strains at the east and west springlines versus distance for the central pipe joint, as actuator displacement increases. In this test the pipe joint was at the fault. In the figures, the "crescent moon" symbol is at a joint location. The strains are all tensile, and greatest at the more southern pipe sections.

Figure 2.3.17 shows the strains at the crown and invert distance for the central pipe joint, as actuator displacement increases. In this test the pipe joint was at the fault. In the figures, the "crescent moon" symbol is at a joint location. The strains are tensile, and greatest at the more southern pipe sections.

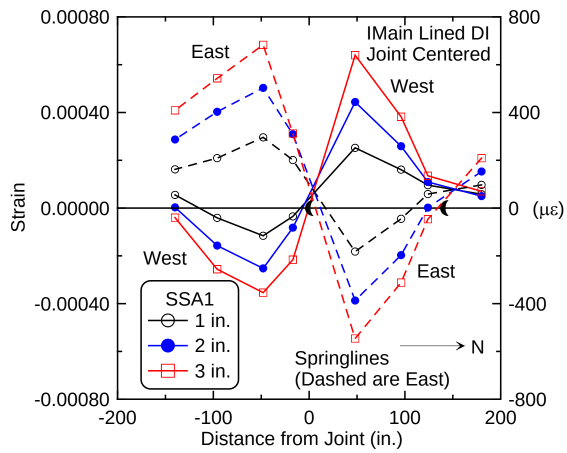

Figure 2.3.16. Strains at Springlines vs. Distance from Center Joint

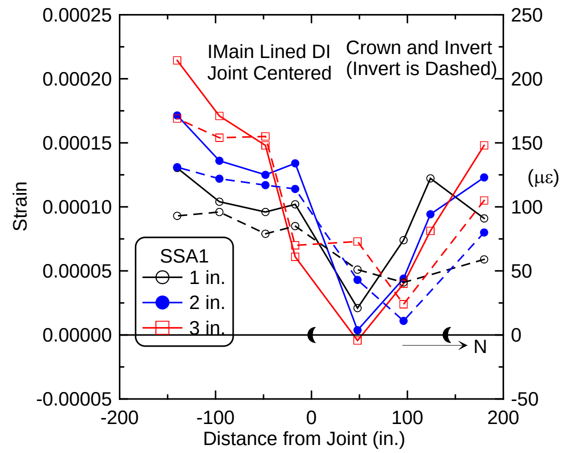

Figure 2.3.17. Strains at Crown and Invert vs. Distance from Center Joint

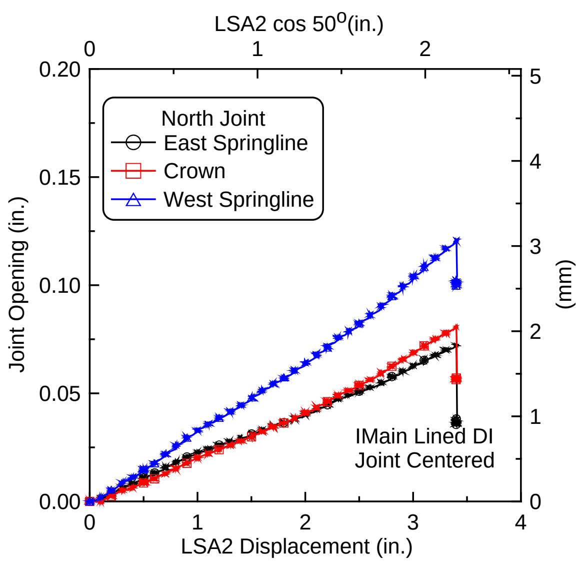

Figure 2.3.18. Displacements at North Joint

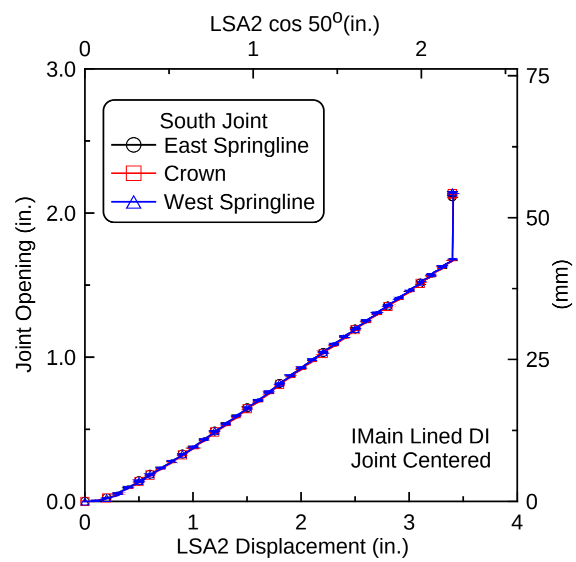

Figure 2.3.19. Displacements at South Joint

Joint Displacements

Three DCDTs were placed at each of the two bell and spigot joints in the portion of the pipe that was buried in soil. Figures 2.3.20 and 2.3.21 show the displacements measured at the east and west springlines and crown of the pipe at the north and south joints, respectively. Displacements at the north joint are an much smaller than those at the south joint. Prior to liner rupture the maximum joint opening of the north joint was roughly 0.11 in (3 mm) on the west springline. At the south joint, the displacements at the three locations were similar until the liner broke. At liner break the joint opening was about 3.4 in. (86.4 2 mm) of actuator movement. This corresponds to an axial displacement of 2.2 in. (1.4 mm).

End Forces

Four load cells were placed outside the test basin at each end to measure the end forces when the basin was displaced. Figure 2.3.22 and 2.3.23 show the end forces at the north end and south end, respectively, of the test basin. Once the liner broke, the end forces reduced to zero. Figure 2.75 shows the sum of all four load cells at the north and sound end of the test pipe. Figure 2.76 shows total north end force versus total south end force.

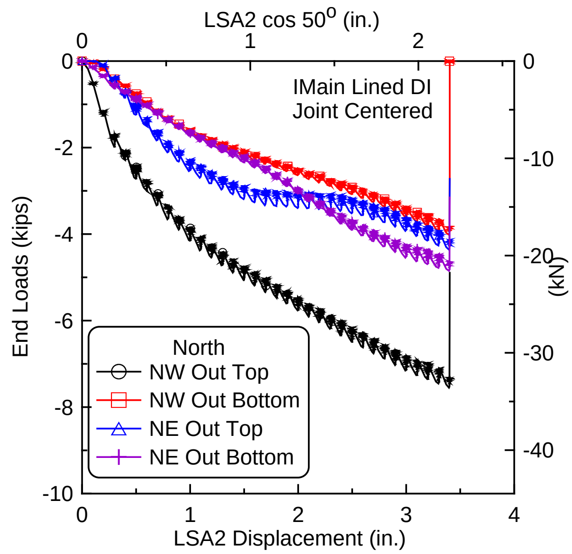

Figure 2.3.20. End Forces, North End, Outside Test Basin

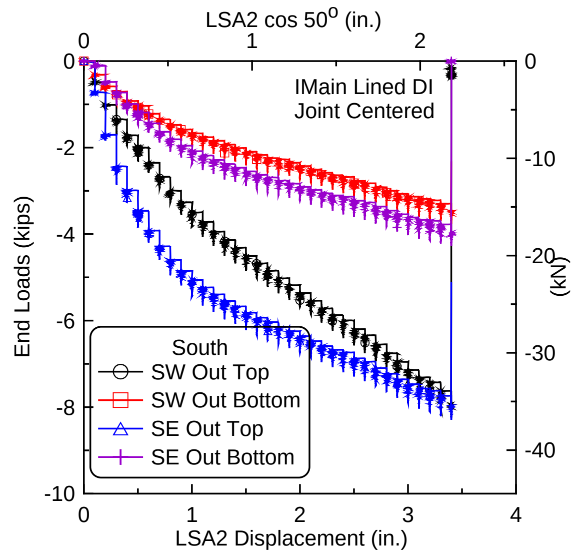

Figure 2.3.21. End Forces, South End, Outside Test Basin

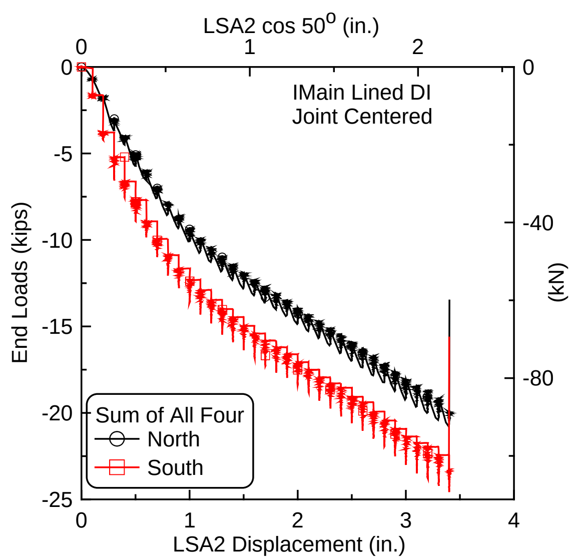

Figure 2.3.22. Total End Forces, North and, South, Outside Test Basin

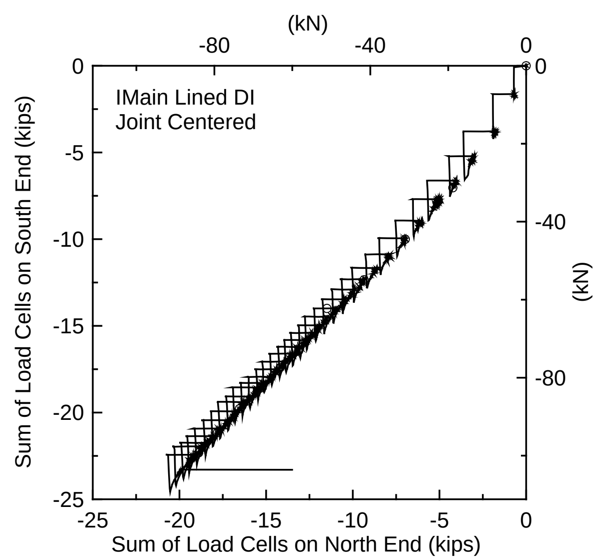

Figure 2.3.23. North vs. South End Forces, Outside Test Basin

2.3.5. Summary of IMain Joint Centered Test

This section presents the measurements made during a large-scale joint centered test of ductile iron pipe that was lined with the InsituformMain® System, referred to as IMain in this report. The test was performed in the large test basin in the Bovay Laboratory at Cornell University. The testing configuration and procedures are described. A pipe joint was centered on the fault. The instrumentation is reported, along with the soil placement procedures. Data are given for the test basin movements, pipe internal pressures, strain gage measurement, joint displacements, and end forces. The liner failed at an axial joint opening of roughly 2.2 in. (55.9 mm). Figure 2.3.24 is a photograph of the lined, joint centered pipe being excavated after the test.

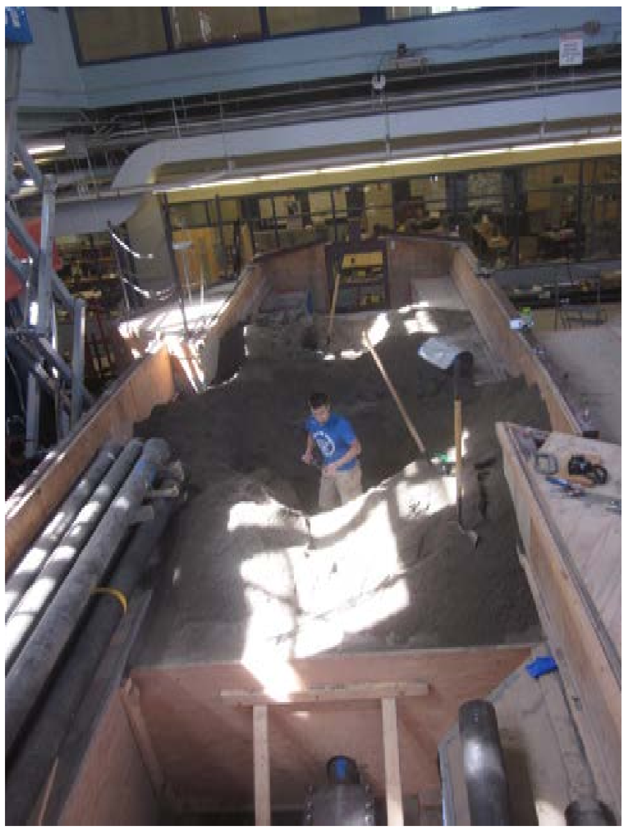

Figure 2.3.24. Photo of Excavation of Pipe after Joint CenteredTest

2.4. Axial Pull Tests on InsituformMain® System Lined DI Pipe

2.4.1. Test Purpose and Descriptions

This section of the annual report presents the results of large-scale axial pull and combined axial pull and rotation tests on lined ductile iron (DI) pipes connected with bell-spigot joints that were lined with InsituformMain® System. The tests were performed in September through November, 2012 and their primary purpose was to a) determine if there is preferential failure when pulling on the bell end or the spigot end, b) determine if the rate of axial pull affects the load-displacement results, and c) investigate the effects of an initial join rotation of potential debonding between the liner and the host pipe.

2.4.2. Test Configuration and Procedure

Testing was done on sections of bell-and-spigot lined DI pipes placed in a load frame which was positioned on the low reaction wall. Figure 2.4.1 is a photograph of the load frame, taken from the north end looking south. At the north end the pipe was connected to a UB clamp ("Testing of UB Clamps," Cornell NEESR Research Group, Dec., 2012) which was attached to the north end cross-member of the test frame. The south end of the pipe was also clamped in a UB clamp which was connected to a hydraulic actuator which was connected to the cross-member at the south end of the test frame. Instrumentation was installed and the actuator pulled on the pipe section from the south end.

The pipe sections were 15 ft (4.57 m) long in total. There was either a 6-ft (1.83-m)-long spigot section connected to a 9-ft (2.74 m)-long bell, or a 9-ft (2.74 m)-long section connected to a bell 6-ft (1.83-m)-long spigot. Thus, the actuator could either pull on a bell end or a spigot end, depending on the north-south orientation of the test pipe.

Figure 2.4.1. Load Frame Used for Rate Testing

Table 2.4.1 gives information about the trial configurations, indicating test date, specimen type, the lengths and pipe sections on the north and south end, and which section was attached to the actuator. Note that Specimens 1 and 4 were cut from the pipe surrounding the north joint of the pipe centered and joint centered tests in the large test-basin. ("IMain Lined Ductile Iron Pipe Centered Tension in Soil Test Basin," Cornell NEESR Research Group, Mar., 2013.; "IMain Lined Ductile Iron Joint Centered Tension Test in Soil Test Basin." Cornell NEESR Research Group, Mar., 2013.) The north joints in those tests underwent the least movement, so they were candidates for this rate testing, even though they disturbed to some degree. The other tests were done on new lined pipe sections. Table 2.4.2 lists the test rates and instrumentation used in the tests.

Table 2.4.1. Trial Configurations for IMain Axial Pull Tests

Trial No.	Date	Specimen	North Pipe Section	South Pipe Section	Pull On
1	09-19-2012	From Joint Centered Test, North Joint	9-ft-long Spigot	6-ft-long Bell	Bell End
2	10-3-2012	New Pipe	6-ft-long Spigot	9-ft-long Bell	Bell End
3	10-9-2012	New Pipe	9-ft-long Spigot	6-ft-long Bell	Bell End
4	11-1-2012	From Pipe Centered Test, North Joint	9-ft-long Bell	6-ft-long Spigot	Spigot End
5	11-16-2012	New Pipe	6-ft-long Bell	9-ft-long Spigot	Spigot End
6	11-21-2012	New Pipe	9-ft-long Bell	6-ft-long Spigot	Spigot End

Table 2.4.2. Test Rates and Instrumentation for IMain Axial Pull Tests

Trial No.	Target Pull Rate (in./min)	Initial Rotation (degrees)	No. of Strain Gages	No. of DCDTs	No. of String Pots	No. of Load Cells	Other[a]
1	0.2	-	4	4	-	-	Actuator
2	0.2	-	16	-	4	-	Actuator
3	20.0	-	16	-	4	-	Actuator
4	2.0	0.5	30	1[b]	4	1[b]	Actuator
5	0.2	0.5	28	1[b]	4	1[b]	Actuator
6	0.2	1.0	24	1[b]	4	1[b]	Actuator

a – Other is the load cell and displacement of the actuator
b – These are used for the rotation measurements at the joint

2.4.3. Test Results

<u>Trial 1</u>

Rate test Trial 1 was a shake-down test of the loading system. The joint had been previously tested in the joint centered test in the large test basin, but had experienced very small displacements during testing. The target loading rate was 0.2 in./min (5.1 mm/min.) The pull for this test was on the bell end of the specimen. Figure 2.4.2 shows the resulting force vs. displacement curve. The maximum force in this test was 20.3 (90.3 kN) kips at a joint opening of 0.22 in. (5.6 mm). Figure 2.4.3 shows the force vs. displacement for each DCDT. In this test there was no liner break, but there was visible liner slip at the end of the bell side of the

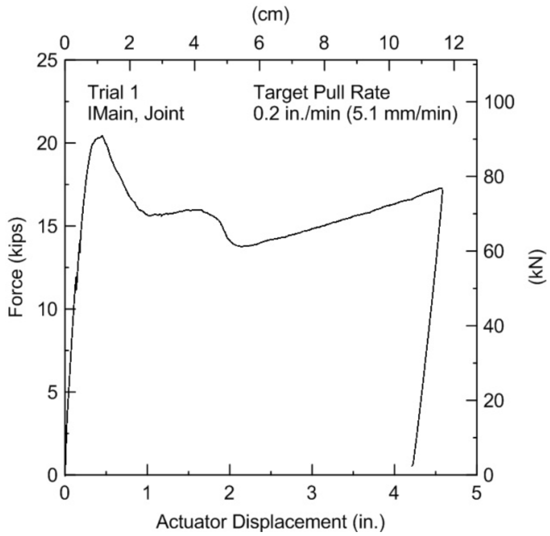

Figure 2.4.2. Force vs. Displacement, Trial 1

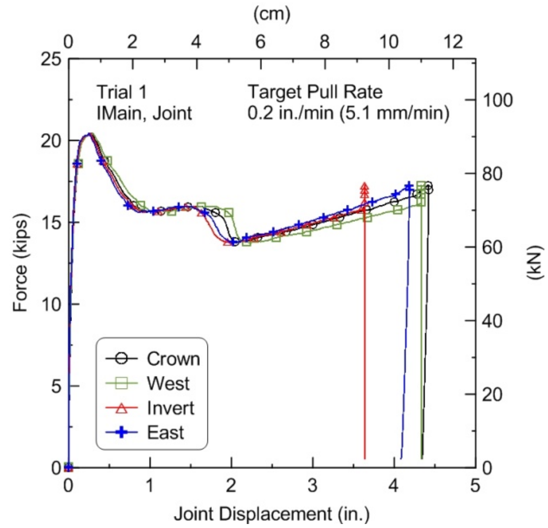

Figure 2.4.3. Force vs. Joint Opening, Trial 1

joint [the 6 ft 1.83 m) section]. Visual inspection after the test indicated debonding between the liner and mortar at the end of the bell side. There was debonding both between the liner and mortar, and between the mortar and DI on the bell side at the joint.

Trial 2

The pipe for Trial 2 was a new section of IMain lined DI and the target loading rate for Trial 2 was 0.2 in./min (5.1 mm/min.) The lined DI pipe specimen was pulled from the bell side and was clamped at the north end to the test frame, and to the hydraulic actuator at the south end using UB clamps. It was supported at the bottom at several locations to prevent bending under its own weight. Four string potentiometers were placed at the crown, invert, and the two sides of the pipe spring line in order to measure displacements around the joint. Strain gages were placed on the west and east side of the joint at 8, 12, 16, and 20 in. (20.3, 30.5, 40.6, and 50.8 cm, respectively) far from the center of the joint. The maximum force in this test was 31.9 (141.9 kN) kips at a joint opening of 0.19 in. (4.83 mm). Figure 2.4.4 shows the force vs. actuator displacement, and Fig. 2.4.5 shows the force vs. joint opening for each string potentiometer. Figures 2.4.6 through 2.4.9 show the strain gage measurements on the east and west pipeline for both the spigot and bell side vs. the average joint displacement that was measured by the string potentiometers.

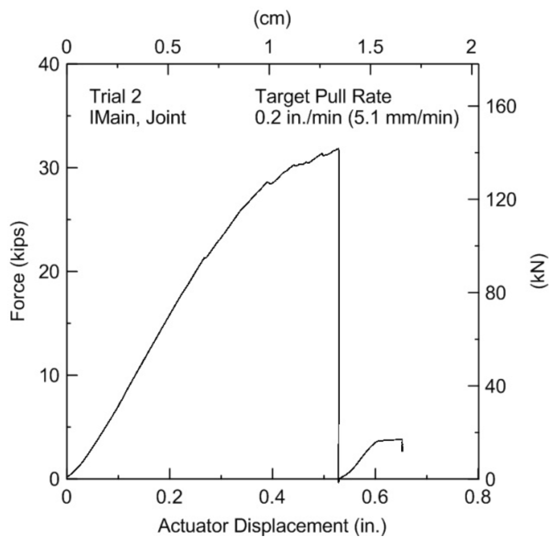

Figure 2.4.4. Force vs. Displacement, Trial 2

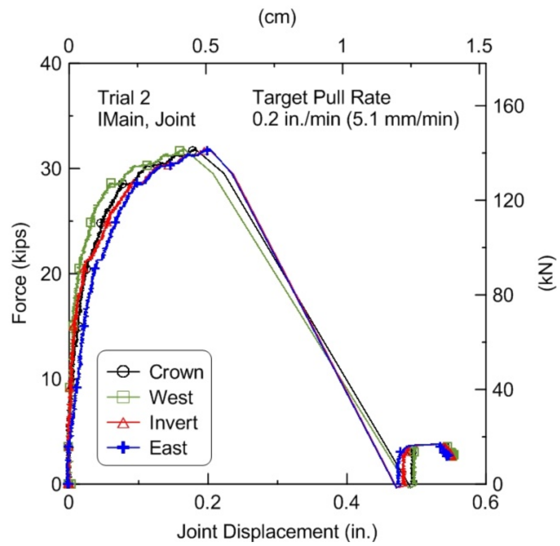

Figure 2.4.5. Force vs. Joint Opening, Trial 2

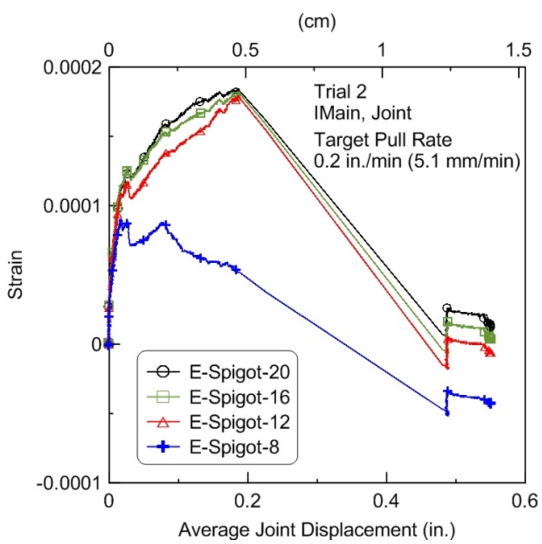

Figure 2.4.6. East Springline Strains, Gages at 8, 12, 16, and 20 in. from Joint, Trial 2, Spigot Side

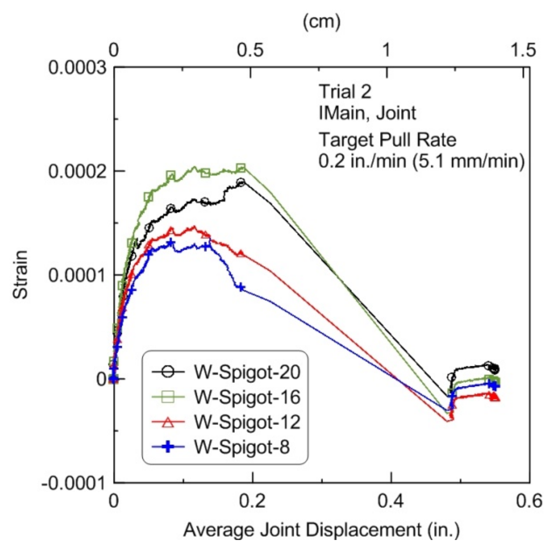

Figure 2.4.7. West Springline Strains, Gages at 8, 12, 16, and 20 in. from Joint, Trial 2, Spigot Side

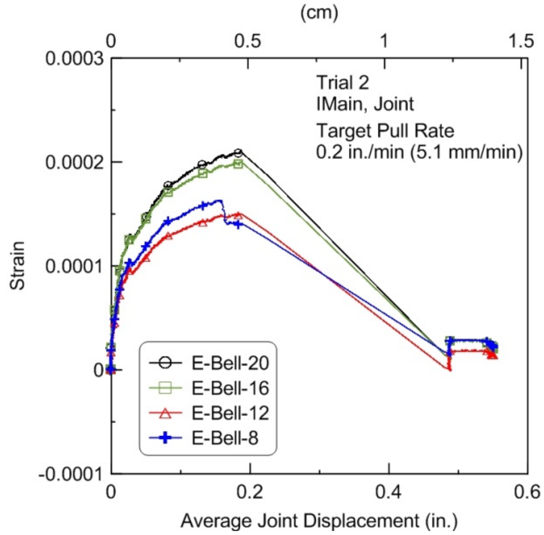

Figure 2.4.8. East Springline Strains, Gages at 8, 12, 16, and 20 in. from Joint, Trial 2, Bell Side

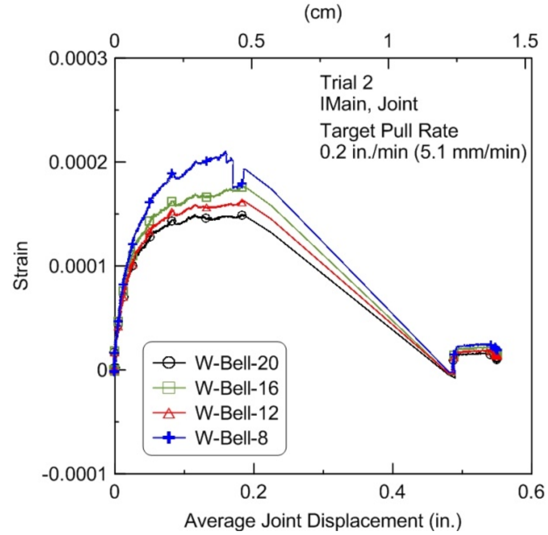

Figure 2.4.9. West Springline Strains, Gages at 8, 12, 16, and 20 in. from Joint, Trial 2, Bell Side

Trial 3

The pipe for Trial 3 was a new section of IMain lined DI. The target loading rate for Trial 3 was 20 in./min (508 mm/min.), and the specimen was pulled from the bell side. Strain gages were placed on the west and east side of the joint at 3, 5, 7, and 9 in. (7.62, 12.7, 17.8, and 22.86 cm, respectively) far from the center of the joint. The actuator force versus actuator displacement is shown in Fig. 2.4.10. The joint openings measured with the string pots are smaller than the actuator movements up to about 0.3 in. (7.6 mm), and then the incremental movements are quite similar. All string pots displacements were very similar. The liner broke at a force of 31.8 kips (141.4 kN) and at an average joint displacement of 0.20 in. (5.1 mm). Figure 2.4.7 shows the force vs. joint opening for each string potentiometer. Figures 2.4.12 through 2.4.15 show the strain gage measurements on the east and west pipeline for both the spigot and bell side vs. the average joint displacement that was measured by the string potentiometers.

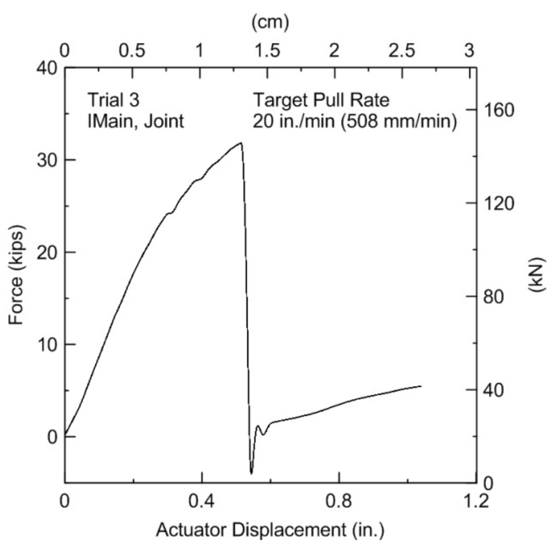

Figure 2.4.10. Force vs. Displacement, Trial 3

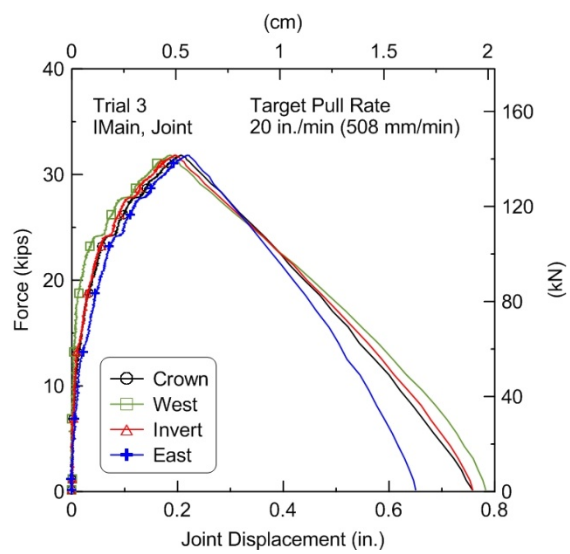

Figure 2.4.11. Force vs. Joint Opening, Trial 3

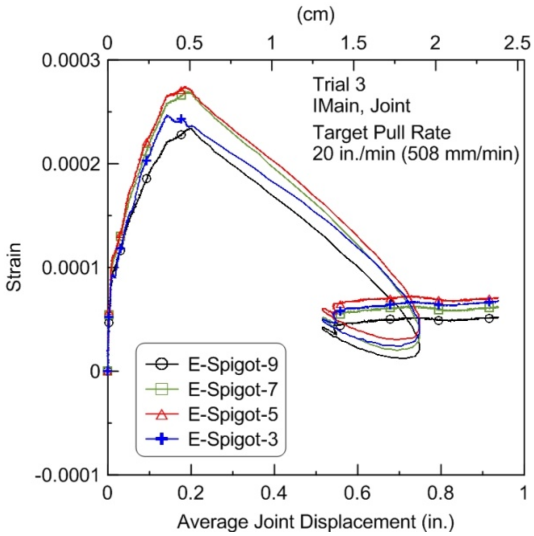

Figure 2.4.12. East Springline Strains, Gages at 3, 5, 7, and 9 in. from Joint, Trial 3, Spigot Side

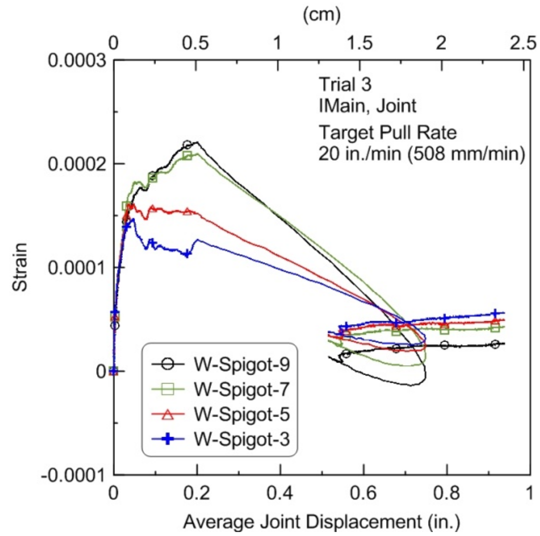

Figure 2.4.13. West Springline Strains, Gages at 3, 5, 7, and 9 in. from Joint, Trial 3, Spigot Side

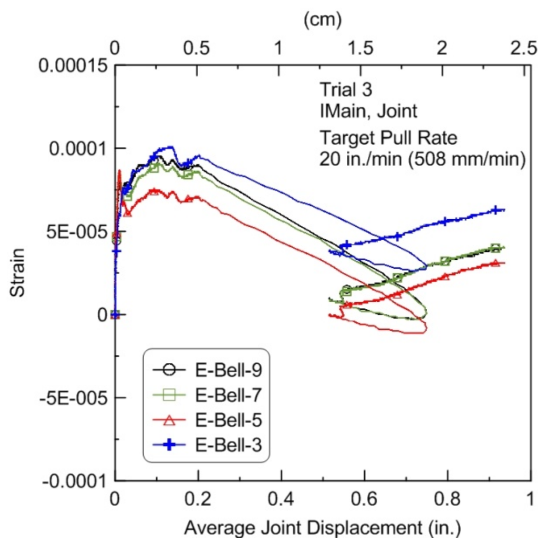

Figure 2.4.14. East Springline Strains, Gages at 3, 5, 7, and 9 in. from Joint, Trial 2, Bell Side

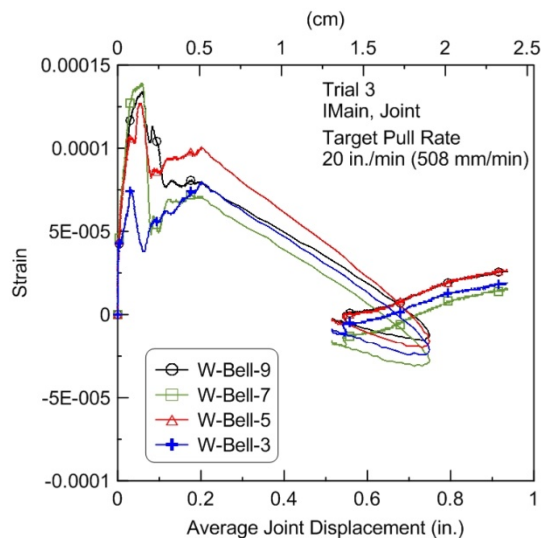

Figure 2.4.15. West Springline Strains, Gages at 3, 5, 7, and 9 in. from Joint, Trial 2, Bell Side

<u>Trial 4</u>

Trial 4 was a combined monotonic axial pull and prescribed rotation test with the axial displacement being applied at a constant loading rate equal to 2 in./min (50.8 mm/min). The pipe specimen for Trial 4 was a previously tested section of IMain lined DI. The test specimen was taken from the northern-most join of the large-scale test basin experiment when the center of a pipe was centered on the joint (pipe centered test). The pull for this test was on the spigot end of the specimen. An initial joint rotation of 0.5º was applied using a screw jack beneath the bell at the joint located 3 in. (7.6 cm) into the bell side from the bell face. This rotation was applied before the actuator began making the axial pull.

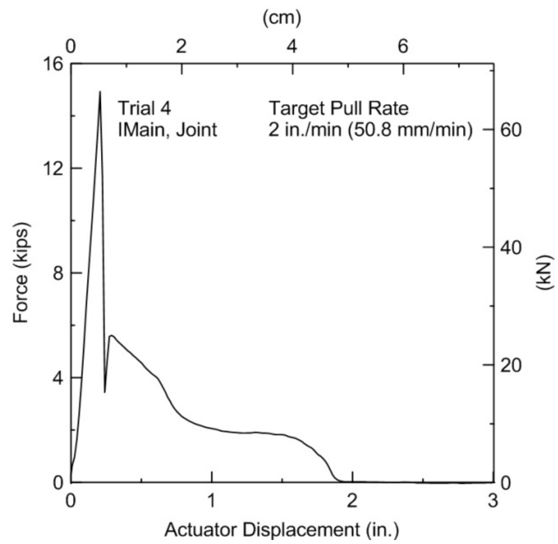

Figure 2.4.16. Force vs. Displacement, Trial 4

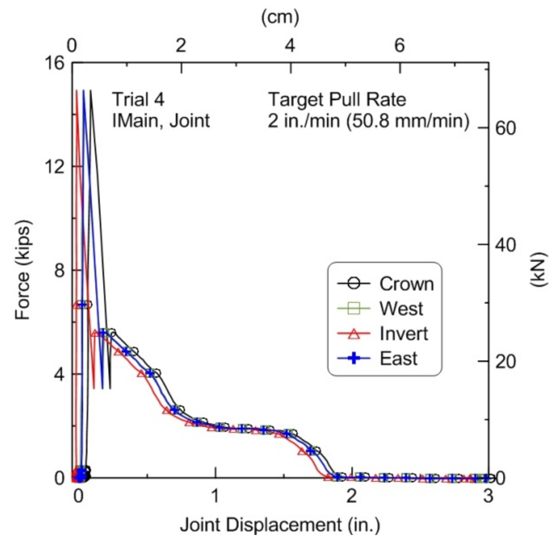

Figure 2.4.17. Force vs. Joint Opening, Trial 4

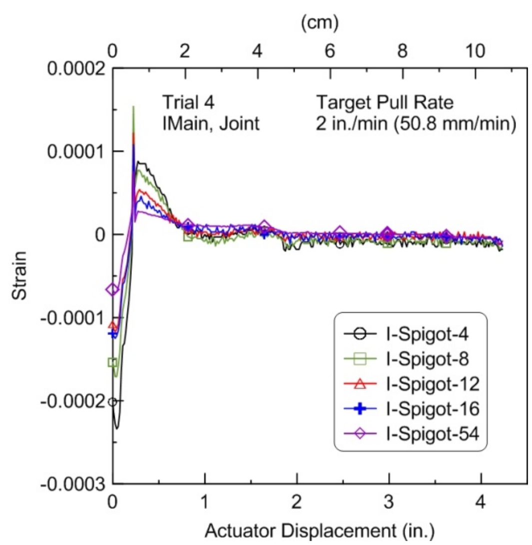

Figure 2.4.18. Pipe Invert Strains, Gages at 4, 8, 12, 16, and 54 in. from Joint, Trial 4, Spigot Side

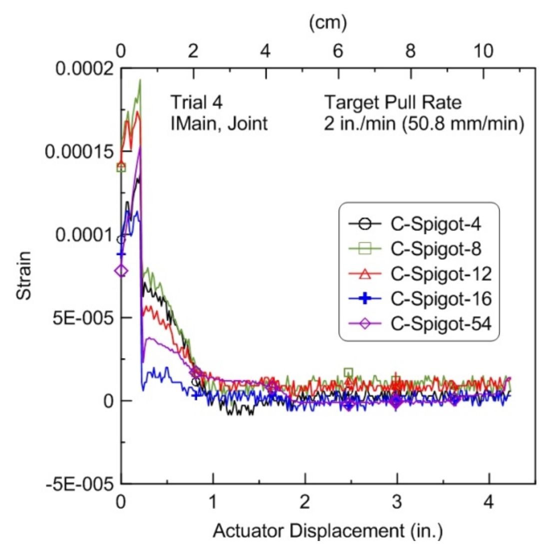

Figure 2.4.19. Pipe Crown Strains, Gages at 4, 8, 12, 16, and 54 in. from Joint, Trial 4, Spigot Side

Figure 2.4.16 shows the force vs. actuator displacement, and Fig. 2.4.17 shows the force vs. joint opening for each string potentiometer. The maximum force in Trial 4 was 14.7 kips (65.4 kN) at an average joint opening of 0.02 in. (0.5 mm). The test was continued until the liner broke completely at a displacement of 0.16 in. (4.1 mm). Strain gages were placed on the pipe crown and invert at 4, 8, 12, 16, and 54 in. (10.16, 20.32, 30.48, 40.64, and 137.16 cm, respectively) far from the center of the joint on the spigot side, and on the pipe crown and invert at 4, 8, 12, 16, and 34 in. (10.16, 20.32, 30.48, 40.64, and 86.36 cm, respectively) far from the center of the joint on the bell side. The evolution of stains at these locations vs. the actuator displacement is shown in Figs. 2.4.18 through 2.4.21.

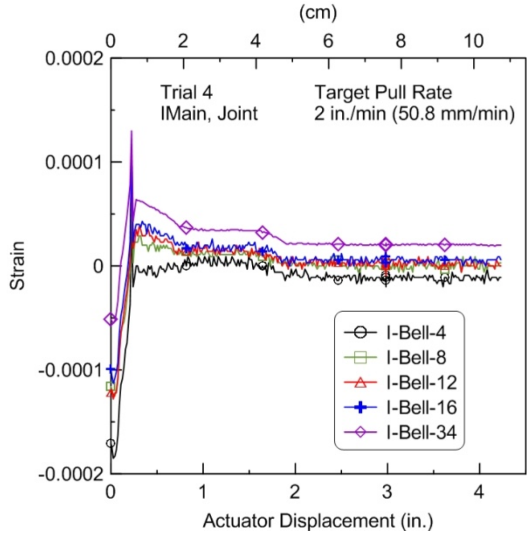

Figure 2.4.20. Pipe Invert Strains, Gages at 4, 8, 12, 16, and 34 in. from Joint, Trial 4, Bell Side

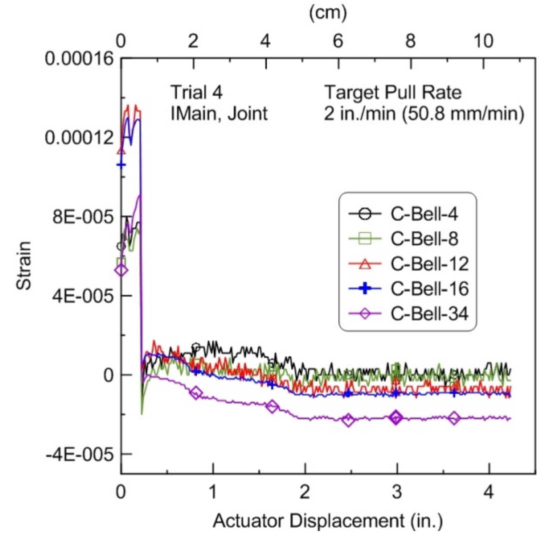

Figure 2.4.21. Pipe Crown Strains, Gages at 4, 8, 12, 16, and 34 in. from Joint, Trial 4, Bell Side

<u>Trial 5</u>

The pipe specimen for Trial 5 was a new test section of IMain lined DI. The target loading rate for Trial 5 was 0.2 in./min (5.1 mm/min.) and the location of pull for this test was on the spigot end of the specimen. In Trial 5 an initial joint rotation of 0.5º was applied using a screw jack beneath the bell at the joint. This rotation was applied before the actuator began making the axial pull. Figure 2.4.22 shows the actuator force vs. actuator displacement, and Fig. 2.4.23 shows the force vs. joint opening for each string potentiometer. The initial joint opening at the crown is positive and the invert is negative because, as the joint was forced upward to cause the initial rotation, the joint opened at the crown and closed at the invert. In Trial 5 the liner failed at a force of 25.8 kips (114.8 kN) at a joint opening of 0.21 in. (5.3 mm). Strain gages were placed on the pipe crown and invert at 4, 8, 12, 16, and 54 in. (10.16, 20.32, 30.48, 40.64, and 137.16 cm, respectively) far from the center of the joint on the spigot side, and on the pipe crown and invert at 4, 8, 12, 16, and 36 in. (10.16, 20.32, 30.48, 40.64, and 91.44 cm, respectively) far from the center of the joint on the bell side. The evolution of stains at these locations vs. the actuator displacement is shown in Figs. 2.4.24 through 2.4.27.

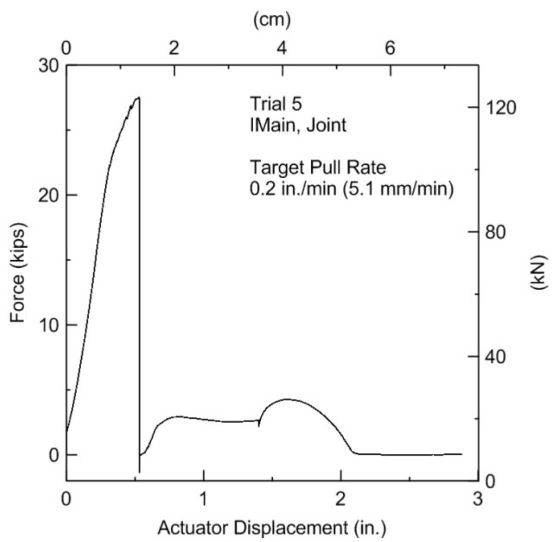

Figure 2.4.22. Force vs. Displacement, Trial 5

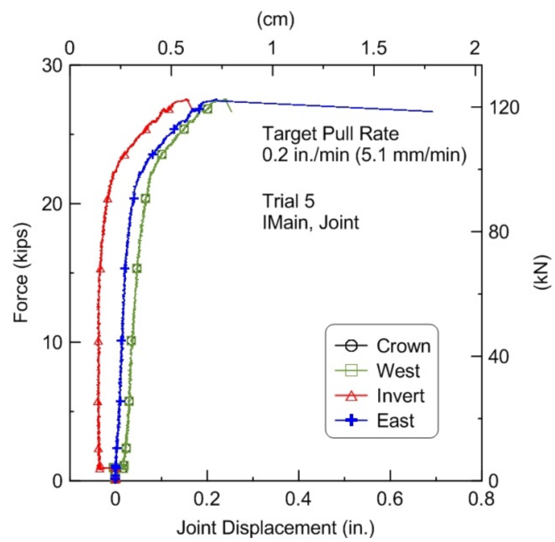

Figure 2.4.23. Force vs. Joint Opening, Trial 5

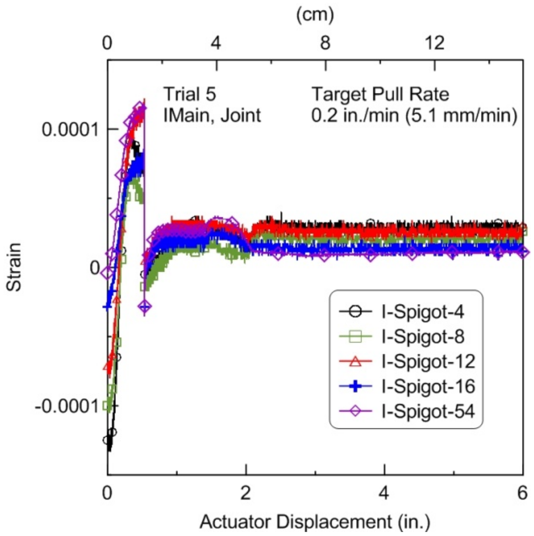

Figure 2.4.24. Pipe Invert Strains, Gages at 4, 8, 12, 16, and 54 in. from Joint, Trial 5, Spigot Side

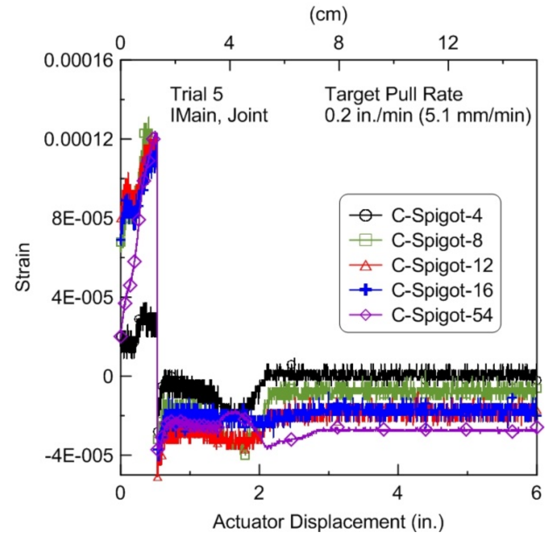

Figure 2.4.25. Pipe Crown Strains, Gages at 4, 8, 12, 16, and 54 in. from Joint, Trial 5, Spigot Side

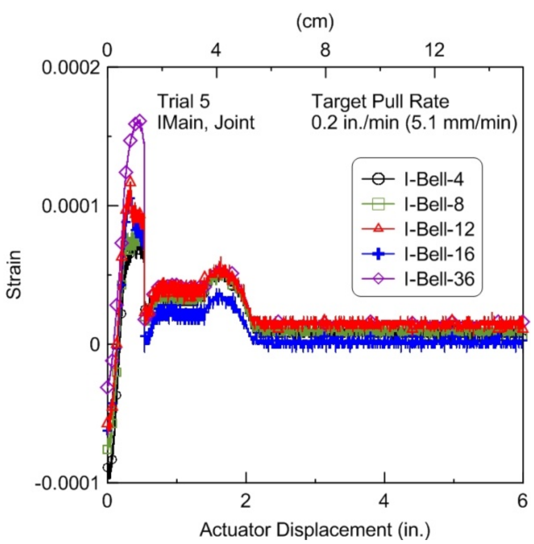

Figure 2.4.26. Pipe Invert Strains, Gages at 4, 8, 12, 16, and 36 in. from Joint, Trial 5, Bell Side

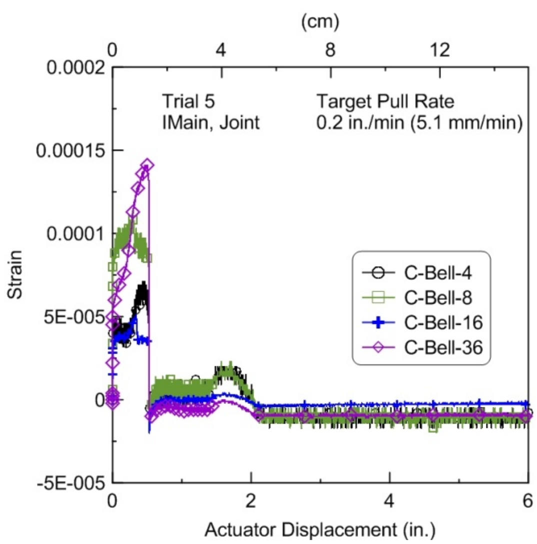

Figure 2.4.27. Pipe Crown Strains, Gages at 4, 8, 12, 16, and 36 in. from Joint, Trial 5, Bell Side

Trial 6

The pipe for Trial 6 was a new test section of IMain lined DI. The target loading rate for Trial 6 was 0.2 in./min (5.1 mm/min.), with the location of pull on the spigot end of the specimen. In Trial 6 an initial joint rotation of 1º was applied using a screw jack beneath the bell at the joint. This rotation was applied before the actuator began making the axial pull. Figure 2.4.12 shows the applied vertical force vs. the resulting joint rotation. As the specimen was pulled, the joint tended to straighten out. Figure 2.4.12 shows the actuator force vs. actuator displacement, and Fig. 2.4.13 shows the actuator force vs. the joint opening measured by each string pot. In Trial 6 the liner slipped at a force of 21.2 kips (94.3 kN) at a joint opening of 0.46 in. (11.7 mm).

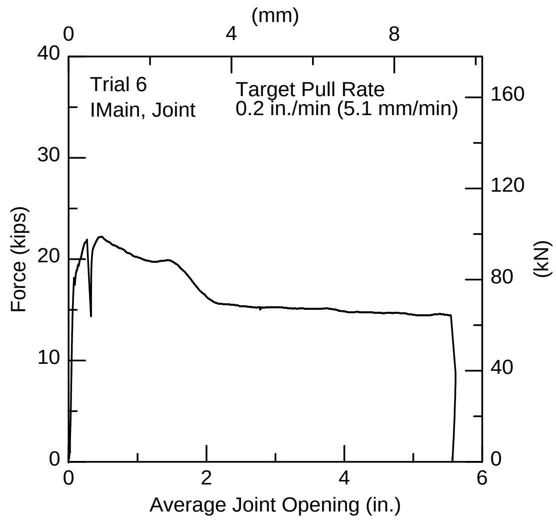

Figure 2.4.28. Force vs. Displacement, Trial 6

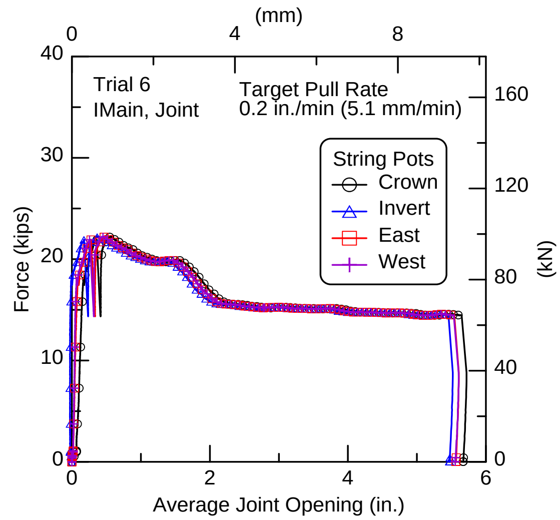

Figure 2.4.29. Force vs. Joint Opening, Trial 6

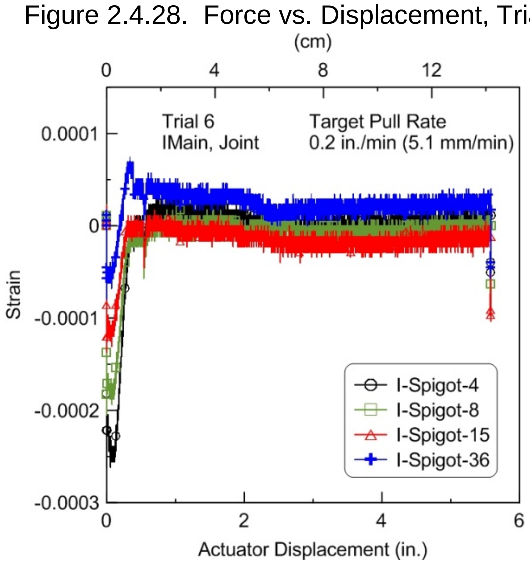

Figure 2.4.30. Pipe Invert Strains, Gages at 4, 8, 15, and 36 in. from Joint, Trial 6, Spigot Side

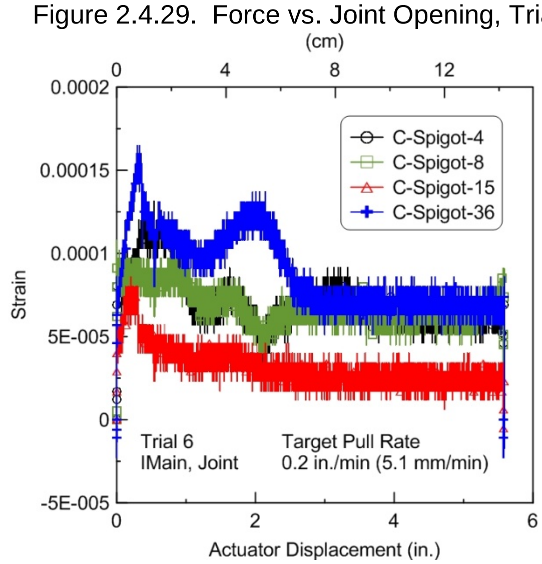

Figure 2.4.31. Pipe Crown Strains, Gages at 4, 8, 15, and 36 in. from Joint, Trial 6, Spigot Side

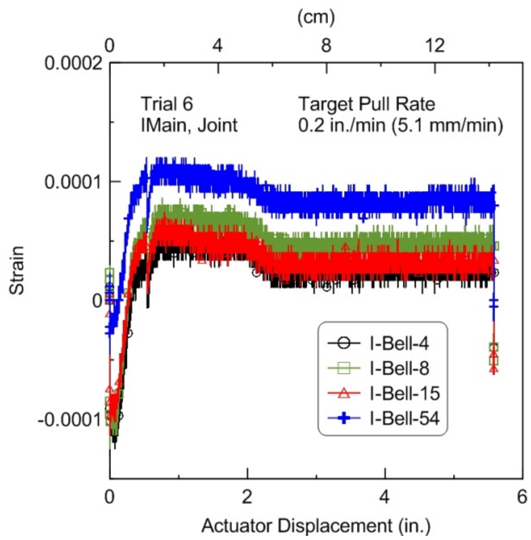

Figure 2.4.32. Pipe Invert Strains, Gages at 4, 8, 15, and 54 in. from Joint, Trial 6, Bell Side

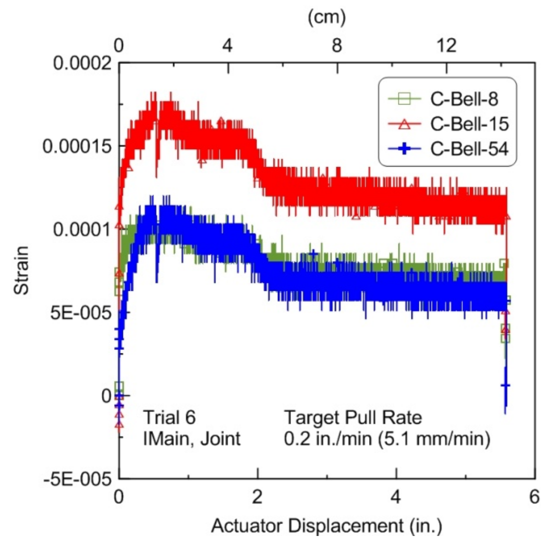

Figure 2.4.33. Pipe Crown Strains, Gages at 8, 15, and 54 in. from Joint, Trial 6, Bell Side

2.4.4. Load Rate Comparisons – Trials 2 and 3

Figure 2.4.34 shows the average joint opening versus time for Trial 2, which had a target joint opening rate of 0.2 in./min (5.1 mm/min.). The data were used to determine the joint opening rate during the test using Eq. 1. When the data were used to determine the joint opening rate using the sampling rate of 10 Hz, there was a great amount of “noise” in the resulting rates.

$$\dot{\delta}(t) = \frac{\delta_j - \delta_i}{t_j - t_i = \Delta t} \qquad (1)$$

where $\dot{\delta}(t)$ = joint opening rate

δ = average joint opening

t = test time, and

Δt = data sampling interval = 0.1 sec for Trial 2

The data from Trial 2 were fitted to a polynomial curve. The expression for joint opening as a function of time, δ(t), is given by:

$$\delta(t)(\text{in.}) = 5.05\times10^{-2} - 4.09\times10^{-4}t - 3.04\times10^{-6}t^2 + 2.54\times10^{-8}t^3 \qquad (2)$$

(r^2 = 0.9992)

where t is the time in seconds.

The open circle symbols and blue line on Figure 2.4.34 are the curve-fitted data, which agree well with the measured average joint opening. The third-order polynomial Eq. 2 can be differentiated, the joint opening displacement rate can be determined throughout the test. Multiplying by 60 sec/min gives the rate in in./min. The continuous joint opening rate for Trial 2 is shown in Figure 2.4.35.

The data from Trail 3 were evaluated the same way described above. Figure 2.4.36 shows the average joint opening versus time for Trial 3, which had a target joint opening rate of 20 in./min (508 mm/min.). Here the sampling rate was 500 Hz. The open circle symbols and blue line on Figure 2.4.36 are the curve-fitted data,

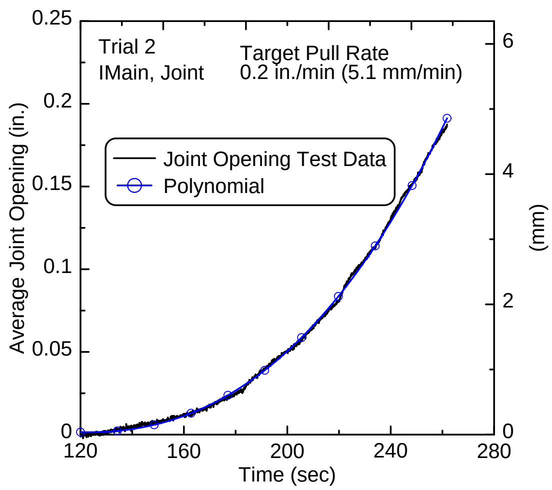

Figure 2.4.34. Average Joint Opening vs. Time, Trial 2

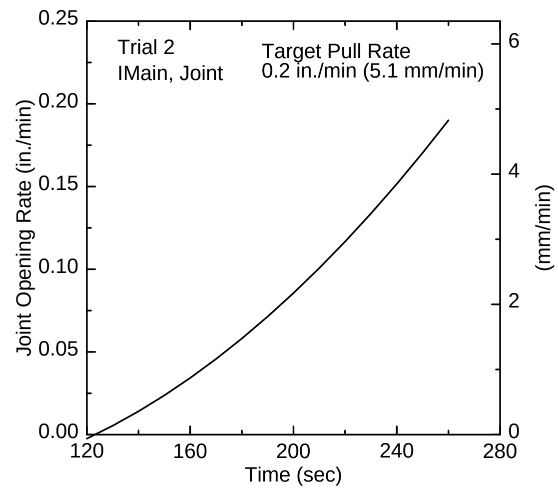

Figure 2.4.35. Continuous Joint Opening Rate vs. Time, Trial 2

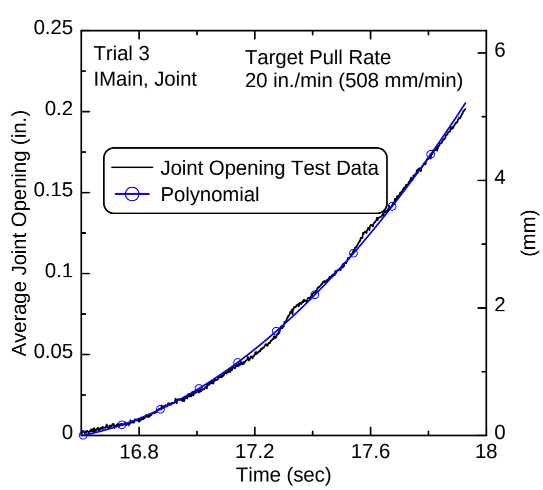

Figure 2.4.36. Average Joint Opening vs. Time, Trial 3

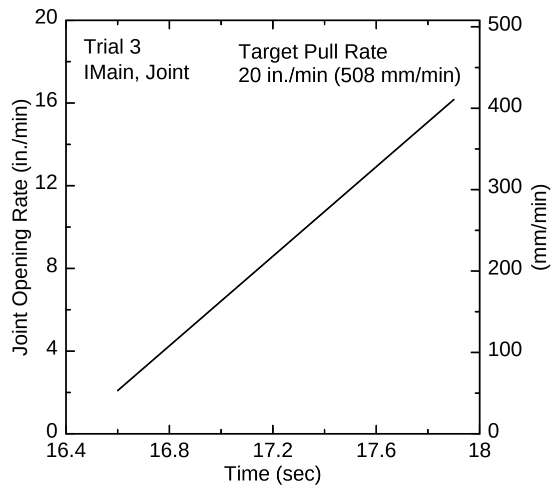

Figure 2.4.37. Continuous Joint Opening Rate vs. Time, Trial 3

which agree well with the measured average joint opening. The second-order polynomial for Trial 3 is given in Eq. 3. The continuous joint opening rate for Trail 3 is shown in Fig. 2.4.37.

$$\delta(t)(\text{in.}) = 24.28 - 2.96\,t + 9.02\times10^{-2}\,t^{2} \qquad (3)$$

(r^2 = 0.9987)

Figure 2.4.38 shows the ratio Trial 2 to Trial 3 joint opening rates versus joint opening. As the joint opening increases the ratio of rates decreases. However, for all joint openings the rate for Trial 3 was on the roughly two orders of magnitude greater than that for Trial 2.

Table 2.4.3 gives the failure mode, maximum force, and joint opening at failure for Trials 2 and 3. There are nearly identical.

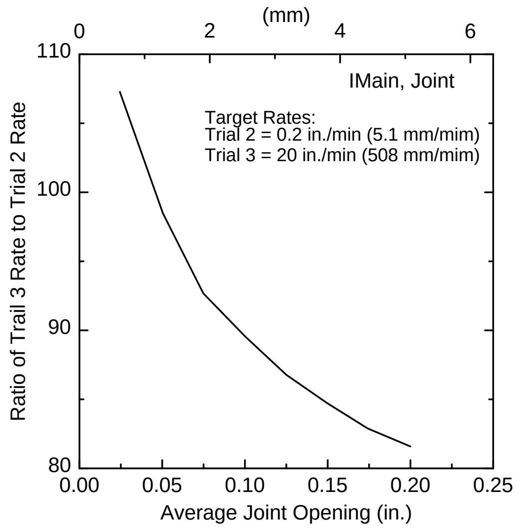

Figure 2.4.38. Ratio of Test Rates for Trials 2 and 3

Table 2.4.3. Test Results for Trials 2 and 3

Trial No.	Specimen	Loading Rate (in./min)	Pull On	Failure Mode	Max. Force (kips)	At Joint Opening of (in.)
2	New Pipe	0.2	Bell End	Liner Break	31.9	0.19
3	New Pipe	20	Bell End	Liner Break	31.8	0.20

2.4.5. Summary of IMain Axial Pull Tests

This report presents the measurements made during a series of six full-scale test of IMain lined ductile iron pipe joints. The purpose of the tests was to:

a) Determine if there was a preference for the liner to break at different locations depending on whether the bell was pulled or the spigot was pulled,
b) Determine the strength of the IMain liner in tension, and the displacement at failure,
c) Investigate progressive debonding between the liner and mortar or the mortar and DI, or both, and
d) Determine if the rate of loading had an effect on liner strength.

The results from this series of tests on specimens that have not been previously tested showed that there is no preferential failure of the liner based on the location of pull (i.e. bell-side pull or spigot-side pull). Specifically, even though in Trial 3 the specimen was pulled from the spigot side and in Trial 5 the specimen was pulled from the bell side, the liner failed very close [within 0.5 in. (1.27 cm) distance] to the edge of the spigot at the joint in both tests. Overall, the liner failed consistently within a range of 0.18 in. and 0.22 in. (0.46 cm and 0.56 cm, respectively) when the specimens were not previously tested, and the maximum force that was reached during the axial pull was approximately 32kips (142.34 kN). When the liner was subjected to combined axial pull and rotation, the maximum force was approximately 26 kips (115.65 kN), but the displacement was again within the range of 0.18 in. and 0.22 in. (0.46 cm and 0.56 cm, respectively). This pattern of liner failure with rupture is shown in Fig. 2.4.39 where the backbone curves of Trials 2, 3, and 5 are presented. Figure 2.4.40 shows the backbone curves of Trials 5 and 6 which were combined axial pull and rotation tests on new specimens. The failure mechanisms were different in there two tests; the specimen in Trial 5 failed due to liner rupture, whereas the liner in Trial 6 fully debonded from the bell-side segment during the test. As a result the maximum force in Trial 5 is greater than the maximum force in Trial 6. Trials 2 and 3 were axial pull tests performed at loading rates of 0.2 in./min (5.1 mm/min) and 20 in./min

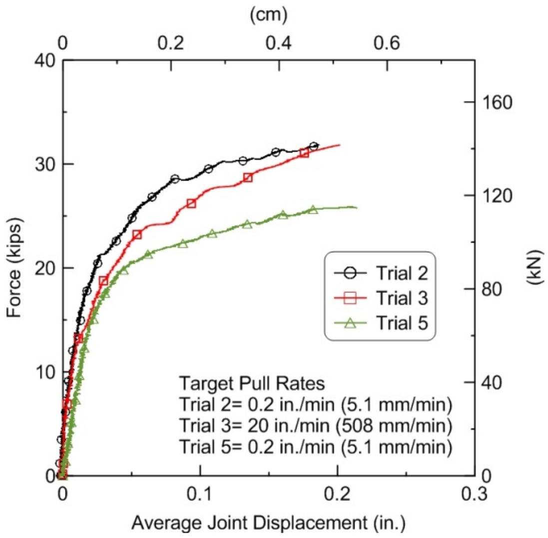

Figure 2.4.39. Trial 2, Trial 3, and Trial 5 Backbone Curves

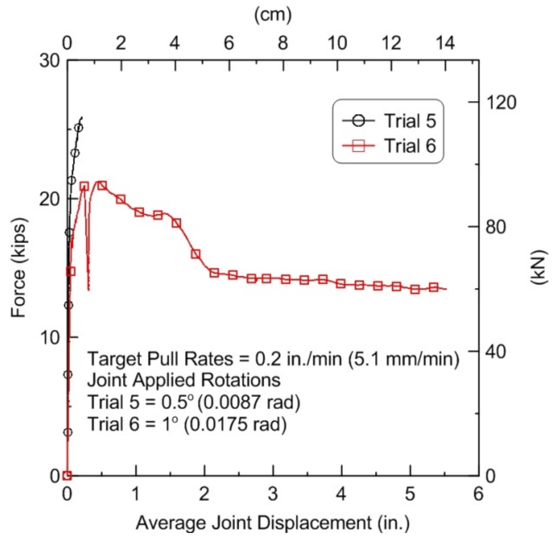

Figure 2.4.40. Trial 5 and Trial 6 Backbone Curves

(508 mm/min), respectively. The backbone curves of these two tests are presented in Fig. 2.4.39 and do not indicate any significant effect of the loading rate on the response of joints lined with InsituformMain® System. Table 2.4.4 provides a summary of the test results.

Table 2.4.4. Summary of IMain Pull Tests

Trial No.	Specimen	Loading Rate (in./min)	Pull On	Failure Mode	Max. Force (kips)	At Joint Opening of (in.)
1	From Joint Centered Test, North Joint	0.2	Bell End	Liner Slip	20.3	0.22
2	New Pipe	0.2	Bell End	Liner Break	31.9	0.19
3	New Pipe	20	Bell End	Liner Break	31.8	0.20
4	From Pipe Centered Test, North Joint	2.0	Spigot End	Liner Break[a]	14.7	0.02 – 0.16
5	New Pipe	0.2	Spigot End	Liner Break	25.8	0.21
6	New Pipe	0.2	Spigot End	Liner Slip	21.2	0.46

a = Rupture started at 0.02 in. and continued to 0.16 in.
1 kip = 4.448 kN; 1 in. = 25.4 mm

2.5. Axial Pull Tests on Starline 2000® Lined DI Pipe

2.5.1. Test Purpose and Descriptions

This section of the annual report presents the results of a series of large-scale axial pull, combined axial pull and rotation, and bending tests on lined ductile iron (DI) pipe connected with bell-spigot joints and lined with Starline2000® System, performed in December 2012 through May, 2013. The purpose of these tests was to a) determine the capacity of the Starline 2000 liner, b) determine if the rate of axial pull affects the load-displacement results, c) investigate the effects of an initial join rotation on potential debonding between the liner and the host pipe, and d) investigate the sensitivity of the lined pipe response to internal pressure.

The liner material was Starline® 2000, referred to as Starline in this report. The Starline System is an internal, cured-in-place pipe (CIPP) composite material made up of woven fabric hose with a polyethylene coating and a specially formulated epoxy resin system. More information about the Starline liner can be found at http://www.progressivepipe.com/downloads/PPM.pdf. Figure 2.5.1 is a schematic of the lining system.

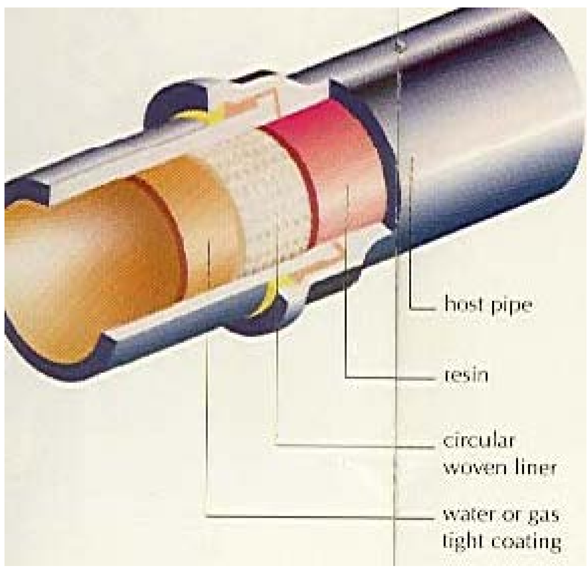

Figure 2.5.1. Schematic of Starline® 2000 System (courtesy of Progressive Pipeline Management)

2.5.2 Test Configuration and Procedure

Testing was done on sections of bell-and-spigot lined DI pipe placed in a load frame. The load frame was positioned on the low reaction wall. Figure 2.5.2. is a photograph of the load frame, taken from the north end looking south. At the north end the pipe was connected to a UB clamp ("Testing of UB Clamps," Cornell University NEESR Group, Dec., 2012) which was attached to the north end cross-member of the test frame. The south end of the pipe also was clamped in a UB clamp which was connected to a hydraulic actuator which was connected to the cross-member at the south end of the test frame. Instrumentation was installed and the actuator pulled on the pipe section from the south end. Testing was done using the same general procedures described in **"**Loading Rate Tests on IMain Lined Bell and Spigot DI Pipe," (Cornell University NEESR Group, April, 2013.)

The pipe sections were varied from 8 to 15 ft (2.44 to 4.57 m) long in total. There was either a two spigot sections with a gap between the two sections with the liner spanning the gap or sections with bell-and-spigot connections.

Figure 2.5.2. Load Frame Used for Testing

Table 2.5.1 gives information about the trial configurations, indicating test date, specimen type, the lengths and pipe sections on the north and south end, and which section was attached to the actuator. The tests were done on new lined pipe sections. Table 2.5.2 lists the test rates and instrumentation.

Table 2.5.1. Trial Configurations for Starline Axial Pull Tests

Trial No.	Date	Specimen	North Pipe Section	South Pipe Section	Pull On
1	12-20-2012	Gap Specimen G1	5-ft-long Spigot	5-ft-long Spigot	Spigot End
2	01-18-2013	Gap Specimen G2	5-ft-long Spigot	5-ft-long Spigot	Spigot End
3	01-31-2013	Gap Specimen G3	5-ft-long Spigot	5-ft-long Spigot	Spigot End
4	04-02-13	Gap Specimen G4	5-ft-long Spigot	5-ft-long Spigot	Spigot End
5	04-17-2013	Joint J2	4-ft-long Spigot	4-ft-long Bell	Bell End
6	04-25-2013	Joint J1	9-ft-long Bell	6-ft-long Spigot	Spigot End
7	05-9-2013	Joint J3	4-ft-long Spigot	4-ft-long Bell	Spigot End

Table 2.5.2. Test Rates and Instrumentation for Starline Axial Pull Tests

Trial No.	Target Pull Rate (in./min)	No. of Strain Gages	No. of DCDTs	No. of String Pots	No. of Load Cells	Other[a]	Nominal Pressure (psi)
1	0.2	4	-	4	-	Actuator	0
2	0.2	4	-	4	-	Actuator	0
3	0.2	16	-	4	-	Actuator	75
4	0.2	12	-	4	-	Actuator	75
5	20	10	-	4	-	Actuator	75
6	20	8	-	4	-	Actuator	75
7	0.2	16	1[b]	4	1[b]	Actuator	75

a – Other is the application of displacement with the actuator
b – These are used for the force and rotation measurements due to applied rotation at the joint

2.5.3. Test Results

Trial 1

Trial 1 was a test of a lined pipe with a gap. The target loading rate was 0.2 in./min (5.1 mm/min.). There was no internal pressure in the pipe specimen during testing. Five cycles of joint opening and joint closing were conducted. The first cycle was a pull until the gages indicated debonding, when the force measured by the actuator reached a plateau. The gap then was pushed back to a position near the initial condition, and multiple cycles of load followed until the liner fully debonded in the south segment during the 5th cycle of loading. Figure 2.5.3 shows the actuator force vs. the average incremental gap opening for all cycles of loading until the end of the test, and Fig. 2.5.4 shows the backbone curve of the test. The maximum force in this test was 10.6 kips (47.29 kN) kips and was reached at a joint opening of 9.84 in. (25 cm).

Trial 2

The pipe for Trial 2 was a new section of Starline lined DI with a gap. The target loading rate for Trial 2 was 0.2 in./min (5.1 mm/min.). There was no internal pressure in the pipe specimen during testing. Seven cycles of joint opening and joint closing were conducted. The maximum force was reached during cycle 4, and then it reached a plateau during the subsequent cycles. The gap was pushed back to a position near the initial condition at the end of each loading and unloading cycle, until the liner fully debonded in the north segment during the 7th cycle of loading. The maximum force was 7.17 kips (31.89 kN) at a gap opening of 1.24 in. (3.15 cm). The actuator force vs. average incremental gap opening is shown in Figure 2.5.5 for all seven cycles. Figure 2.5.6 shows the backbone curve of Trial 2.

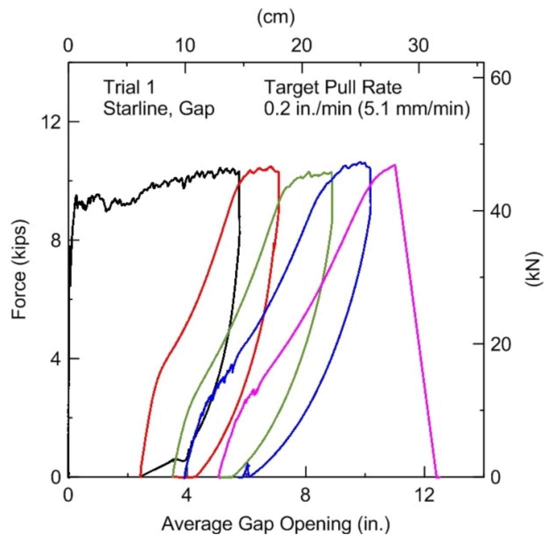

Figure 2.5.3. Force vs. Average Gap Opening, Trial 1

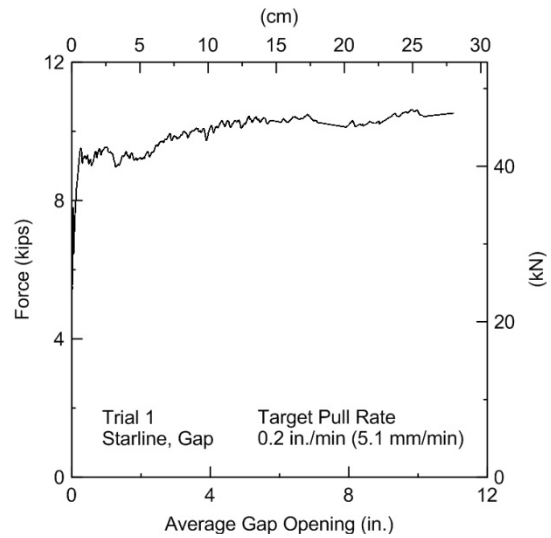

Figure 2.5.4. Backbone Curve, Trial 1

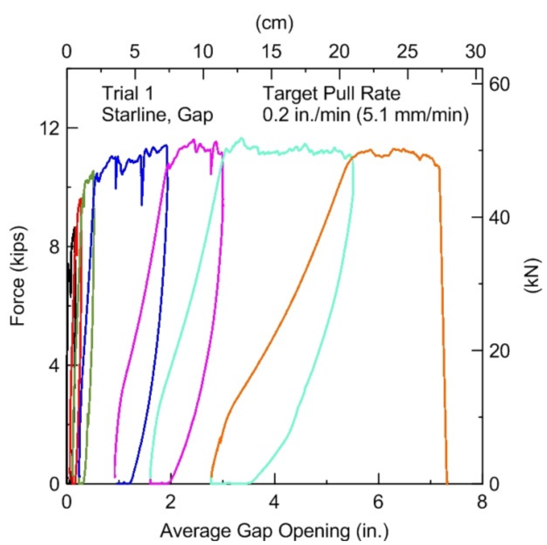

Figure 2.5.5. Force vs. Average Gap Opening, Trial 2

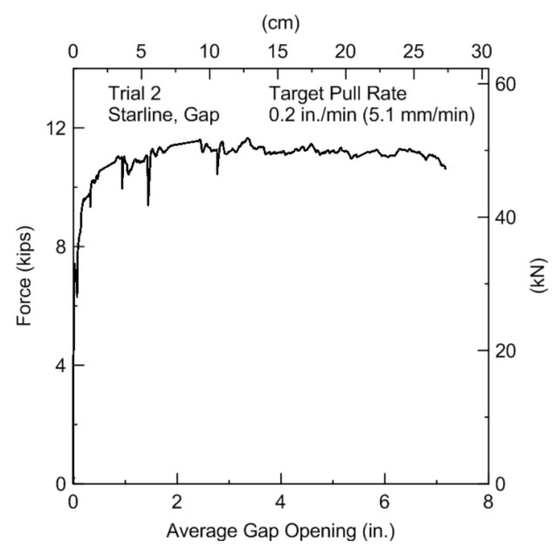

Figure 2.5.6. Backbone Curve, Trial 2

<u>Trial 3</u>

The pipe for Trial 3 was a new section of Starline lined DI with a gap. The target loading rate for Trial 3 was 0.2 in./min (5.1 mm/min.) The pipe was pressurized to 75 psi (517 kPa) internal pressure. The steps of Trial 3 are the following:

1) Step 1: Axial pull until 0.07in. (1.78 mm) of gap opening and unloading until there is no force.
2) Step 2: Axial pull until 0.14in. (3.56 mm) of gap opening and unloading until there is no force.
3) Step 3: Axial pull until 0.37in. (9.4 mm) of gap opening and unloading until there is no force.
4) Step 4: Axial pull until 0.83in. (21.08 mm) of gap opening and unloading until there is no force.
5) Step 5 (Cycle 1): Axial pull until 1.77in. (44.96 mm) of gap opening and unloading up to 0.33in. (8.38 mm) of gap opening and compressive force.
6) Step 6 (Cycle 2): Axial pull until 1.81in. (45.97 mm) of gap opening and unloading up to 0.41in. (10.41 mm) of gap opening and compressive force.

7) Step 7 (Cycle 3): Axial pull until 1.81in. (45.97 mm) of gap opening and unloading up to 0.62in. (15.75 mm) of gap opening and compressive force.
8) Step 8 (Cycle 4): Axial pull until 1.81in. (45.97 mm) of gap opening and unloading up to 0.42in. (10.67 mm) of gap opening and compressive force.
9) Step 9 (Cycle 5): Axial pull until 1.82in. (46.22 mm) of gap opening and unloading up to 0.41in. (10.41 mm) of gap opening and compressive force.
10) Step 10 (Cycle 6): Axial pull until 1.81in. (45.97 mm) of gap opening. Liner ruptured.

The maximum force was reached during step 5 (cycle 1), and then 5 subsequent cycles of loading were applied at similar levels of maximum displacement in each of these cycles. The gap was pushed back to a position near the initial condition at the end of each loading and unloading cycle, until the liner ruptured during axial pull at a gap opening of 1.79 in. (4.55 cm) and a force equal to 18.24 kips (81.14 kN). At the end of cycles 1 through 5 folding of the liner in the gap was observed. The actuator force vs. average incremental gap opening is shown in Figure 2.5.7 for all loading steps. The actuator force vs. incremental gap opening is shown in Figure 2.5.8.

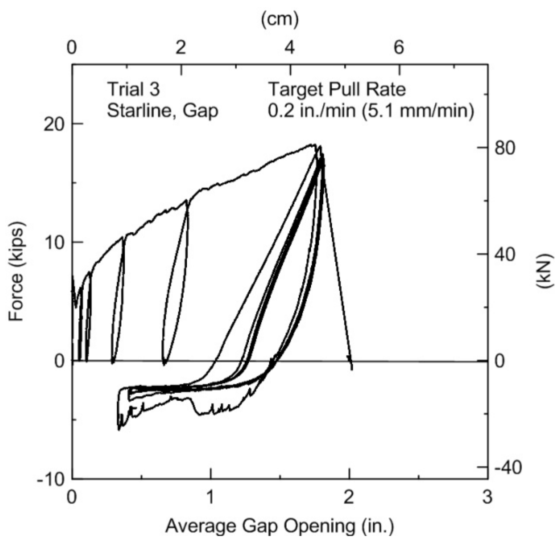

Figure 2.5.7. Force vs. Average Gap Opening, Trial 3

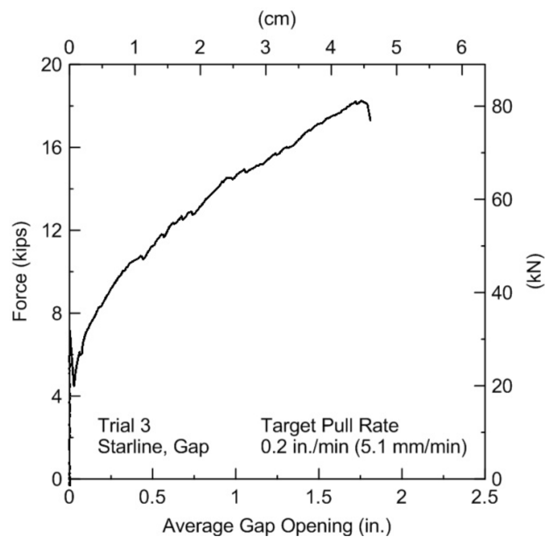

Figure 2.5.8. Backbone Curve, Trial 3

Trial 4

The pipe for Trial 4 was a new section of Starline lined DI with a gap. The target loading rate for Trial 4 was 0.2 in./min (5.1 mm/min.). The pipe was pressurized to 75 psi (517 kPa). In this test target incremental gap openings of 0.25. 0.5, 0.75. 1.0 and 1.0 in. (6.4, 12.7, 19.1, 25.4, and 25,4 mm) were targeted for each cycle. Once the target gap opening was achieved, the gap was closed to near its initial position, and the next incremental gap opening was applied. On the final cycle (cycle 6), the gap was returned to an opening of 0.3 in. (7.6 mm) and the gap was filled with a relatively stiff foam wrapping to investigate folding of the liner within the gap as if the pipe was buried in soil. The foam was placed to see what effect infilling the gap might have on subsequent response. The gap was then opened to failure. The liner failed at a gap opening of 3.12 in. (7.92 cm) and a force of 20.28 kips (90.2 kN). The actuator force vs. average incremental gap opening is shown in Figure 2.5.9 for all loading steps. The actuator force vs. incremental gap opening is shown in Figure 2.5.10.

Trial 5

The pipe for Trial 5 was a new test section of Starline lined DI. The central portion of the specimen was a bell-and-spigot joint. The target loading rate for Trial 5 was 20 in./min (50.8 mm/min.). The pull for this test was on the bell end of the specimen and the specimen was subjected to monotonic loading until liner failure. The liner failed at a peak force of 18.5 kips (82.29 kN) at an incremental joint opening of 3 in. (7.62 cm). The data acquisition system failed during testing and there were no data collected apart from data from the beginning and the end of the test. Figure 2.5.11 shows the actuator force vs. actuator displacement which were the only results acquired during the test.

Trial 6

The pipe for Trial 6 was a new test section of Starline lined DI. The central portion of the specimen was a bell-and-spigot joint. The pipe was pressurized to 75 psi (517 kPa). The target loading rate for Trial 6 was 20 in./min (508 mm/min.). The pull for this test was on the bell end of the specimen. The liner was subjected to monotonic loading and failed at a peak force of 20.7 kips (90.08 kN) at an incremental joint opening of 2.78in. (7.06 cm). The actuator force vs. average incremental joint opening is shown in Figure 2.5.12.

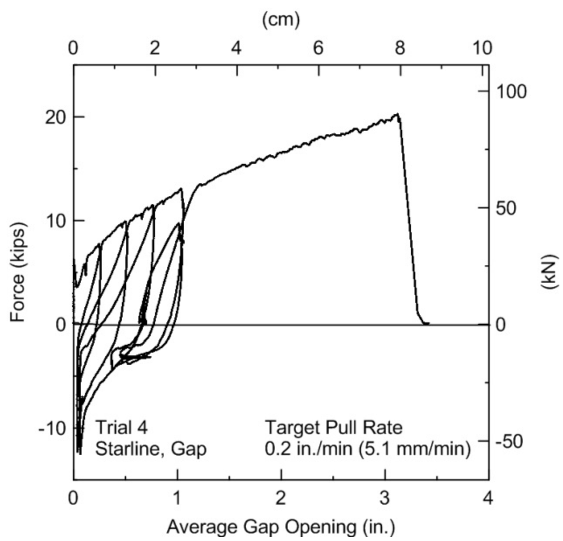

Figure 2.5.9. Force vs. Average Gap Opening, Trial 4

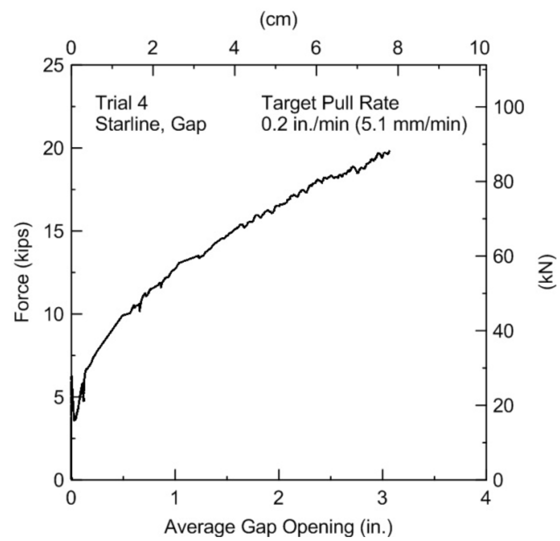

Figure 2.5.10. Backbone Curve, Trial 4

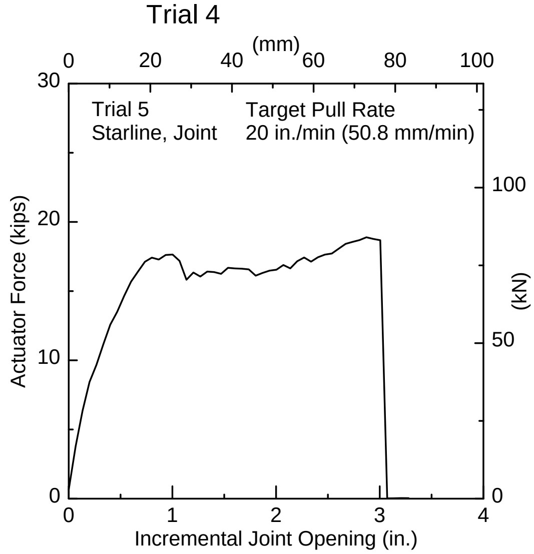

Figure 2.5.11. Force vs. Joint Opening, Trial 5

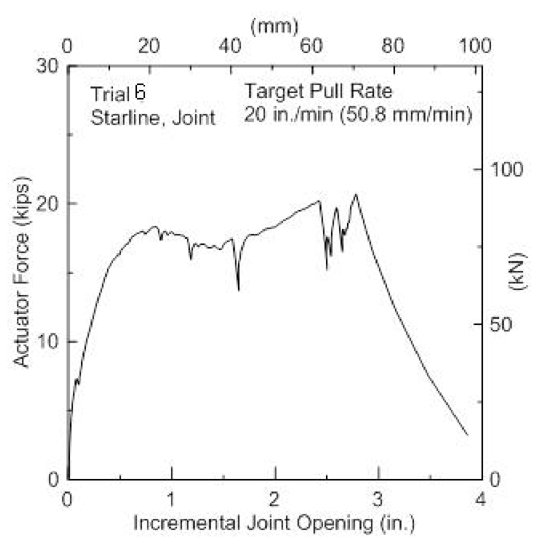

Figure 2.5.12. Force vs. Joint Opening, Trial 6

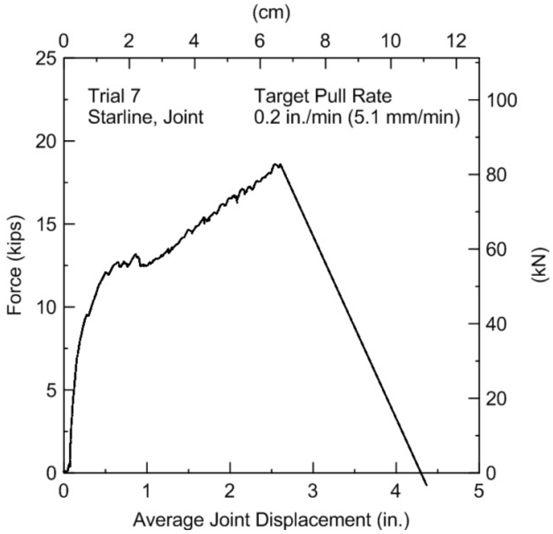

Figure 2.5.13. Force vs. Joint Opening, Trial 7

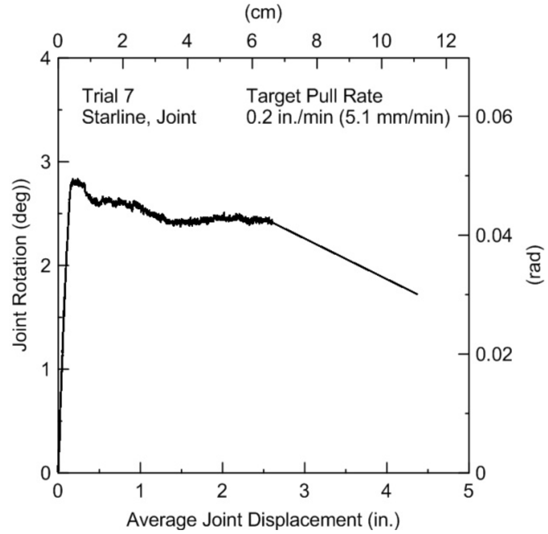

Figure 2.5.14. Joint Rotation vs. Joint Opening, Trial 7

Trial 7

The pipe for Trial 7 was a new test section of Starline lined DI. The central portion of the specimen was a bell-and-spigot joint. The pipe was pressurized to 75 psi (517 kPa). The target loading rate for Trial 6 was 0.2 in./min (5.1 mm/min.). The pull for this test was on the spigot end of the specimen. An initial joint rotation of approximately 2.5º was applied using a screw jack beneath the bell at the joint located 3 in. (7.6 cm) into the bell side from the bell face. This rotation was applied before the actuator began making the axial pull. The liner was then subjected to monotonic axial pull and failed at a peak force of 18.59 kips (82.69 kN) at an average incremental joint opening of 2.61in. (6.63 cm). The actuator force vs. average incremental joint opening is shown in Figure 2.5.13.

2.5.4. Summary of Starline Loading Rate Tests

This report presents the measurements made during a series of seven full-scale tests of Starline lined ductile iron pipe gap and joint specimens. The purpose of the tests was to:

a) Determine the capacity of the Starline 2000 liner.
b) Determine if the rate of axial pull affects the load-displacement results.
c) Investigate the effects of an initial join rotation on potential debonding between the liner and the host pipe.
d) Investigate the sensitivity of the lined pipe response to internal pressure.

The results from this series of tests on showed that there is significant effect of the internal pressure on the response of gap and joint specimens lined with the Starline2000 system. Figure 2.5.15 shows a comparison of the backbone curves of Trials 1 through 4. Internal pressure increases the strength of the lined specimens significantly and changes the failure mechanism from complete debonding of the liner from the host pipe (Trials 1 and 2) to a more abrupt liner rupture at the connection (Trials 3 and 4). Trials 3, 4 and 6 were axial pull tests performed at loading rates of 0.2 in./min (5.1 mm/min), 0.2 in./min (5.1 mm/min), and 20 in./min (508 in./min), respectively. The backbone curves of these three tests are presented in Fig. 2.4.16 and do not indicate any significant effect of the loading rate on the response of joints lined with Starline2000® System, apart from the initial increased stiffness that is observed in Trial 6 where the loading rate is two orders of magnitude higher than in Trials 3 and 4.

Overall, the specimens that were pressurized at a constant pressure of 75 psi (517 kPa) failed consistently at joint/gap openings ranging from 2.6 to 3 in. (6.6 to 7.62 cm) with maximum force ranging from 18.5 to 20.7 kips (82.29 to 92.08 kN). Trials 4, 5, and 6 were conducted with constant internal pressure of 75 psi (517

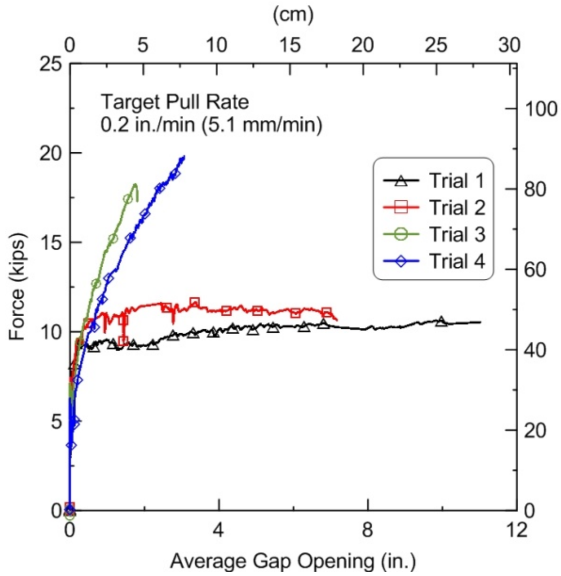

Figure 2.5.15. Backbone Curves, Trials 1, 2, 3 and 4

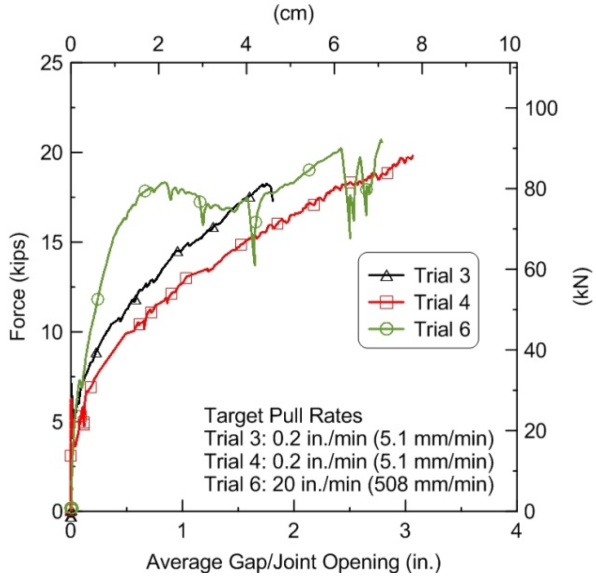

Figure 2.5.16. Backbone Curves,, Trials 3, 4 and 6

kPa) that simulates real field conditions. Table 2.5.3 provides a summary of the test results. Trial 7 was a combined axial pull and rotation test with an applied rotation of approximately 2.5°. When the liner was subjected to combined axial pull and rotation, the debonded length of the liner at the joint was similar to the debonded length that was observed during the pure axial pull tests. Therefore, initial rotation does not seem to have a significant effect of liner debonding.

Table 2.5.3. Summary of Starline Pull Tests

Trial No.	Specimen	Loading Rate (in./min)	Nominal Pressure (psi)	Failure Mode	Max. Force (kips)	At Joint Opening of (in.)
1	New Pipe	0.2	0	Liner Slip	10.6	9.84
2	New Pipe	0.2	0	Liner Slip	7.17	1.24
3	New Pipe	0.2	75	Liner Rupture	18.24	1.79
4	New Pipe	0.2	75	Liner Rupture	20.28	3.12
5	New Pipe	20	75	Liner Rupture	18.5	3
6	New Pipe	20	75	Liner Rupture	20.7	2.78
7	New Pipe	0.2	75	Liner Rupture	18.59	2.61

3.0 UNIVERSITY AT BUFFALO

Experimental Study

3.1 Test Set-up and Instrumentation

The two 50-metric-ton (55 tons), 7 m x 7 m (23 ft. x 23 ft.), re-locatable shake tables at the University at Buffalo (UB) NEES Site (UB-NEES) were utilized in Year 2 and Year 3 to conduct two series of tests on eight full scale ductile iron (DI) water pipelines with 150 mm (6.0 in.) nominal diameter, and 9.14 m (30 ft.) nominal length, as shown in Figure 3.11. Each pipeline specimen had two push-on joints located at its 1/3 spans. All the eight DI pipeline specimens were reinforced with cured in place pipeline (CIPP) liner technology as shown in Figure 3.1.2. Two different types of CIPP liners commonly used in practice in the US were selected to retrofit the pipeline specimens. Four DI pipeline specimens were reinforced with Insituform IMain liner, manufactured by Insituform Technologies, LLC, Chesterfield, Missouri, and four DI pipeline specimens were reinforced by Starline® 2000 liner, manufactured by Progressive Pipeline Management, LLC, West Deptford, New Jersey. Monotonic, cyclic and dynamic (seismic) tests were performed on the eight pipeline specimens under transient ground deformations (TGD). Two shake tables were required to simulate the differential axial motions at two adjacent weak joints separated by a 3.66-m (12-ft.) pipeline segment. Joint movements were derived from numerical models of seismic wave interaction with jointed pipelines conducted by researchers at Cornell University (Dimitra Bouziou, personal communication, 2013; Shi and O'Rourke, 2008; Wang and O'Rourke, 2008). Because the models account for soil-pipeline interaction, soil was not included in the tests at the University at Buffalo.

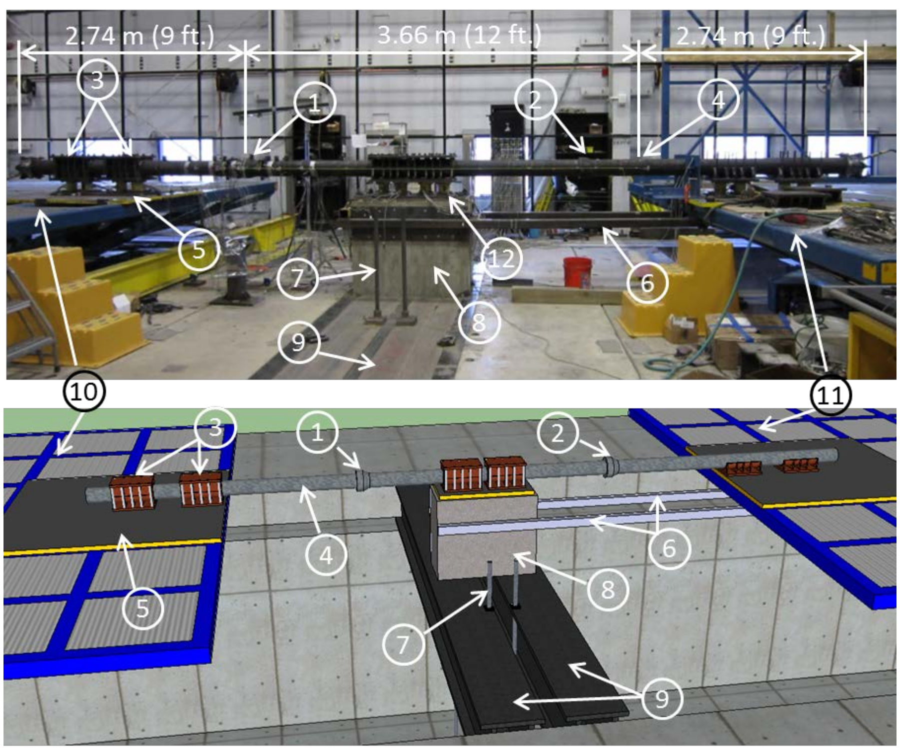

1. West Joint
2. East Joint
3. Steel Clamp
4. Pipe Specimen
5. Mounting Plate
6. HSS Beam
7. Post-tension Steel Rod
8. Central Concrete Pedestal
9. Steel Girder
10. West Shake Table
11. East Shake Table
12. Load Cell

Figure 3.1.1. Three-Dimensional Overview of Test Set-up

The main objectives of the experimental study were: (1) to develop a test set-up for evaluating the seismic response of full-scale water pipelines reinforced with CIPP liners under TGD, (2) to characterize the seismic response and failure mechanisms of full-scale water pipelines with two types of CIPP liners (Insituform IMain liner and Starline® 2000 liner) under TGD, (3) to quantify the contribution of the two CIPP lining systems to the seismic performance of pressurized push-on pipe joints under TGD and, (4) to compare the different failure characteristics of the DI pipeline joints reinforced with the two types of CIPP liners under both static and dynamic loading.

Over 100 sensors were deployed along each DI pipeline specimen to measure the response of each joint. Most of the instrumentation sensors were located in the vicinity of the two push-on joints of each DI pipeline specimen. Figure 3.1.3 shows a close-up view of a typical instrumented push-on joint. Four potentiometers and eight LED sensors of the KRYPTON system were placed around the joints to measure the joint opening and rotation in both the axial and transverse directions of the pipeline. Moreover, four string potentiometers were installed close to the joint as secondary instrumentation to measure the axial joint opening in the event that the potentiometers have reached their capacity. Four accelerometers were installed close to the joints for the dynamic tests to measure accelerations on the spigot and the bell of the joint. Because the Starline® 2000 liner is relatively flexible with a low tensile capacity, a steel joint-restraint was installed before each test to protect the joint from initial loading when tightening the steel clamps at the two ends of the pipeline and adjusting the shake tables. The two threaded steel bars of the joint-restraint system were removed at the beginning of each test after completing all the calibration of the shake table and instrumentation.

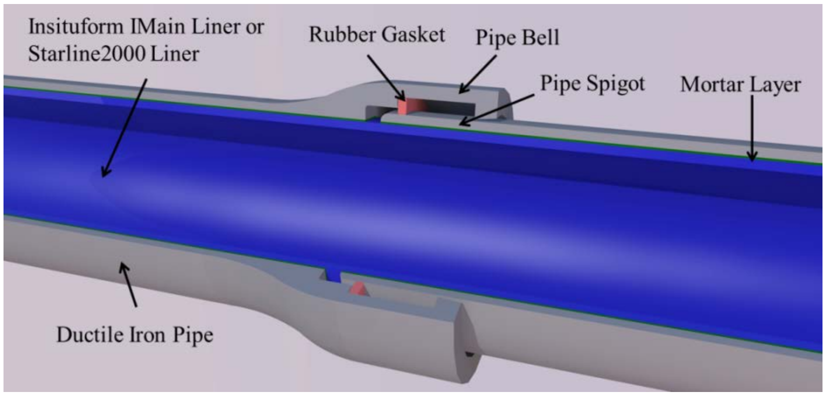

Figure 3.1.2. Cross Section of DI pipe with Two Types of CIPP Liner: Insituform IMain Liner or Starline® 2000 Liner

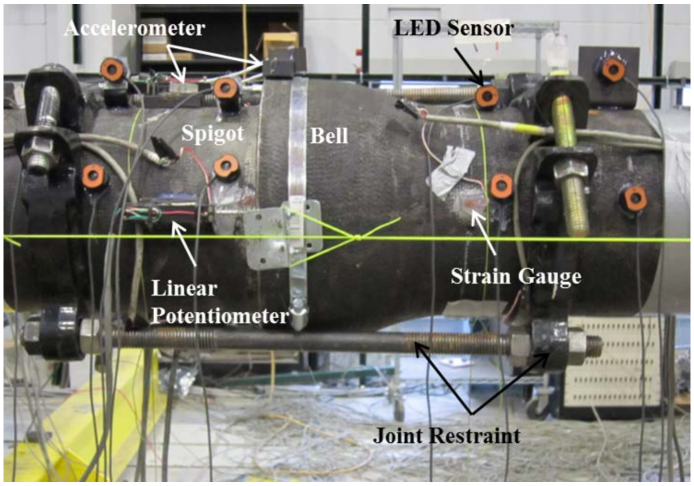

Figure 3.1.3. Close-up View of Instrumented Push-on Joint

Figure 3.1.4. Tool for Liner Inspection

An inspection of the liner was performed on all the tested pipeline specimens that exhibited liner failure to determine the exact failure locations along the liner's length. As shown in Figure 3.4, a special inspection tool incorporating a camera attached to a stainless steel pole was assembled to observe the damage of the liner inside the pipelines after the tests. The camera could be rotated inside the pipeline to inspect the inner surface of the liner and find the shape and location of the failure plane in the liner.

3.2 Test of DI Pipelines with Insituform IMain liner

Table 3.2 1 lists the test protocol for the four DI pipeline specimens reinforced with the Insituform IMain liner. This test protocol included single- and double-joint tests of water-pressurized DI pipeline specimens under monotonic, cyclic and dynamic (seismic) loading. For the single-joint dynamic tests, two different input motions were considered. The first input motion was the near-field Rinaldi ground motion recorded during the 1994 Northridge earthquake. The second input motion, originated from the far-field Joshua-Tree (J-T) records from the 1992 Landers Earthquake. For the double-joint dynamic tests, asynchronous Rinaldi input motions were utilized at each joint to represent the effect of wave propagation along the pipe specimen. The relative joint opening time histories obtained from the numerical analysis at Cornell University were used as the input ground motions for the seismic tests. Figure 3.2.1 shows the full-scale (100%) ground motions used for the seismic tests on the pipeline specimens reinforced with the Insituform IMain liner.

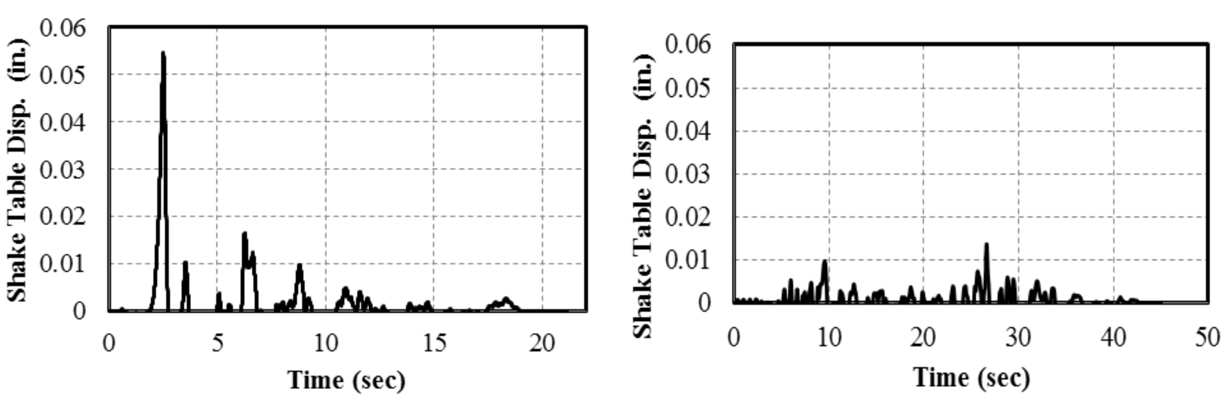

(a) Full-Scale Rinaldi Input Motion (b) Full-Scale Joshua-Tree Input Motion

Figure 3.2.1. Input Motion for Dynamic Tests of Pipeline with Insituform IMain Liner (Bouziou, 2013; Shi and O'Rourke, 2008; Wang and O'Rourke, 2008).

Table 3.2.1. Test Protocol for Shake Table Tests of DI Pipe with IMain Liner

Test No.	Specimen No.	Joint Name	Test Description	Input Loading Description	Test Date
1	SP1	East Joint	Monotonic Tensile Test (Single Joint)	Ramp Loading (1.27 mm/min. or 0.05 in./min.)	11-21-2011
2		West Joint	Cyclic Tensile Test (Single Joint)	Cyclic Load (5.08 mm/min. or 0.2 in./min.)	11-21-2011
3	SP2	East Joint	Cyclic Tensile Test (Single Joint)	Cyclic Load (1.27 mm/min. or 0.05 in./min.)	12-05-2011
4		East Joint	Cyclic Tensile Test (Single Joint)	Cyclic Load with Different Loading rates	12-07-2011
5		West Joint	Dynamic Test (Single Joint)	From 50% to 125% Rinaldi GM	12-12-2011
6		West Joint	Dynamic Test with Damaged Liner (Single Joint)	150% Rinaldi GM	12-16-2011
7	SP3	Double Joints	Dynamic Tests with Dual Shake Tables	From 50% to 200% Rinaldi GM	12-21-2011
8	SP4	East Joint	Dynamic Test (Single Joint)	From 300% to 570% J-T GM	02-17-2012
9		West Joint	Dynamic Test (Single Joint)	550% J-T GM	02-23-2012

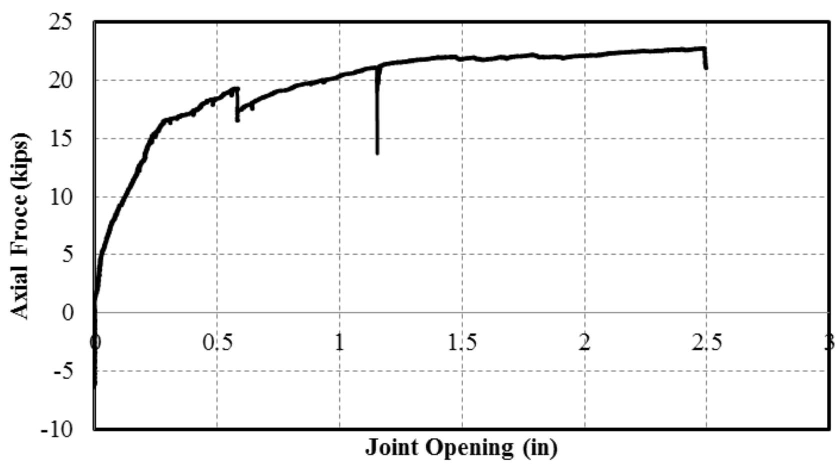

Figure 3.2.2. Axial Force-Joint Opening Relationships from Monotonic Test on SP1 East Joint

For the tests on the DI pipeline specimens reinforced with the Insituform IMain liner, two basic modes of failure were observed during the test series. The first failure mode was characterized by ductile response due to debonding of the liner from the pressurized DI pipe, as shown in Figure 3.2.2, for the monotonic test on the SP1 east joint (Test No. 1 in Table 3.2.1). The force-displacement relationship of the joint is ductile with a joint opening of 63.5 mm (2.5 in.) and a peak axial force of 100 kN (22.5 kips) without failure of the liner.

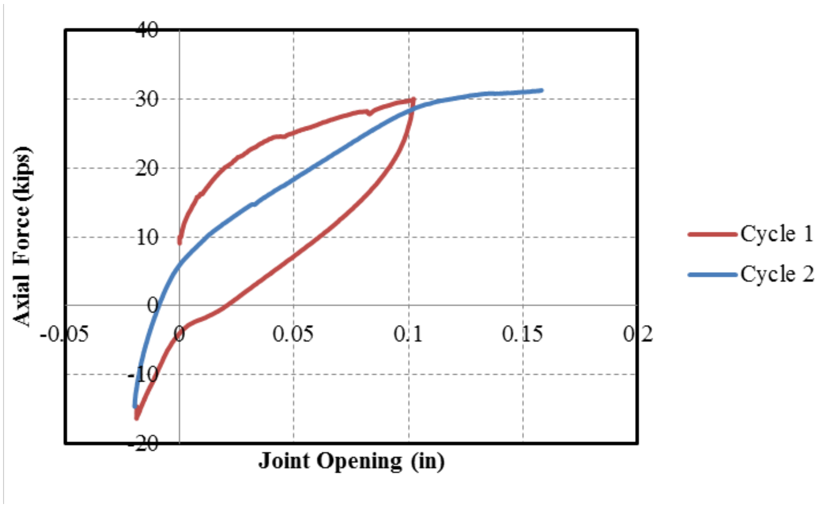

Figure 3.2.3. Axial Force-Joint Opening Hysteretic Responses from Cyclic Tensile Test on SP1 West Joint

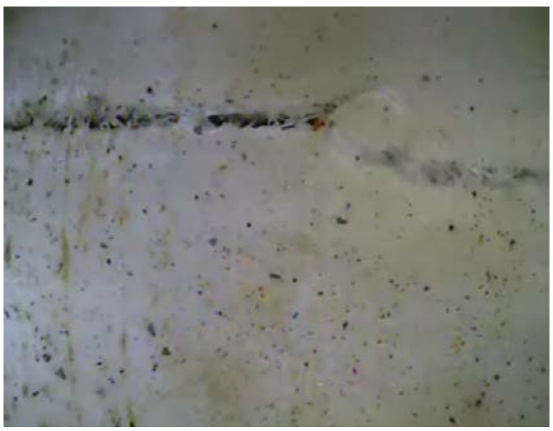

Figure 3.2.4. Liner Failure of SP1 West Joint

The second mode of failure was characterized by a brittle failure of the liner at much reduced joint opening, as shown in Figure 3.2.3 for the cyclic tensile test on the SP1 west joint (Test No. 2 in Table 3.2.1). Failure of the liner occurred in the second cycle of loading at a peak axial force of 139 kN (31.3 kips) and a joint opening of only 4.06 mm (0.16 in.) The gasket in the push-on joint accommodated this large joint opening without leakage. Figure 3.2.4 shows a typical non-uniform failure in the Insituform IMain liner close to the spigot end of SP1 west joint after the cyclic tensile tests.

Figure 3.2.5 shows the hysteretic response of the SP2 east joint, which was tested under cyclic tensile loading with a loading rate of 1.27 mm/min (0.05 in./min) (Test No.3 in Table 3.1). It was observed that when the joint opening is smaller than 0.25 mm (0.01 in.) the joint exhibits a constant stiffness of approximately 150 kN/mm (850 kips/in.) during loading. However, after the joint opening exceeds 0.25 mm (0.01 in), the axial stiffness of the joint decreases significantly. This stiffness degradation associated with a ductile response is mainly attributed to the debonding between the liner and the pipeline, which has led to a continuous increase of the un-bonded length of the liner as the test progressed. It is important to note that the loading rate in the range of 1.27 mm/min (0.05 in./min) to 127 mm/min. (5.0 in/min.) did not affect significantly the behavior of the push-on joints, as shown in Figure 3.2.6 for the cyclic tests conducted on the SP2 east joint (Test No. 4 in Table 3.2.1).

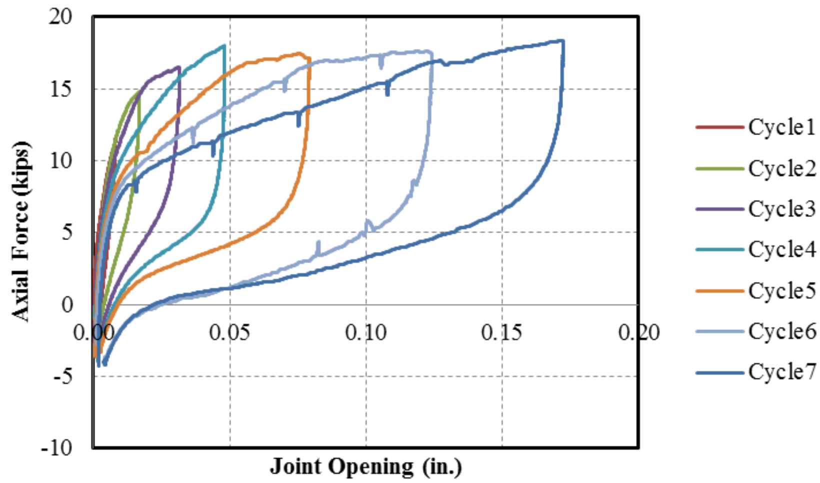

Figure 3.2.5. Axial Force-Joint Opening Hysteretic Responses from Cyclic Tensile Test on SP2 East Joint

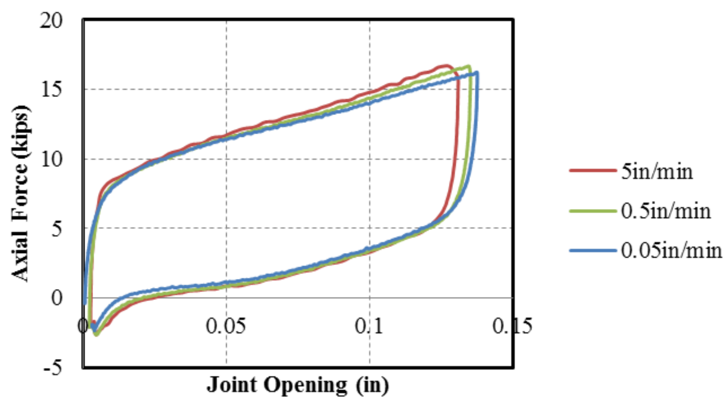

Figure 3.2.6. Axial Force-Joint Opening Hysteretic Responses from Cyclic Tensile Tests on SP2 East Joint

Figure 3.2.7 compares the axial force-joint opening hysteretic responses from all the seismic tests. For the single-joint seismic tests with the Rinaldi ground motion (Test No.5 in Table 3.1), the SP2 west joint did not fail up to amplitude of 125% of full-scale. This set of tests was terminated due to a malfunction of the west shake table, which caused the liner to fail in the joint prior the start of the next scheduled test to amplitude of 150% of full-scale. For the single-joint seismic tests with J-T input motion (Test No.8 in Table 3.2.1), the SP4 east joint remained undamaged for amplitude of 570% of the full-scale. For the double-joint seismic tests with the Rinaldi ground motion (Test No.7 in Table 3.2.1), only the SP3 west joint failed at amplitude of 200% of full-scale. These test results indicate that the pipeline specimens reinforced with the Insituform IMain liner were able to accommodate very high intensities of ground motions. Also, the characteristics of the input motions (near-field vs. far-field) did not affect significantly the behavior of the push-on joints, as evidently shown in Figure 3.2.8 for the 190% Rinaldi and 550% Joshua-Tree dynamic tests.

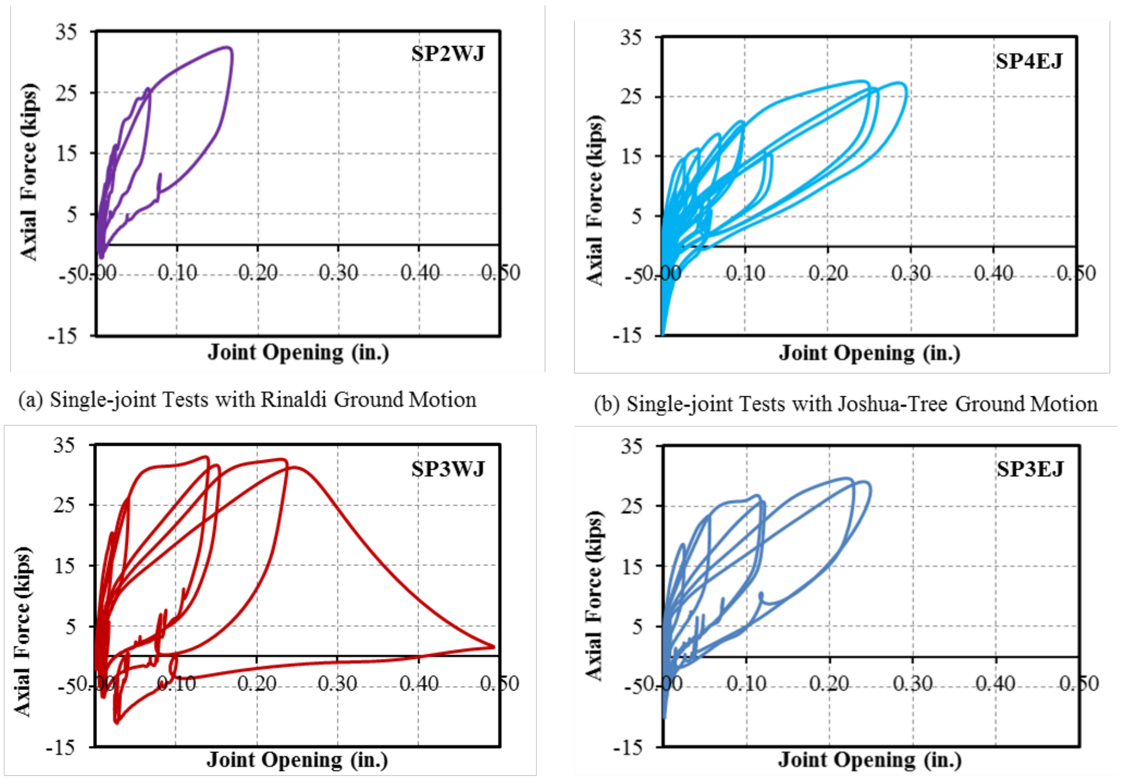

(a) Single-joint Tests with Rinaldi Ground Motion

(b) Single-joint Tests with Joshua-Tree Ground Motion

West Joint

East Joint

(c) Double-joint Tests with Rinaldi Ground Motion

Figure 3.2.7. Axial Force-Joint Opening Hysteretic Responses of DI Joints Retrofit with Insituform IMain Liner under Seismic Loading

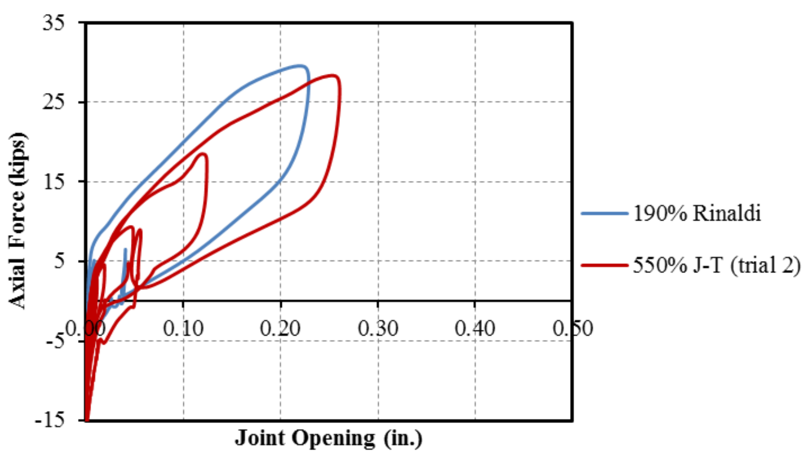

Figure 3.2.8. Axial Force-Joint Opening Hysteretic Responses for the 190% Rinaldi and 550% Joshua-Tree Dynamic Tests

An inspection of the liner was performed on the four tested pipeline specimens that exhibited liner failure to determine the exact failure locations along the liner's length. The inspection was conducted using the special inspection tool described above. The results of the inspection indicated that the liner failed almost at the center of each joint or at the end of the spigot inside the bell of the push-on joint. The shape of the liner fractures were a zigzag pattern with some parts of the liner remaining attached, as shown in Figure 3.2.9.

Figure 3.2.9. Failure Plane of Insituform IMain Liner

3.3 Tests of DI Pipelines with Starline® 2000 Liner

Table 3.3.1 lists the test protocol for the four DI pipeline specimens reinforced with the Starline® 2000 liner. Similar to the tests performed in Year 2, single- and double-joint tests on the pressurized DI pipeline specimens under monotonic, cyclic and dynamic (seismic) loading were conducted. Figure 3.3.1 shows the full-scale (100%) ground motions used for the seismic tests on the pipeline specimens reinforced with the Starline® 2000 liner. The relative joint opening time histories obtained from the numerical analysis at Cornell University were again used as input motions for the seismic tests.

Four basic failure modes for the DI pipeline specimens reinforced with the Starline® 2000 were observed during this test series. The first failure mode was characterized by a “ductile” debonding of the liner from the DI pipeline, as shown in Figure 3.3.2 for the monotonic tensile test on the SP1 east joint (Test No. 1 in Table 3.3.1). After applying a water pressure of 310 kPa (45 psi) to the pipeline specimen, the valves located at the two ends of specimen were closed before the start of the monotonic test. Therefore, the internal water pressure dropped with the elongation of the joint. No liner failure or water leakage was observed in this test.

Table 3.3.1. Test Protocol for Shake Table Tests of DI Pipelines with Starline® 2000 Liner

Test No.	Specimen name	Joint name	Test description	Input Loading description	Test date
1	SP1	East Joint	Monotonic tensile (single Joint)	Ramp loading (1.27 mm/min. or 0.05 in./min.)	02-22-2013
2		West Joint	Monotonic tensile (single Joint)	Ramp loading (2.54 mm/min. or 0.1 in./min.)	02-26-2013
3	SP2	East Joint	Cyclic tensile (single joint)	Cyclic loading with 330 kPa (48 psi) water pressure (1.27 mm/min.~5.08 mm/min. or 0.05 in./min.~0.2 in./min.)	03-01-2013
4		West Joint	Cyclic tensile (single joint)	Cyclic loading with 110 kPa (16 psi) water pressure (1.27 mm/min.~5.08 mm/min. or 0.05 in./min.~0.2 in./min.)	03-06-2013
5	SP3	East Joint	Seismic (single joint)	From 100% to 200% Rinaldi	03-13-2013
6		West Joint	Seismic (single joint)	From 300% to 900% Joshua-Tree	03-19-2013
7	SP4	Double Joints	Seismic (double joints)	From 50% to 2.25*260% Rinaldi	03-22-2013

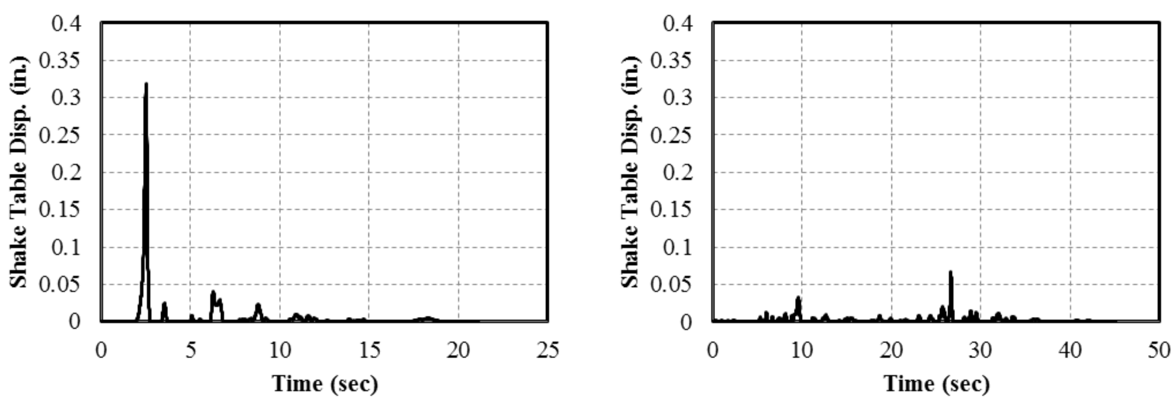

(a) Full-scale Rinaldi Input Motion (b) Full-scale Joshua-Tree Input Motion

Figure 3.3.1. Input Motion for Dynamic Tests of Pipeline with Starline® 2000 Liner (Dimitra Bouziou, personal communication, 2013; Shi and O'Rourke, 2008; Wang and O'Rourke, 2008).

The second failure mode was characterized by a combination of "ductile" debonding of the liner from the DI pipeline and partial failure of the liner at the end of the spigot, as shown in Figure 3.3.3 for the monotonic tensile test on the SP2 west joint (Test No. 2 in Table 3.3.1). In this test, the water pressure was regulated manually and was maintained at approximately 320 kPa (46 psi). The liner remained undamaged when the SP2 west joint opening reached 121 mm (4.78 in.). However, the liner folded into the gap between the spigot and the bell when the joint was closed resulting in a partial failure of the liner when the joint was subjected to high axial compressive forces, as shown in Figure 3.3.4.

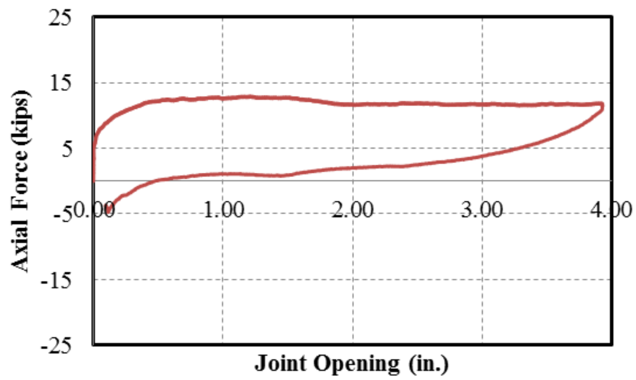

Figure 3.3.2. Axial Force-Joint Opening Relationships from Monotonic Tensile Test on SP1 East Joint

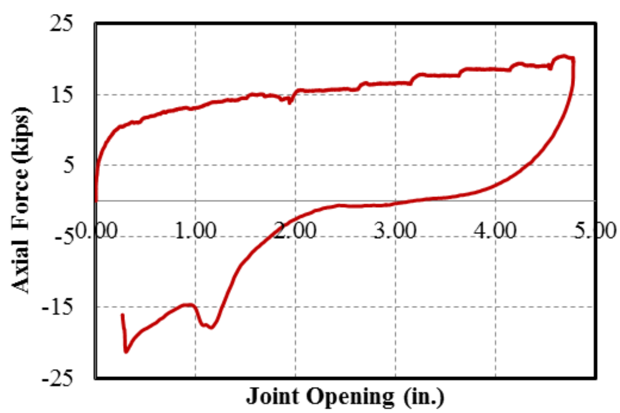

Figure 3.3.3. Axial Force-Joint Opening Relationships from Monotonic Tensile Test on SP1 West Joint

The third failure mode was observed during the cyclic tensile tests (Test No. 3 and 4 in Table 3.3.1) and was characterized by a tensile failure of the liner at reduced joint openings, as shown in Figure 3.3.5. Two cyclic tensile tests with a constant internal water pressure of 330 kPa (48 psi) and 110 kPa (16 psi) were performed on the SP2 east joint (EJ) and west joint (WJ), respectively. Significant pinching effects were observed during the tests when the peak joint openings exceeded 0.4 in. The liner in both joints failed in tension at a joint opening of 55.9 mm (2.2 in.) Loud noises were heard during the tests and sever water leakage was observed at the moment the liner failed in both joints. Figure 3.3.6 shows the liner debonding and failure after pulling out the spigot from the bell of the damaged push-on joint after the test.

(a) Liner Folding (b) Liner Failure

Figure 3.3.4. Liner Folding and Failure of SP1 West Joint

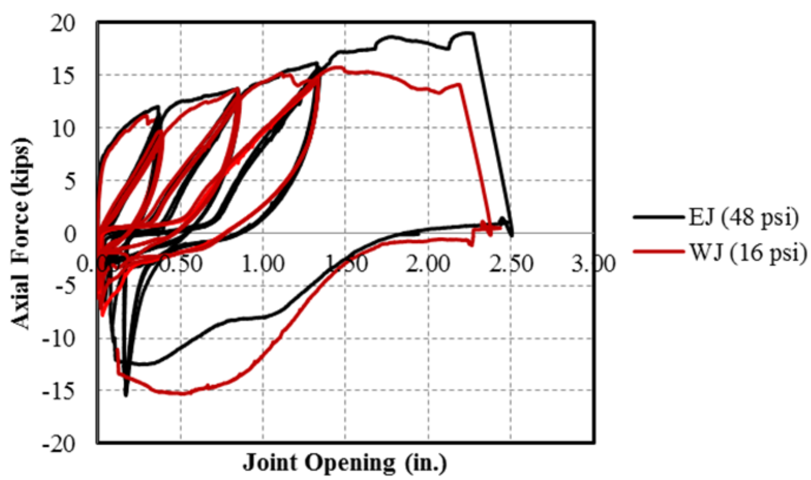

Figure 3.3.5. Axial Force-Joint Opening Hysteretic Responses from Cyclic Tensile Test on SP2 Specimen

The fourth failure mode was characterized by a brittle failure of the liner in tension at a very small joint opening, as shown in Figure 3.3.7 for the single-joint test with Rinaldi ground motion (Test No. 5 in Table 3.3.1). In this seismic test series, the SP3 east joint failed prematurely under the 160% Rinaldi input motion. No water leakage was observed during these tests as the gasket in the push-on joint accommodated the small joint opening and prevented water from leaking.

Figure 3.3.8 compares the axial force-joint opening hysteretic responses from all the seismic tests. For the single-joint seismic tests with the J-T ground motion (Test No. 6 in Table 3.3.1), the SP3 west joint failed at amplitude of 900% of full-scale. For the double-joint seismic tests with the Rinaldi ground motion (Test No. 7 in Table 3.3.1), the SP4 west joint failed at an amplitude equal to 2.25 * 260% of full-scale. These test results indicate that the pipeline specimens reinforced with Starline® 2000 liner were able to accommodate very high intensities of ground motions. The response of the joints reinforced with Starline® 2000 liner are insensitive to the different characteristics of seismic ground motions, i.e. the near-field directivity ground motions with single strong displacement pulse (Rinaldi ground motion) or the far-fault ground motions with

Figure 3.3.6. Liner Damage in SP3 East Joint after Cyclic Test

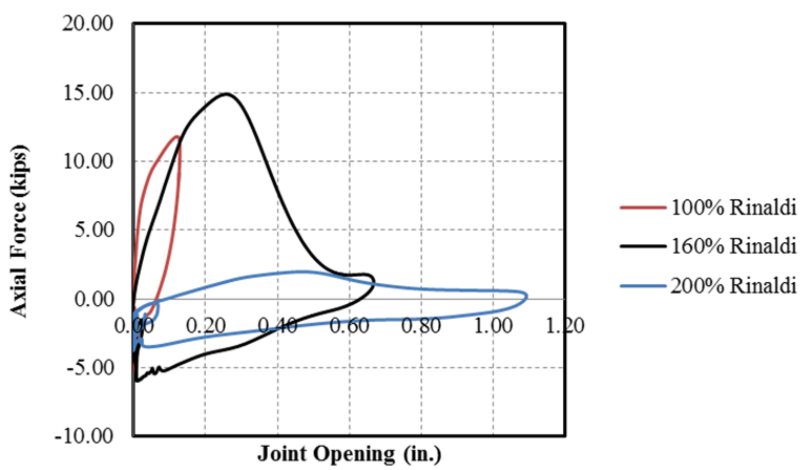

Figure 3.3.7. Axial Force-Joint Opening Hysteretic Responses from Single-Joint Test with Rinaldi Ground Motion on SP3 East Joint

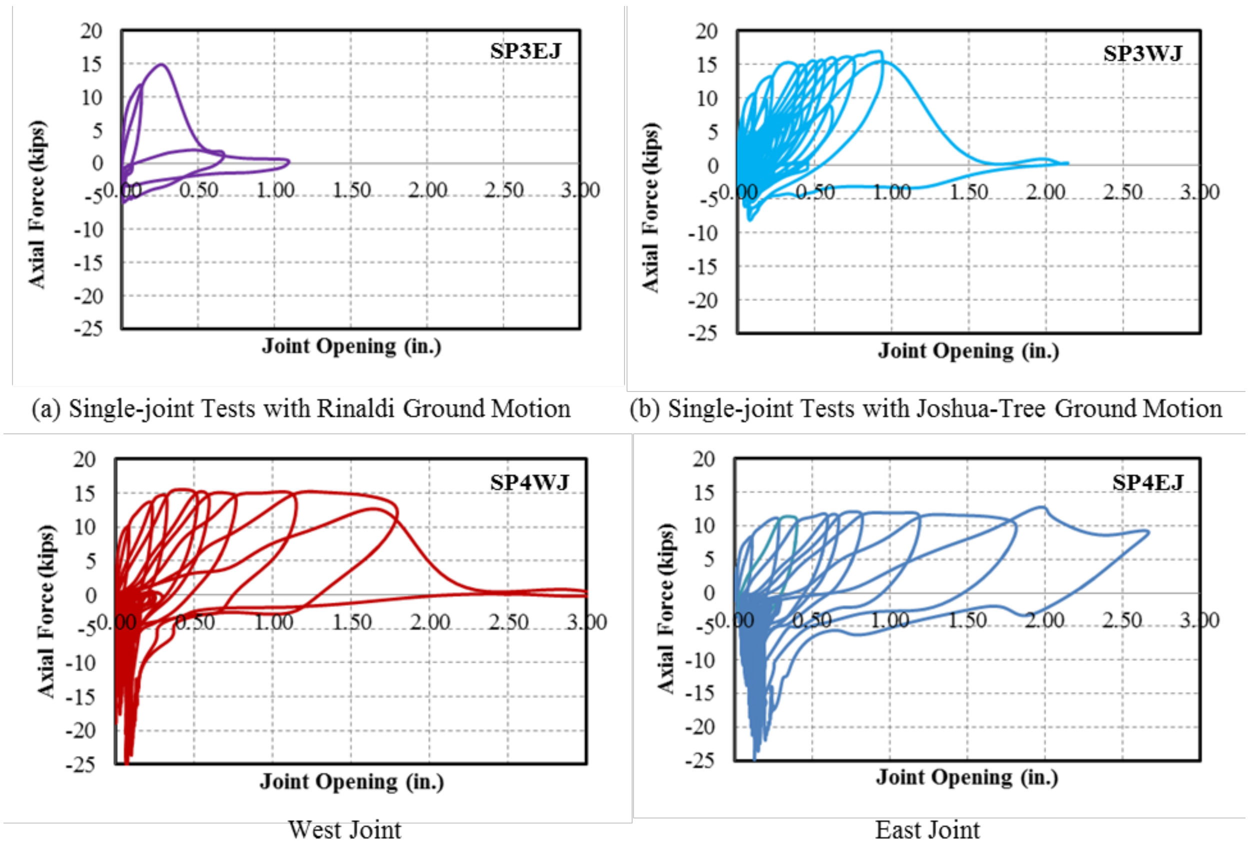

(a) Single-joint Tests with Rinaldi Ground Motion

(b) Single-joint Tests with Joshua-Tree Ground Motion

West Joint

East Joint

(c) Double-joint Tests with Rinaldi Ground Motion

Figure 3.3.8. Axial Force-Joint Opening Hysteretic Responses of DI Joints Reinforced with Starline® 2000 Liner under Seismic Loading

several displacement pulses (J-T ground motion). However, there could be some exception. When the initial bond between the liner and the DI pipeline is strong and the reinforced joint is subjected to a ground motion with a single strong displacement pulse, the debonding mechanism between the liner and the pipeline may not fully develop. In this case, the reinforced joint would behave in a brittle fashion and fail very early at a smaller joint opening. The tests results showed that pinching effect becomes significant after the joint opening exceeds about 12.7 mm (0.5 in), as shown in Figure 3.3.8 (b) and (c). In this case failure is induced by unfolding of the unbonded bulged liner in the joint. The near-field forward directivity ground motions with single strong displacement pulses (such as the Rinaldi ground motion) are more likely to cause the liner to fold into the gap between the spigot and the bell and lead to high compressive forces and large residual joint opening. However, the pinching effect is not favorable to the seismic behavior of the lined joint; the repetitive folding and compression of the liner between the spigot and the bell is likely to cause accumulated damage to the liner and thus, accelerate the failure of the liner.

The inspection of the liner was performed on the tested pipeline specimens to determine the exact location of the failure in the liner and the debonding length between the liner and the DI pipeline. Table 3.3.2 summarizes the liner inspection results from all the tested joints. In most of the tests the liner failure locations were very close to the end of the spigot. The liner at the end of the spigot becomes the weak link of the reinforced joint because of the poor initial bond between the liner and the pipeline. Moreover, the interaction between the liner and the spigot end during the tests could lead to accumulated damage to the liner and result in a liner failure concentrated at the spigot end of the joint. As shown in Figure 3.3.9, a linear relation between the peak joint opening and the total debonding length is observed from the tests results. A

Table 3.3.2. Summary of Liner Inspection

Test Name	Water Pressure	Joint Name	[1]Peak Joint Opening	Total Debonding Length	[2]Failure Location
Initial Debonding Length	NA		0	6.35 mm (0.25 in.)	
Monotonic Tests	310 kPa (45 psi), (closed valve)	EJ of SP1	97.8 mm (3.85 in.)	1010 mm (39.75 in.)	NA
Monotonic Tests	46 psi	WJ of SP1	120 mm (4.72 in.)	1321 mm (52 in.)	19.1 mm (0.75 in.)
Cyclic Tests	330 kPa (48 psi)	EJ of SP2	57.9 mm (2.28 in.)	718 mm (28.25 in.)	19.1 mm (0.75 in.)
Cyclic Tests	16 psi	WJ of SP2	54.1 mm (2.13 in.)	889 mm (35 in.)	12.7 mm (0.5 in.)
Single-joint Seismic Tests with Rinaldi Ground Motion	338 kPa (49 psi)	EJ of SP3	6.86 mm (0.27 in.)	159 mm (6.25 in.)	6.35 mm (0.25 in.)
Single-joint Seismic Tests with Joshua-Tree	330 kPa (48 psi)	WJ of SP3	23.11mm (0.91 in.)	387 mm (15.25 in.)	133 mm (5.25 in.)
Double-joint Seismic Tests with Rinaldi Ground Motion	330 kPa (48 psi)	WJ of SP4	42.2 mm (1.66 in.)	457 mm (18 in.)	6.35 mm (0.25 in.)
Double-joint Seismic Tests with Rinaldi Ground Motion	330 kPa (48 psi)	EJ of SP4	66.0 mm (2.60 in.)	673 mm (26.5 in.)	NA

Note: (1) If the liner did not fail in the test, the peak joint opening is the maximum joint opening. Otherwise, the peak joint opening is the joint opening at the moment of liner failure. (2) The distances were measured from the end of the spigot of each joint.

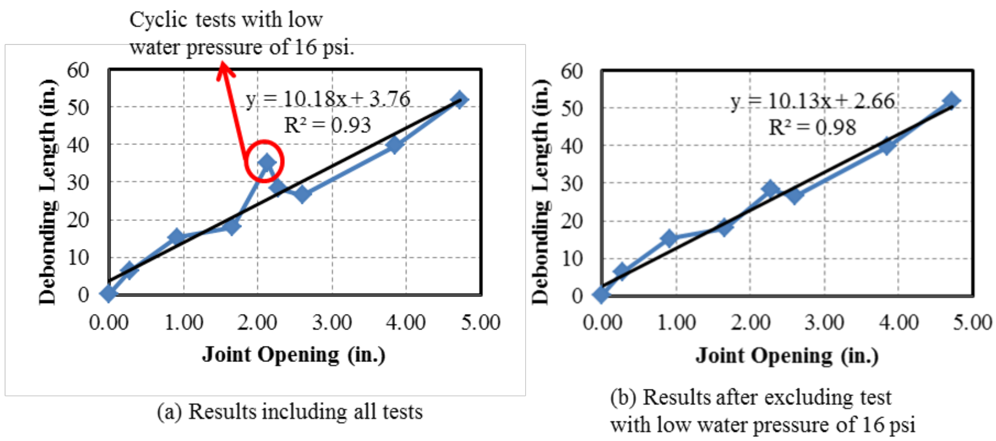

Figure 3.3.9. Relation between Joint Opening and Liner Debonding Length

better linear relation is obtained in Figure 3.3.9 (b) after removing the low pressure (110 kPa / 16 psi) cyclic tensile test. The total debonding measured after each test is about 10 times that of the peak joint opening.

3.4. Comparison of Test Results of Pipeline with Insituform IMain liner and Starline® 2000 liner

This section compares the seismic performance of the DI pipeline specimens reinforced with the two different types of CIPP liner considered in this research (Insituform IMain and Starline® 2000 liners) under two different ground motions (Rinaldi and J-T ground motions).

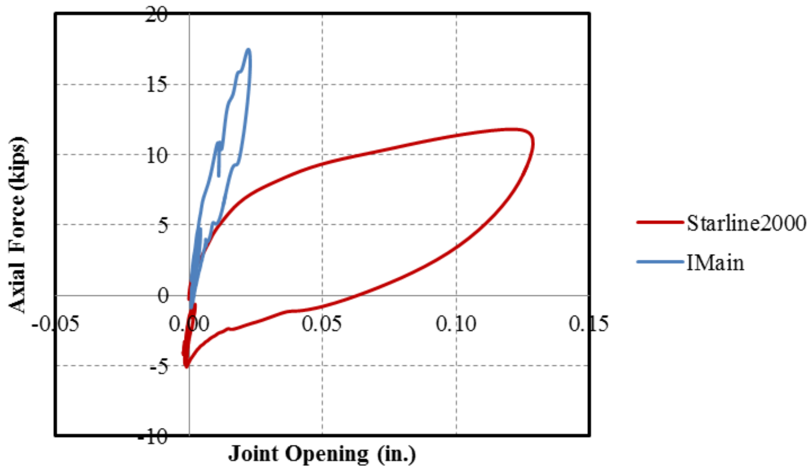

Figure 3.4.1. Single-Joint Seismic Tests with Full-Scale Rinaldi Ground Motion

Figure 3.4.1 compares the seismic behavior of the two types of CIPP liner under the full-scale (100%) Rinaldi ground motion. The DI pipelines reinforced with both types of CIPP liners can accommodate the full-scale Rinaldi ground motion without failure but exhibit very different behaviors. The DI joint reinforced with the IMain liner remains almost linear elastic with an initial stiffness of approximately 190 kN/mm (1000 kips/in) and a secant stiffness of 144 kN/mm (760 kips/in.) at the maximum opening. No residual deformation or axial compressive forces can be observed at the end of the test. Also, very little energy was dissipated by the joint. However, the DI joint reinforced with the Starline® 2000 liner was much more ductile with a lower initial stiffness of 36 kN/mm (190 kips/in). The joint started to "yield" under an axial force about 22.2 kN (5.0 kips) and the axial stiffness reduced significantly. A small residual deformation and a residual compression force of 22.7 kN (5.1 kips) occurred at the end of the test. Moreover, much more energy was dissipated by the Starline® 2000 joint than by the IMain joint.

Figure 3.4.2 compares the seismic behavior of the DI pipelines reinforced with the two types of liners under the J-T ground motions at different intensities. Clearly, the DI joint reinforced with the Starline® 2000 liner is much more flexible than the joint reinforced with the IMain liner. Both joints, however, exhibited a nonlinear plastic response under the J-T ground motions. Again, the Starline® 2000 joint is much more ductile and dissipates more energy than the IMain joint. Moreover, the IMain joint experiences much higher peak tensile force at smaller peak joint openings. Larger residual compressive forces are induced in the IMain joint than in the Starline® 2000. Finally, significant pinching effect with large residual deformations in the liner can be observed in the Starline® 2000 joint when the J-T ground motion is scaled up to 500% of its full-scale intensity.

Figure 3.4.3 compares the response of the two types of CIPP liners under high intensity Rinaldi ground motions that damaged the liner in the joints. Only the west joints failed during the tests, while the east joints remained in good condition. The west IMain joint failed at 200% Rinaldi while the west Starline® 2000 joint failed at 2.25 * 260% Rinaldi. It is clearly seen that the IMain joints are much stiffer with a larger axial capacity and fails at a much a smaller joint openings than the Starline® 2000 joints.

Overall, the results from the tests conducted at the University at Buffalo indicate that pipelines reinforced with both types of CIPP liners can accommodate very high intensity ground motions. The DI joints reinforced with the Starline® 2000 liner are more ductile and could accommodate higher ground motion intensities compared to Joints reinforced with the Insituform IMain liner. Debonding between the liner and the DI pipelines confirms that it is beneficial to the seismic response of the lined joints. Debonding increases the deformation capacity of the joints and helps the DI joints to dissipate more energy during an earthquake event. Moreover for the Starline® 2000 liner, pinching effect was observed when the joint opening exceeded 12.7 mm (0.5 in.). This is not favorable for the seismic behavior of the joint as partial damage accumulates when the liner is folding into the gap between the spigot and the bell of the push-on joint.

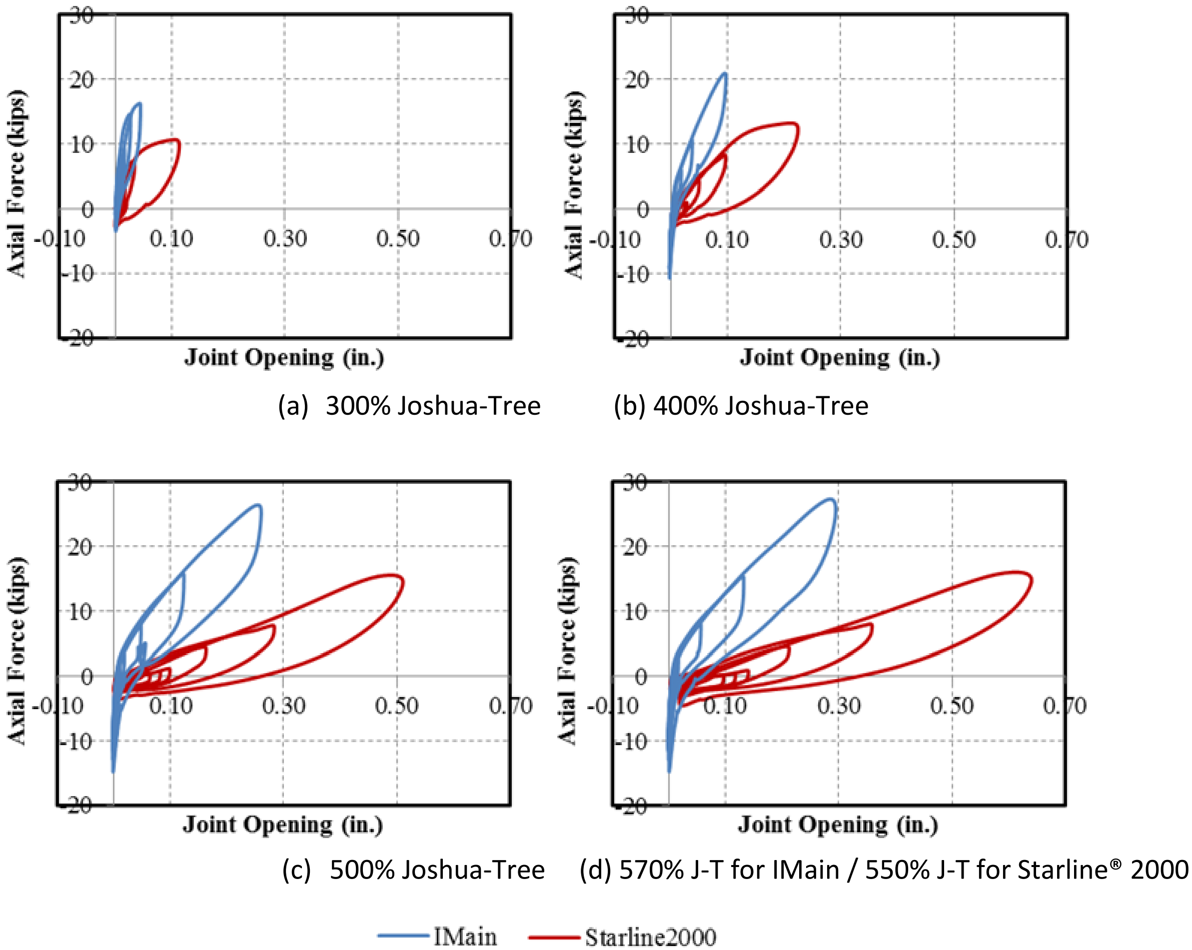

Figure 3.4.2. Single-Joint Seismic Tests with Joshua-Tree Ground Motion

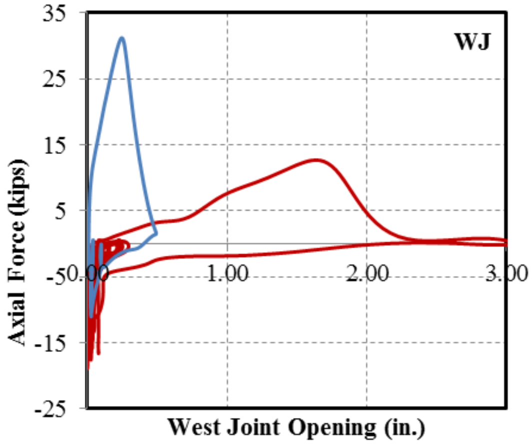

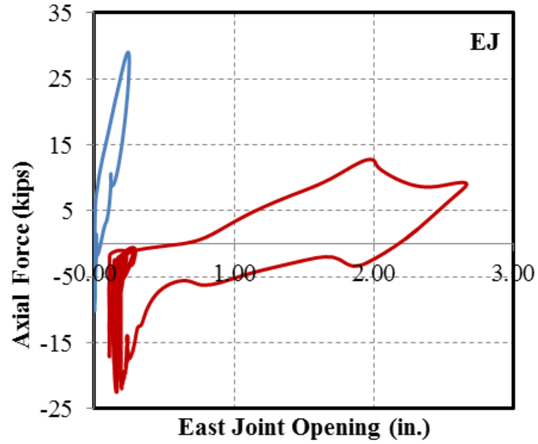

(a) West Joint (b) East Joint

Figure 3.4.3. Double-Joint Seismic Tests with Rinaldi Ground Motion

4. 0 CSULA / Education, Outreach and Training Activities

Progress Report for Year 3

4.1. Integrating Diverse Undergraduate Student Researchers.

Two graduate and two undergraduate research students (including two undergraduate Hispanic women) have been working on analytical and experimental aspects of the project at CSULA. The students have completed the Ductile Iron Pipe experiment with four point loading at CSULA's Strength of Materials laboratory (Figures 4.1.1 and 4..12).

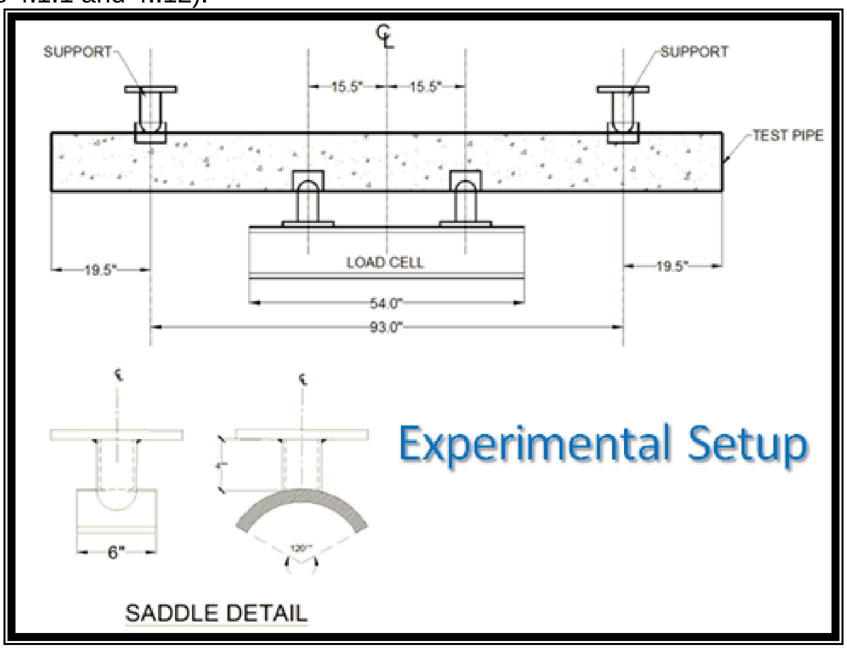

Figure 4.1.1. Details of Experimental Setup of Four Point Pipe Bending Test

Figure 4.1.2. Four Point Bending Test of a DI Pipe at CSULA Strength of Materials Laboratory

In parallel analytical studies of the same experiment was completed with a nonlinear finite element model with material non linearity. The model is shown in Figure 4.1.3 and the stress contour results are shown in Figure 4.4.4.

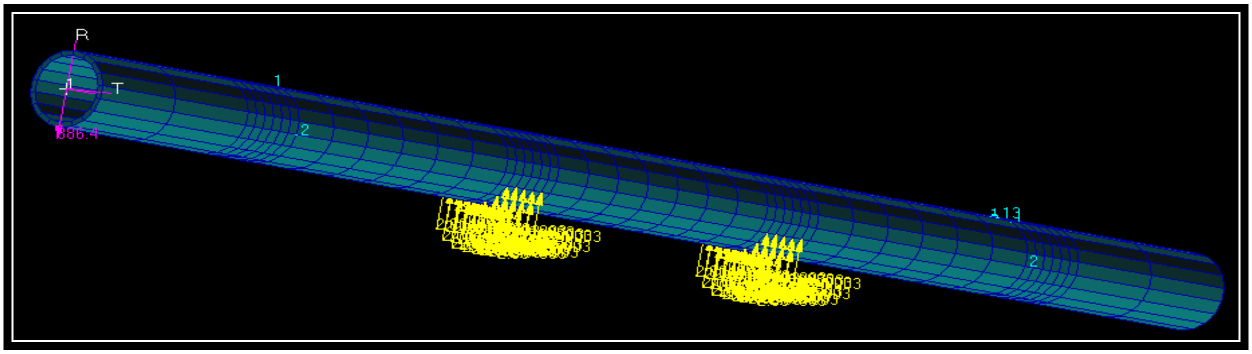

Figure 4.1.3. Non Linear Finite Element Model of the Pipe Experiment

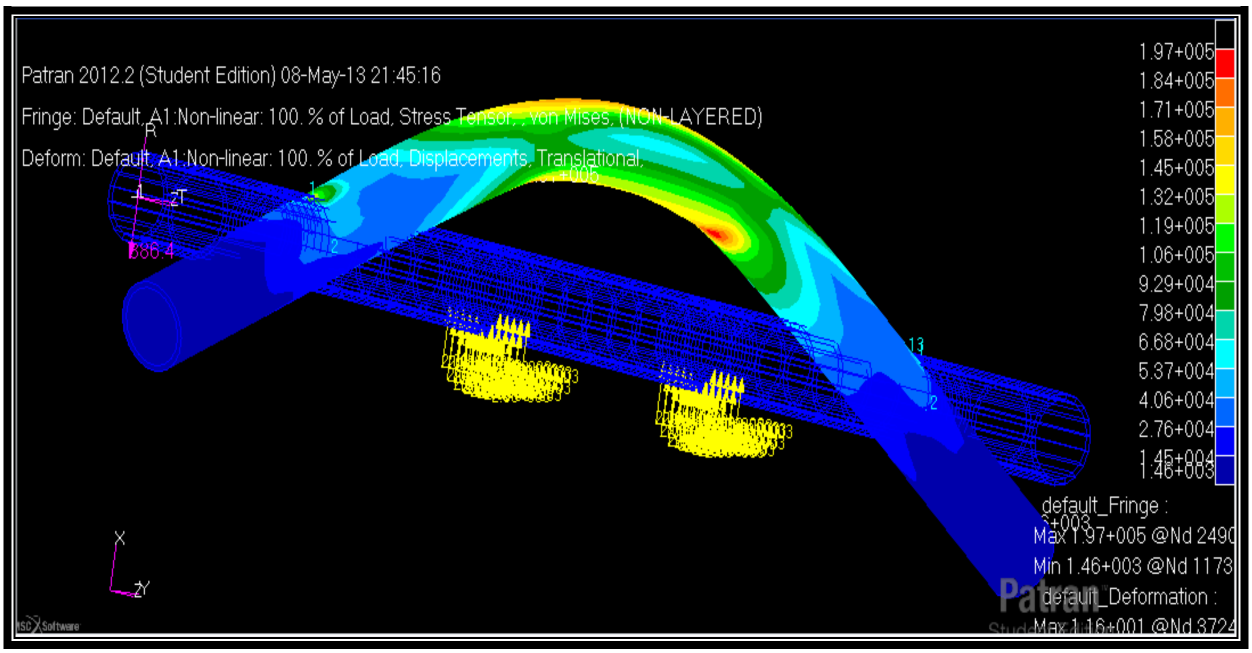

Figure 4.1.4. Stress Contours of Non Linear Finite Element Analysis Results

Figure 4.1.5 depicts the comparison of experimental and analytical results of strain versus applied load at mid span of the pipe (where load value shown is the applied load at one actuator point, whereas there are two such loads on the pipe.) As illustrated in the figure, reasonable correlation of experimental to analytical results is obtained.

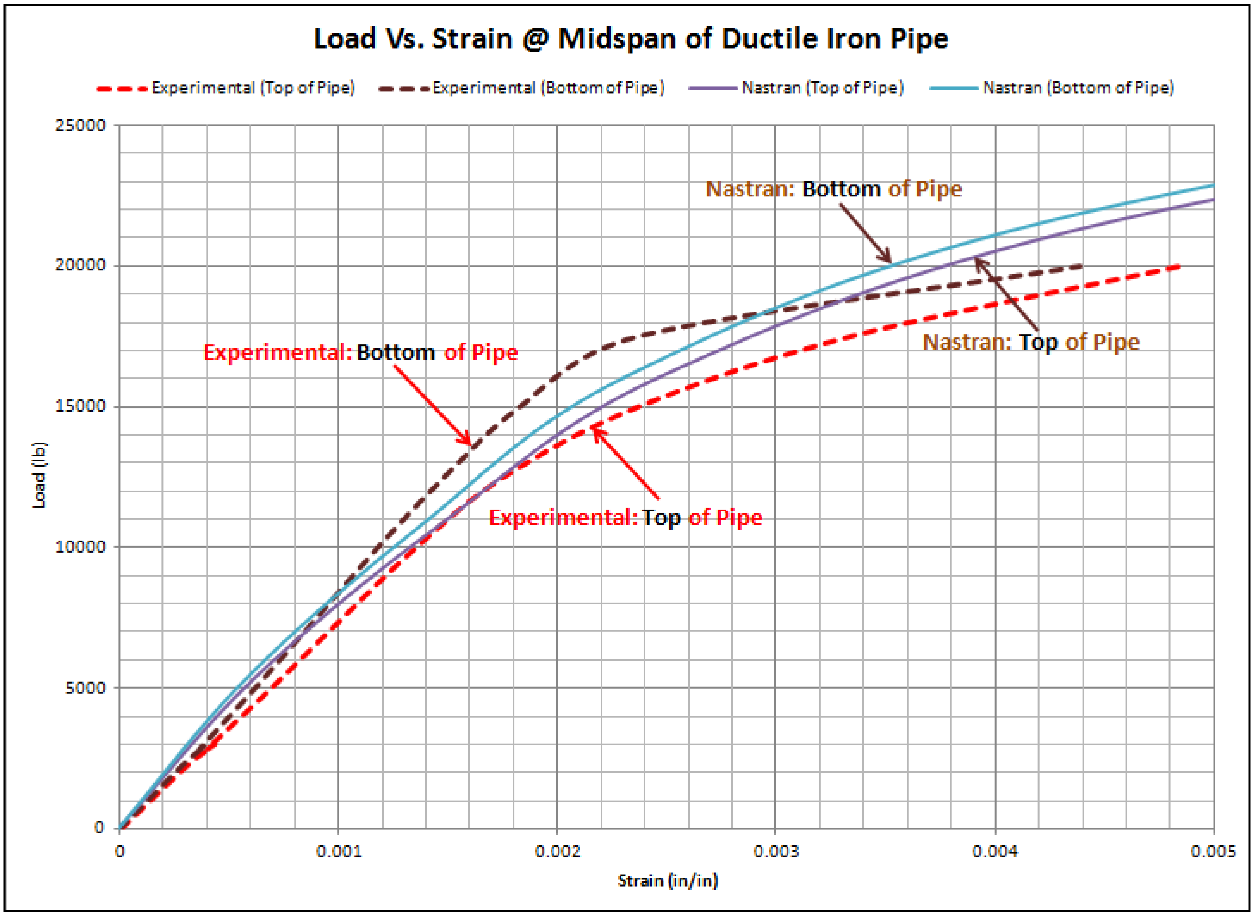

Figure 4.1.5. Comparison of Experimental and Non Linear Finite Element Analysis Results

The research concepts were introduced in a Freshman Civil Engineering Design course (CE 195) in spring 2013. The students were required to do a preliminary design of a new water conveyance system and support facilities, including a dam, pump station, and a pipeline that supplies water to a local community. The project required the preliminary design of a one-mile long pipeline from a pump station at a base of a dam to a storage facility at the top of a hillside. Students determined reservoir capacity, location, dam configuration and pipeline alignment based on the given constraints. As the pipeline crossed an earthquake fault, the students learned about fault-crossing design of pipeline as well. There were about 35 freshman students that represent a very diverse student group at CSULA.

4.2. Annual Field Trip to a LADWP Facility.

On March 14, 2013 approximately 25 students from CSULA participated in a field trip organized by the Los Angeles Department of Water and Power (LADWP) to observe pipe laying of earthquake resistant joint ductile iron pipes (ERJDIP).This is the very first time LADWP used this pipe joints that had the capability to lock joints in the event of an earthquake thereby minimizing any damage. The students observed firsthand the use of this innovative technology in the field. Figures 4.2.1 and 4.2.2 show students participating in the site visit along with LADWP employees.

Figure 4.2.1. Student Field Trip to an LADWP Pipe-Laying Site

Figure 4.2.2. Student Field Trip to an LADWP Pipe- Laying Location

4.3. Research Experiences for Undergraduates (REU) Program.

We were slightly less successful this year in recruiting undergraduate applicants for the REU 2013 program. Applications were received from four states (California, Georgia, Massachusetts and New York) with a couple of international inquiries as well. Similarly, efforts to recruit diverse applicants were less effective this year, with the applicant pool consisting of only one Hispanic, one Asian and three Caucasians. This year's REUs, include a male, Clarkson University sophomore from New York who is interested in expanding his understanding of "the correlation between creating buildings, and the people who utilize the infrastructure." The second REU is a Hispanic woman from California State University, Los Angeles, who participated in last year's LADWP short course and field trip. She has already indicated an intention to pursue a doctoral degree, and feels that this REU fellowship will allow her to "explore my ever growing interest in structural analysis and my developing knowledge of the vulnerability of ductile iron pipes." She also indicated that she wishes to serve as a mentor/role model to other women of color "to inspire more women to help diversify the pool of engineers."

4.4 Outreach and Technology Transfer to Water Supply Industry.

The annual 2-day short course, entitled "Water Supply Seismic System Performance, Planning, and Asset Management," has been postponed to September 26-27, 2013. The intentional postponement is to take advantage of final research findings that would offer broader impacts to improving design and operation of system performances of pipelines based on material that will be available this Fall.

REFERENCES

Bouziou, Dimitra (2013), personal communication.

Cornell University NEESR Group, ”Capacity Testing of UB Clamps,” Dec., 2012.

Cornell University NEESR Group, ”Axial Push Tests on Ductile Iron Pipes,” January 23, 2013.

Cornell University NEESR Group, “Unlined Ductile Iron Tension in Soil Test Basin,” Feb., 2013

Cornell University NEESR Group, “IMain Lined Ductile Iron Pipe Centered Tension in Soil Test Basin,” Mar., 2013.

Cornell University NEESR Group, “IMain Lined Ductile Iron Joint Centered Tension Test in Soil Test Basin,” Mar., 2013.

Cornell University NEESR Group, “Loading Rate Tests on IMain Lined Bell and Spigot DI Pipe,”, April, 2013.

http://www.insituform.com/CompanyInformation/~/~/media/Corporate/Files/Insituform/InsituMain%20Brochure.ashx

Shi, P. and O’Rourke, T.D. (2008). Seismic Response Modeling of Water Supply Systems. *Technical Report MCEER-08-0016*. Multidisciplinary Center for Earthquake Engineering Research, Buffalo, NY.

University at Buffalo NEES Group. (2012). “Shake Table Tests of Ductile Iron Pipe Retrofitted with Insituform IMain Liner”. Technical Report, University at Buffalo, NY.

University at Buffalo NEES Group. (2013). “Shake Table Tests of Ductile Iron Pipe Retrofitted with Starline2000 Liner”. *Technical Report*, University at Buffalo, NY.

Wang, Y. and O’Rourke, T.D. (2008). Seismic Performance Evaluation of Water Supply Systems. *Technical Report MCEER-08-0015*. Multidisciplinary Center for Earthquake Engineering Research, Buffalo, NY.